Appendix A

Temperature Analysis

Appendix A
Temperature Analysis:
Thermal Patterns, Source Assessment and Analytical Framework

Thermal Patterns

Overview

Extensive water temperature monitoring has occurred in the Grande Ronde River basin during the past decade. Two types of temperature data exist for the Grande Ronde River and tributaries: continuous measurements (temporal) and forward-looking infrared radiometer (spatial) thermal imagery. Several temperature patterns for the mainstem Grande Ronde River were observed from this data:

- Longitudinal temperature trends have slightly varied on an annual basis, but the general temperature condition has not changed;
- The upper 30 river miles is the location of rapid temperature change;
- Warm summertime mainstem temperatures (>75^{o}F) persist throughout the Grande Ronde mainstem below Meadow Creek to the Wallowa River confluence at Rondowa;
- Almost no cold-water "refugia" areas were observed in the FLIR temperature profiles for both the Grande Ronde River and Catherine Creek, once water temperatures are elevated; and
- Tributary temperatures at the mouth are greater than 64 ^{o}F (Excluding Clear Cr.).

Temporal Temperature Patterns

In an attempt to quantify the temporal thermal patterns of the Grande Ronde River and tributaries, several academic institutions and government agencies have been collecting continuous stream temperature data. Digital thermistors have excellent temperature resolution (±0.2^{o}C) and are capable of collecting thousands of measurements at user defined time intervals. Continuous temperature data can also have a spatial component when longitudinal sampling (i.e., multiple monitoring sites along a particular stream reach) is performed. **Image A-1** displays where continuous data exists and where associated median 7-day statistics have been calculated.

Image A-1. Streams with Continuous Temperature Data

Temperature Compliance

A seven-day moving average of daily maximums (7-day statistic) was adopted as the statistical measure of the stream temperature standard. Absolute numeric criteria are deemed action levels and water quality standard compliance (Recall **Table 4**).

Maximum temperatures in the mainstem during July and August commonly exceed 77^{o}F. This temperature level can cause rapid mortality to salmonids. Brett (1952) and Bell (1984) found the upper *incipient lethal limit* for salmonids to be 77^{o}F (25^{o}C). Continuous temperature data has shown that vast reaches of the Grande Ronde mainstem are elevated above ranges considered protective of salmon and trout populations. In fact, present conditions exceed *sub-lethal* temperature ranges (64^{o}F to 74^{o}F), and clearly fall in the *incipient lethal* temperature limits in much of river. This data indicates that the mainstem of the Grande Ronde River from Rondowa (RM 82) to the Clear Creek confluence (RM 200.5) does not support summertime salmonid migrations, spawning and rearing based on scientifically accepted aquatic life thermal limitations.

Recall **Table 4**. Applicable Water Temperature Standards *OAR 340-41-725(2)(b)(A)* WATER TEMPERATURE STANDARD	**7-Day Statistic**
Basic Absolute Criterion – Applies year long in all streams in the basin, with the exception of those that qualify for the *salmonid spawning, egg incubation and fry emergence criterion* -or- *bull trout criterion*.	≤64°F (17.8°C)
Salmonid Spawning, Egg Incubation and Fry Emergence Criterion – Applies to stream segments designated as supporting native salmonid spawning, egg incubation and fry emergence for the specific times of the year when these uses occur.	≤55°F (12.8°C)
Bull Trout Criterion – Applies to waters determined by the Department to support or to be necessary to maintain the viability of Bull Trout in the basin.	≤50°F (10.0°C)

Figure A-1. Grande Ronde River Median 7-Day Temperature Statistics for 1992 to 1999.

Note that the number of years represented in each monitoring site is displayed

Bars display minimum and maximum values

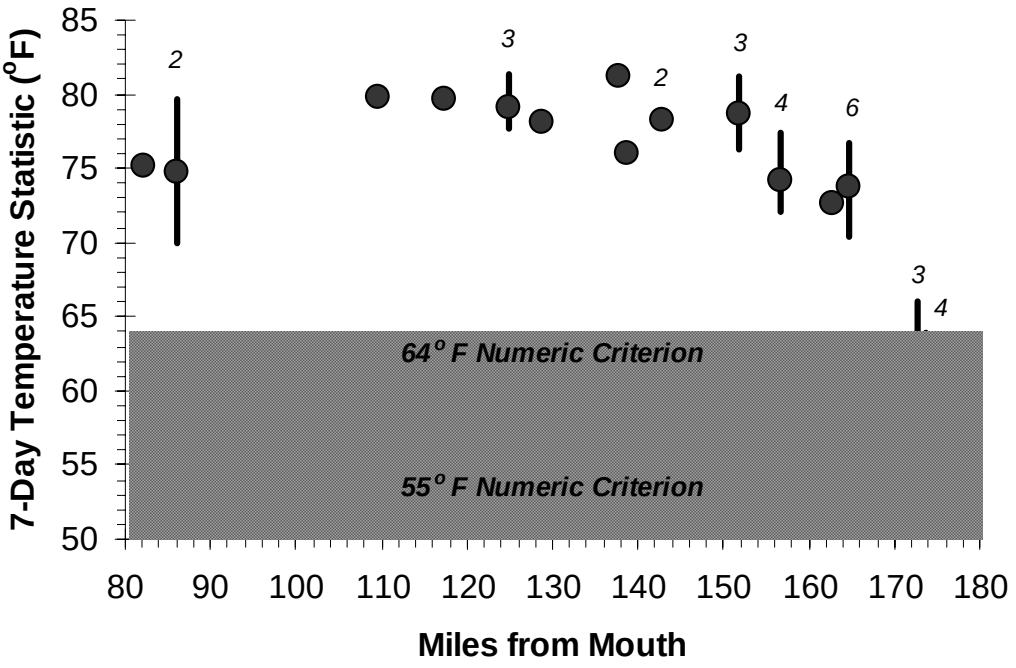

Calculated 7-day averaged maximum daily temperatures for the Grande Ronde River from the headwaters to Rondowa occurring between 1992 to 1999 are presented in **Figure A-1**. Although there is some variability in the data between years, there is a distinct pattern of rapid heating from the headwaters to below the Fly Creek confluence. In particular, Vey Meadow Valley (miles 165.8 to 171.8 from mouth) corresponds to an area of rapid temperature increase (i.e., a median 7-day temperature statistics of 62.8°F above Vey Meadow to 73.8°F below Vey Meadow). Bohle (1994) found that stream temperatures increased 1.3°F per mile (0.5°C per kilometer) through the unconstrained Vey Meadows reach where stream cover was low and channels were wide and shallow. Once the mainstem has heated to mid-70°F in the Grande Ronde River, it remains at a relatively warm temperature throughout the remaining 80 river miles to the Wallowa River confluence.

ODEQ deployed a total of 15 Vemco thermistors in the Upper Grande Ronde Basin during the summer of 1999. Calculated 7-day temperature statistics for these stations using summer 1999 data is presented in **Table A-1**.

Table A-1. 7-Day Temperature Statistics for the Upper Grande basin in 1999.

Temperature Site	Max Temperature		7-Day Statistic	
	Date	(^{o}F)	Date	(^{o}F)
Grande Ronde R. upstream Clear Cr.	07/29/99	61.2	07/27/99	59.5
Grande Ronde R. downstream Vey Meadows	07/28/99	77.7	07/25/99	75.1
Grande Ronde R. upstream Meadow Cr.	07/28/99	81.1	07/27/99	78.4
Grande Ronde R. at Pierce Lane	07/29/99	81.5	07/27/99	80.4
Grande Ronde R. at Striker Lane	08/27/99	83.3	08/23/99	79.8
Grande Ronde R. at Palmer Junction	07/28/99	72.3	07/25/99	70.0
Grande Ronde R. at Rondowa	07/28/99	77.7	07/25/99	75.1
North Fork Catherine Cr. at mouth	08/19/99	64.4	07/27/99	62.5
South Fork Catherine Cr. at mouth	08/04/99	64.4	07/27/99	62.0
Catherine Cr. at Goodley Road	08/28/99	80.8	08/23/99	77.8
Catherine Cr. upstream Union	08/06/99	75.2	07/31/99	71.7
Indian Cr. at mouth	08/04/99	83.7	07/27/99	81.2
Willow Cr. at Courtney Road	07/27/99	73.6	07/17/99	70.9
Lookingglass Cr. upstream Hatchery	07/28/99	64.9	07/25/99	63.8
Wallowa R. at Rondowa	08/28/99	72.3	08/23/99	71.1

Daily Temperature Patterns

Figure A-2 displays the longitudinal distribution of daily maximum temperatures between July 15 and August 31 between 1992 and 1997. Again, the pattern of heating follows a rapid increase from the headwaters of the Grande Ronde to below Vey Meadow (Rivermiles 212-194) where median daily maximum temperatures increase 20^{o}F over 18 river miles (1.1^{o}F per RM –or- 0.4^{o}C per kilometer). **Figure A-2** also shows that median maximum daily temperatures remain relatively constant from Vey Meadow (Rivermile 194.0) to the head of the State Ditch (Rivermile 150).

Daily temperature patterns are presented in **Figure A-3**. Stream temperature generally cools throughout the night and into the early morning hours. Rapid heating during mid-morning and early afternoon periods is common. Maximum daily temperatures occur during afternoon and early evening periods when heat energy delivery peaks.

Figure A-2. Grande Ronde Mainstem Longitudinal Box Plot of Daily Maximum Temperatures Occurring Between July 15 and August 31, 1992 to 1997 (ODEQ Data)

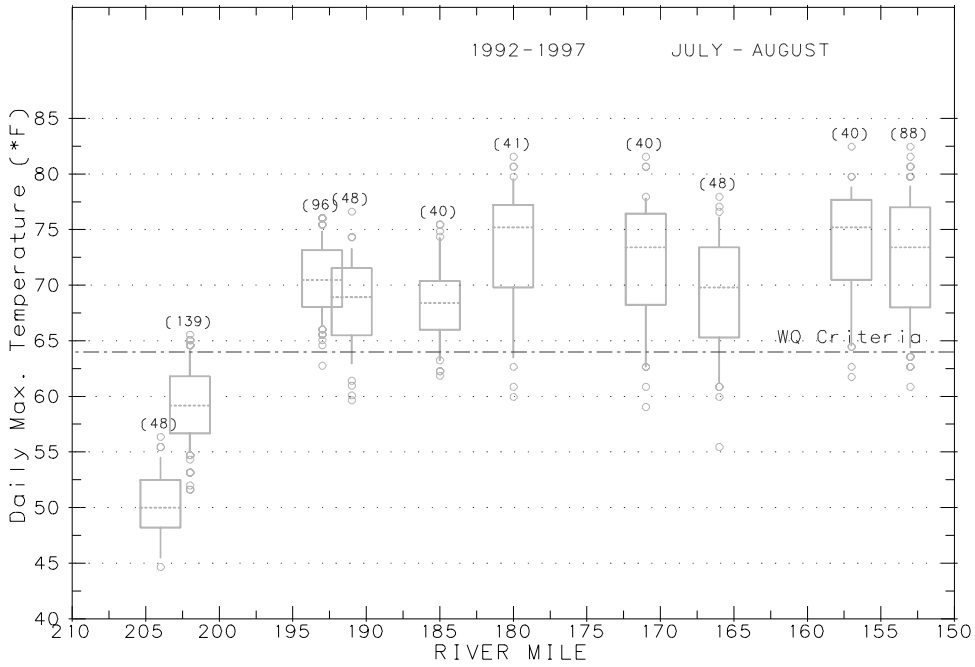

Figure A-3. Grande Ronde Mainstem Daily Temperature Profiles August 20, 1999

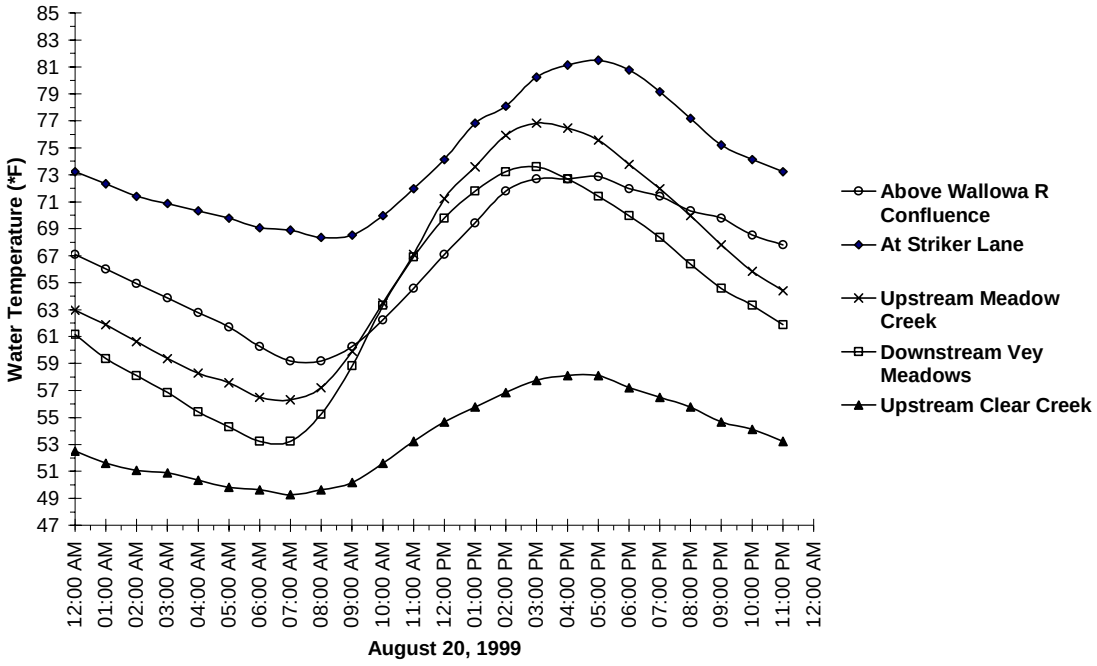

Seasonal/Annual Temperature Patterns

Section 303(d)(1) requires this TMDL to be "established at a level necessary to implement the applicable water quality standard with seasonal variations." Both stream temperature and flow vary seasonally from year to year. Water temperatures are coolest in winter and early spring months. Stream temperatures exceed State water quality standards in summer and early fall months (June, July, August and September) (**Figure A-4**). Warmest stream temperatures correspond to prolonged solar radiation exposure, warm air temperature, low flow conditions and decreased groundwater contribution. These conditions occur during summer and early fall. The analysis presented in this TMDL is concerned with summertime periods in which stream temperatures are most critical.

Figure A-4. Summertime 7-Day Temperature Statistic

(ODEQ data, 1999)

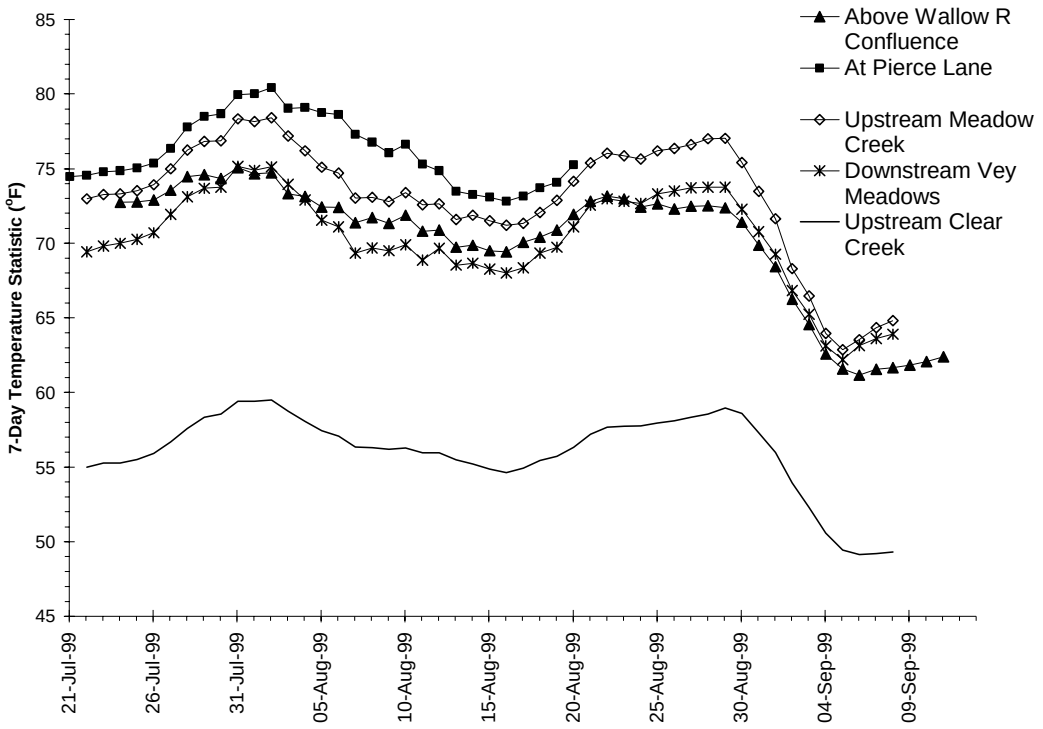

Spatial Thermal Patterns

Forward looking infrared radiometer (FLIR) thermal imagery coupled with color videography and geographic positioning systems (GPS) produces spatially continuous temperature imagery. FLIR and color video images are collected with instruments mounted to a helicopter. The output data consists of GPS-tagged FLIR digital images that cover approximately 100 x 150 meters with less than 1 meter of spatial resolution and $\pm 0.5^{o}C$ accuracy. The spatial continuity of the FLIR data has made it possible to visually observe many of the thermodynamic processes associated with stream heating as they occur. The overriding strength of FLIR temperature analysis is spatial continuity. FLIR temperature analysis includes the development of longitudinal heating profiles that depict thermal effects of tributaries, cool water thermal refugia and source (heating) areas.

Perhaps the greatest contribution of FLIR technology is its ability to display thermal habitat fragmentation of warmed reaches separated by isolated cool-water refugia. Before the advent of FLIR stream temperature analysis, the variability of stream temperature was vastly understated.

This variability has been cited for the continued existence of cold water fish in relatively warm water rivers/streams. McIntosh et al. (1995) and Torgersen et al. (1995) demonstrated that cold water fish commonly utilize cooler reaches and habitats during times that vast portions of rivers/streams maintain stressful and/or lethal warm water temperatures.

Summary statistics for the August 1999 FLIR data are presented in **Table A-2** and **Figure A-5**. A total of 274.5 stream miles were "flown" with FLIR. Mainstem sampling included 91.6 miles, Catherine Creek was sampled along 71.0 miles, and the remaining 111.9 miles were sampled in tributaries. 5.0% of the total stream miles were less than 55^{o}F, while 21.3% of the stream mileage were below 64^{o}F (i.e., temperatures suitable for salmonids). Forty eight percent (48%) of the FLIR sampled stream mileage is in the sub-lethal temperature range and 15.5% of the total stream mileage has incipient lethal temperatures. Thermal stratification occurred in 15.3% of the total mileage flown.

Table A-2. FLIR Derived Water temperatures in the Grande Ronde Sub-Basin

Temperature (°F)	Distance (Miles)	Percent of Total	Mode of Thermal Mortality
Less than 55.0	13.7	5.0%	
55.0 to 59.5	19.3	7.0%	
59.5 to 64.0	25.5	9.3%	
64.0 to 68.5	23.8	8.7%	Sub-Lethal Limit
68.5 to 73.0	48.5	17.7%	
73.0 to 77.5	59.3	21.6%	
Greater than 77.5	42.5	15.5%	Incipient Lethal Limit
Thermally Stratified	41.9	15.3%	
Totals	274.5	100%	

Figure A-5. FLIR Derived Temperature Summary (*1:30-5:00 PM for August 20-26, 1999)*

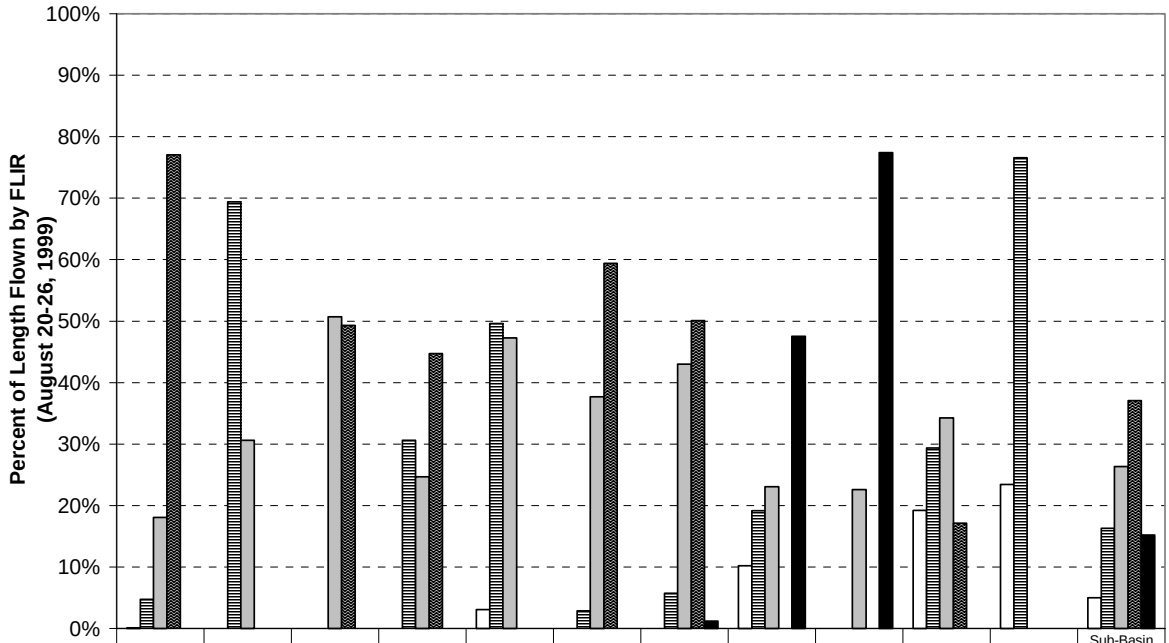

	Mainstem (91.6 miles)	Limber Jim (4.6 miles)	Fly Cr. (13.4 miles)	Sheep Cr. (10.5 miles)	Beaver Cr. (13.3 miles)	McCoy Cr. (9.3 miles)	Meadow (21.1 miles)	Catherine (71.0 miles)	Willow Cr. (10.2 miles)	Indian Cr. (21.2 miles)	Lookingglass (8.0 miles)	Sub-Basin Total (270.5 miles)
Less than 55.0*F	0.1%	0.0%	0.0%	0.0%	3.1%	0.0%	0.0%	10.2%	0.0%	19.2%	23.4%	5.0%
55.0*F to 64*F	4.8%	69.4%	0.0%	30.6%	49.6%	2.9%	5.7%	19.1%	0.0%	29.4%	76.6%	16.3%
64.0*F to 73.0*F	18.0%	30.6%	50.7%	24.7%	47.3%	37.7%	43.0%	23.1%	22.6%	34.3%	0.0%	26.3%
Greater than 73.0*F	77.1%	0.0%	49.3%	44.7%	0.0%	59.4%	50.1%	0.0%	0.0%	17.2%	0.0%	37.1%
Thermally Stratified	0.0%	0.0%	0.0%	0.0%	0.0%	0.0%	1.2%	47.6%	77.4%	0.0%	0.0%	15.3%

Mainstem Longitudinal Profile

The Grande Ronde mainstem was sampled August 20, 1999 between 2:15 PM and 4:12 PM. Longitudinal water temperature increased rapidly within the first 30 miles from the headwaters. Temperatures are consistently warm below the upper Forest Service boundary to Rondowa (RM 82), with the exception of cool water mixing from Lookingglass Creek (RM 85.6). The FLIR profile also indicates that 40.3% of the Grande Ronde River was over the *incipient lethal limit* for salmonids, and 95.1% is over the sub-lethal limit (64 ^{o}F) (**Table A-3**). That is, only *4.9%* of the Grande Ronde River was under 64^{o}F and these areas are largely located in the upper headwater reaches of the river.

Table A-3. Water temperatures in the Grande Ronde Mainstem on 8/20/99

Temperature (°F)	Distance (Miles)	Percent of Total	Mode of Thermal Mortality
Less than 55.0	0.1	0.1%	
55.0 to 59.5	1.0	1.1%	
59.5 to 64.0	3.3	3.6%	
64.0 to 68.5	2.4	2.6%	Sub-Lethal Limit
68.5 to 73.0	14.2	15.5%	
73.0 to 77.5	33.7	36.8%	
Greater than 77.5	36.9	40.3%	Incipient Lethal Limit
Thermally Stratified	0.0	0.0%	
Totals	91.6	100.0%	

Few cool water areas were observed in the Grande Ronde River mainstem following initial stream heating within the upper reaches of the river (see **Figure A-6**). Small areas of water temperature "cooling" were observed, however, river temperatures generally remained well above 75^{o}F within these zones and were not considered thermal habitat/refugia areas.

Lookingglass Creek water temperatures were much lower relative to that of the Grande Ronde mainstem (64.9^{o}F and 79.0^{o}F, respectively) and Lookingglass Creek summer discharge rates are generally similar to that of the Grande Ronde mainstem. Observed Grande Ronde River temperatures increased rapidly downstream of this confluence, indicating that factors causing stream heating in the Grande Ronde River are still present downstream of the confluence. The temperatures above the Lookingglass Creek confluence are extreme and form a lethal thermal barrier for salmonids. Deviation between tributary and mainstem FLIR-derived water temperatures are presented in **Table A-4**. Negative values conditions which tributary mouth temperatures are lower than upstream mainstem temperatures.

Figure A-6. Grande Ronde River Longitudinal Water Temperature Profile for 8/20/99.

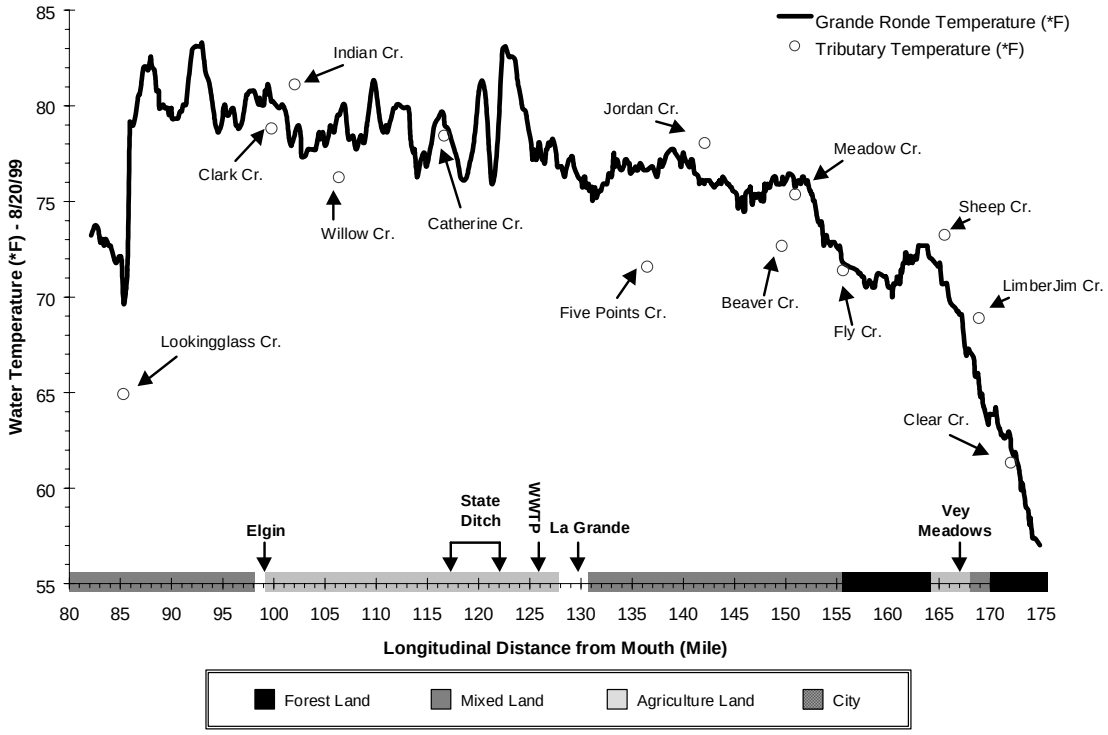

Table A-4. Deviation of tributary mouth temperatures and upstream Grande Ronde River temperatures observed with FLIR on 8/20/99.

Tributary Name	Deviation from Grande Ronde Temperature (^{o}F)	Tributary Name	Deviation from Grande Ronde Temperature (^{o}F)
Clear Cr.	- 1.1	Five Points Cr.	- 5.2
Limber Jim Cr.	+ 4.1	Catherine Cr.	- 1.4
Sheep Cr.	+ 2.7	Willow Cr.	- 3.2
Fly Cr.	- 0.0	Indian Cr.	+ 2.3
Meadow Cr.	- 0.9	Clark Cr.	- 1.4
Beaver Cr.	- 4.0	Lookingglass Cr.	- 14.3
Jordan Cr.	+2.9		

Continuous Monitoring Data Comparison

It may be helpful to remind the reader that FLIR images represent the temperature of the outer most surfaces. **Figure A-7** presents both the spatial (FLIR derived profile) and temporal (continuous Vemco) temperature data collected at 4 PM on 8/20/99. Observed FLIR temperature data correspond with continuous temperature data collected from devices placed at the bottom of the stream channel. Such a tight correlation between observed FLIR and continuous temperatures suggests that that the Grande Ronde River is not thermally stratified.

Figure A-7. Grande Ronde mainstem measured FLIR temperature profile and continuous (Vemco) temperature data near 4:00 PM August, 20, 1999

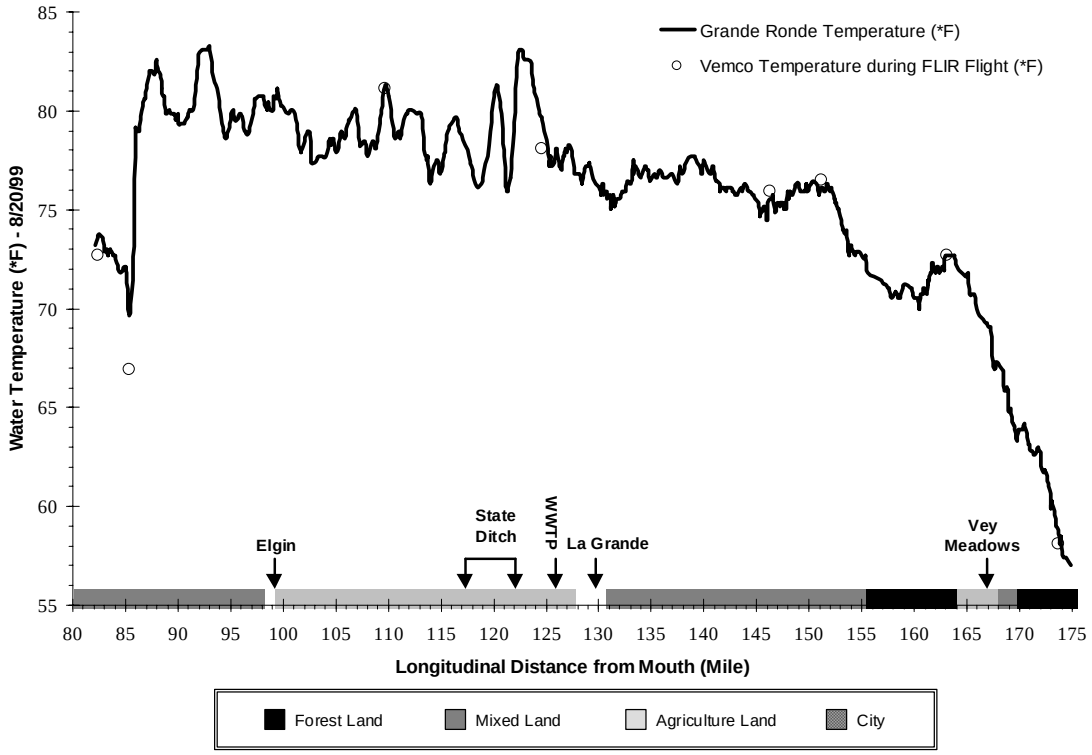

Stream Mixing and Reynolds Number

The *Reynolds Number* is commonly used to define the upper and lower critical velocities for the transition between laminar and turbulent flow. The *Reynolds Number* is a fundamental parameter that represents the relative importance of inertia in comparison with viscous forces in the flow (Martin and McCutcheon, 1999):

$$R_e = \frac{U \times R_h}{\nu} = \frac{U \times \frac{A}{P_w}}{\nu} = \frac{U \times \frac{(W \times D)}{(W + 2D)}}{\nu}$$

Grande Ronde Mainstem Reynolds Number Ranges

(R_e > 2,000 Indicates Turbulent Flow)

Minimum R_e = 11,756

Maximum R_e = 94,967

Where,

A:	Cross-sectional area (m^2)	*U*:	Mean velocity ($m\ s^{-1}$)
D:	Average stream depth (m)	ν:	Kinematic viscosity ($1.007 \times 10^{-6}\ m^2 s^{-1}$)
P_w:	Wetted perimeter (m)	*W*:	Wetted width (m)
R_h:	Hydraulic radius (m)		

Accordingly, calculated *Reynolds Numbers* for the Grande Ronde River indicate that the river experiences turbulent flow and therefore the river is well mixed.

Tributary Longitudinal Profiles

Catherine Creek Temperature Pattern

FLIR longitudinal temperature profiles were collected for Catherine Creek, North Fork Catherine Creek, and South Fork Catherine Creek between 1:38 PM and 2:57 PM on August 21, 1999. It is important to point out that river miles presented with the longitudinal profile were calculated with the "old" Grande Ronde River channel bypassed by the State Ditch (approximately 22 miles).

Below the Catherine Creek forks, the temperarure was 61 ^{o}F (**Figure A-8**). Rapid stream heating was observed within Catherine Creek between the confluence of Scott Creek and Milk Creek. Stream temperatures rose above 64^{o}F within this reach. Further downstream, water temperatures continue to warm between Milk Creek confluence and upstream of Davis Dam (66.0^{o}F to 69.6^{o}F, respectively). Tributary temperatures are similar to mainstem temperatures upstream of Davis Dam and do not appear to influence mainstem temperatures.

Continuous and FLIR temperatures correlate well upstream of Davis Dam (**Figure A-9**). However, thermal stratification is apparent below Davis dam because FLIR temperature increases downstream of Davis Dam do not match temperatures measured by continuous monitors at the bottom of water column. Therefore, caution should be used when interpreting FLIR water temperature data downstream of Davis Dam because it likely does not reflect water column temperatures below the stratified surface layer. Accordingly, approximately 63% of the mainstem Catherine Creek is thermally stratified below the North and South Forks.

Both North and South Fork Catherine Creek temperatures were below 64^{o}F (**Figure A-10** and **Figure A-11**).

Based on FLIR derived longitudinal temperature profiles, 29% of the Catherine Creek system has water temperatures below the sub-lethal limit (64 ^{o}F) (**Table A-5**). These cold water areas are located exclusively in the North and South Forks and the uppermost 3.6 miles of Catherine Creek.

Figure A-8. Catherine Creek Longitudinal Water Temperature Profile
2:04 PM to 2:56 PM August, 21 1999

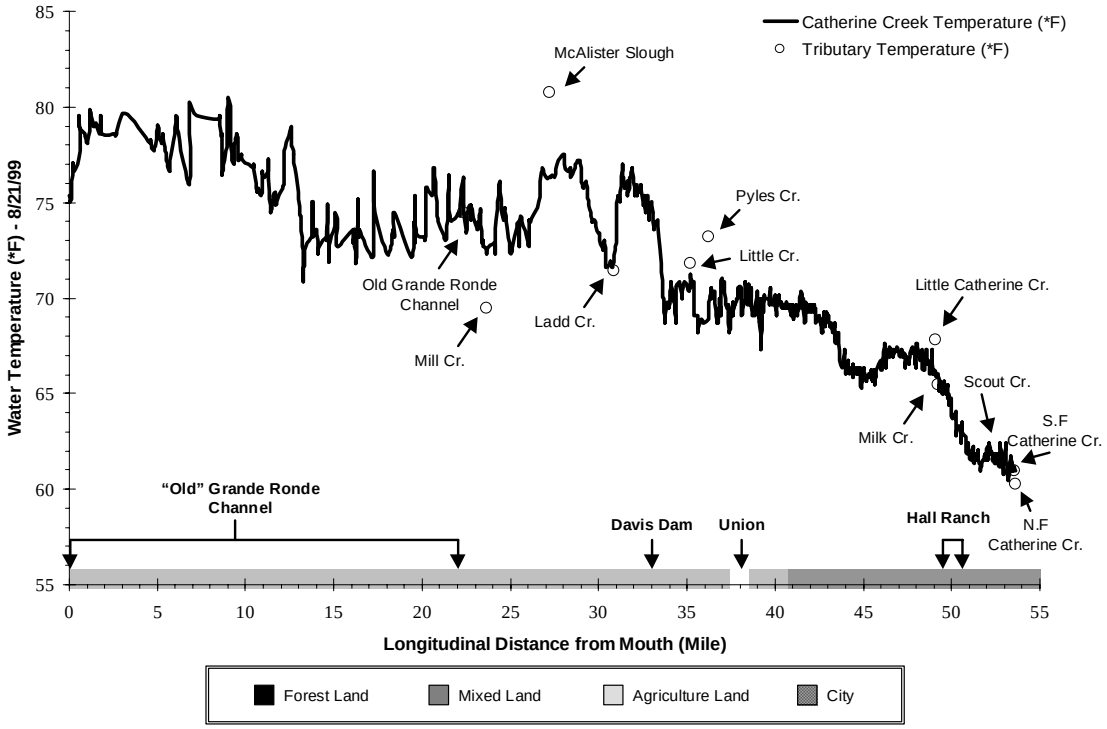

Figure A-9. Catherine Creek FLIR Derived and Continuous (Vemco) Temperature Data
2:04 PM to 2:56 PM August, 21 1999

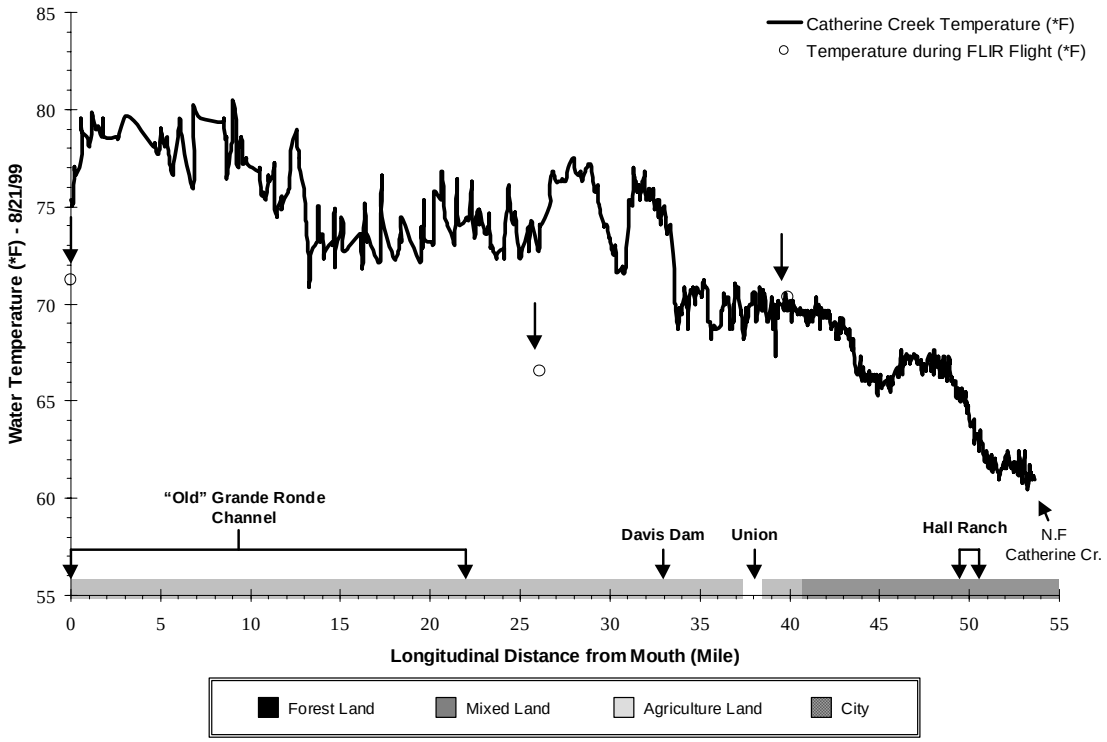

Figure A-10. North Fork Catherine Creek Longitudinal Water Temperature Profile
1:55 PM to 2:04 PM August, 21 1999

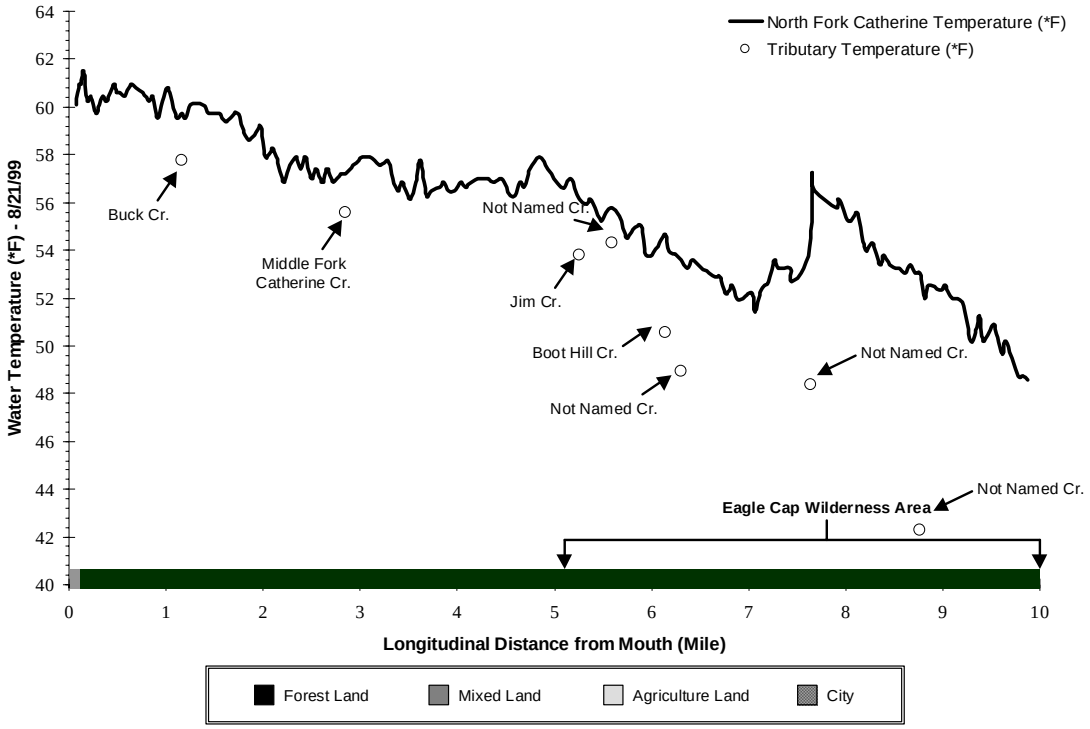

Figure A-11. South Fork Catherine Creek Longitudinal Water Temperature Profile
1:38 PM to 1:46 PM August, 21 1999

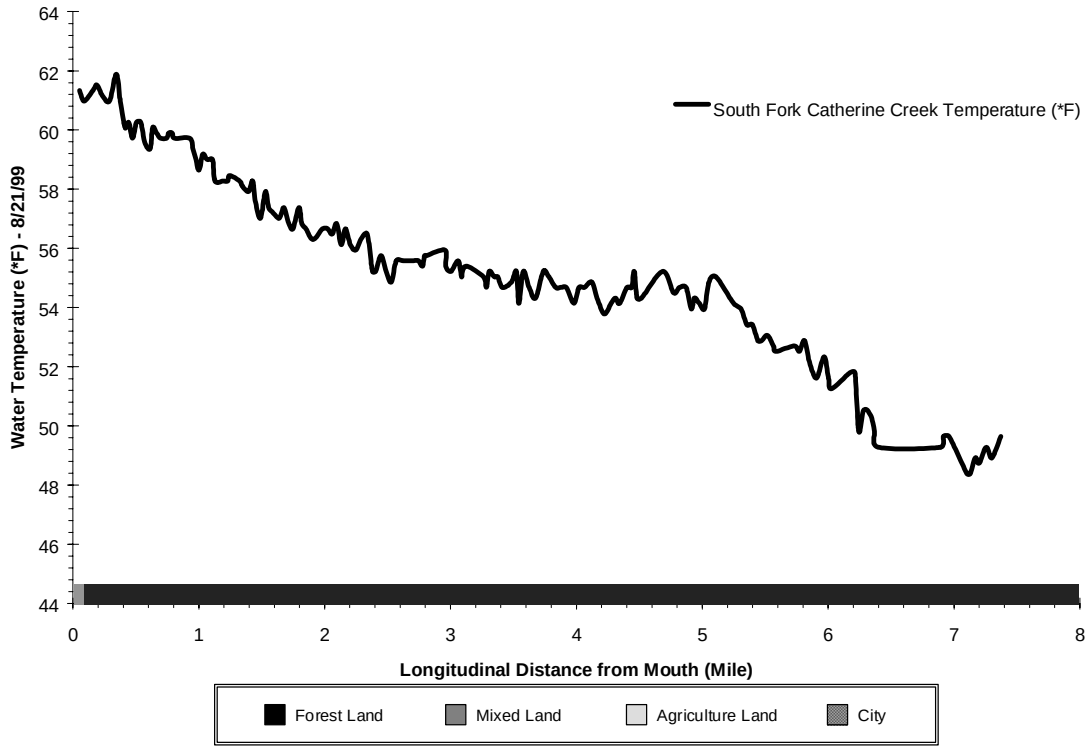

Table A-5. Water temperatures for Catherine Creek on 8/21/99			
Temperature (°F)	**Distance (Miles)**	**Percent of Total**	**Mode of Thermal Mortality**
Catherine Creek - Forks to Mouth			
Less than 55.0	0.0	0.0%	
55.0 to 59.5	0.0	0.0%	
59.5 to 64.0	3.6	6.7%	
64.0 to 68.5	7.0	13.0%	Sub-Lethal Limit
68.5 to 73.0	9.4	17.4%	
73.0 to 77.5	0.0	0.0%	
Greater than 77.5	0.0	0.0%	Incipient Lethal Limit
Thermally Stratified	33.8	62.9%	
Totals	53.8	100.0%	
North Fork Catherine Creek			
Less than 55.0	3.6	36.6%	
55.0 to 59.5	4.6	46.4%	
59.5 to 64.0	1.7	17.0%	
64.0 to 68.5	0.0	0.0%	Sub-Lethal Limit
68.5 to 73.0	0.0	0.0%	
73.0 to 77.5	0.0	0.0%	
Greater than 77.5	0.0	0.0%	Incipient Lethal Limit
Thermally Stratified	0.0	0.0%	
Totals	9.9	100.0%	
South Fork Catherine Creek			
Less than 55.0	3.6	49.3%	
55.0 to 59.5	2.8	38.6%	
59.5 to 64.0	0.9	12.0%	
64.0 to 68.5	0.0	13.0%	Sub-Lethal Limit
68.5 to 73.0	0.0	17.4%	
73.0 to 77.5	0.0	0.0%	
Greater than 77.5	0.0	0.0%	Incipient Lethal Limit
Thermally Stratified	0.0	0.0%	
Totals	7.3	100.0%	
Catherine Creek - System Totals			
Less than 55.0	7.2	10.2%	
55.0 to 59.5	7.4	10.5%	
59.5 to 64.0	6.2	8.7%	
64.0 to 68.5	7.0	9.9%	Sub-Lethal Limit
68.5 to 73.0	9.4	13.2%	
73.0 to 77.5	0.0	0.0%	
Greater than 77.5	0.0	0.0%	Incipient Lethal Limit
Thermally Stratified	33.8	47.6%	
Totals	71.0	100.0%	

Lookingglass Creek Temperature Pattern

FLIR data was collected for Lookingglass Creek between 3:30 and 3:40 on August 25, 1999. Data was collected from the mouth and extended eight river-miles to the Eagle Creek confluence. Observed water temperatures were below the 64°F criteria (**Table A-6**). The effects of tributary streams on mainstem temperature were minimal (**Figure A-12**). In addition, the fish hatchery located near the Jarboe Creek confluence does not appear to influence water temperatures on the FLIR profile.

Table A-6. Water temperatures for Lookingglass Creek on 8/25/99

Temperature (°F)	Distance (Miles)	Percent of Total	Mode of Thermal Mortality
Less than 55.0	1.9	23.4%	
55.0 to 59.5	2.3	28.4%	
59.5 to 64.0	3.9	48.2%	
64.0 to 68.5	0.0	0.0%	Sub-Lethal Limit
68.5 to 73.0	0.0	0.0%	
73.0 to 77.5	0.0	0.0%	
Greater than 77.5	0.0	0.0%	Incipient Lethal Limit
Thermally Stratified	0.0	0.0%	
Totals	8.1	100.0%	

Figure A-12. Lookingglass Creek Longitudinal Water Temperature Profile
3:30 PM to 3:40 PM August, 25 1999

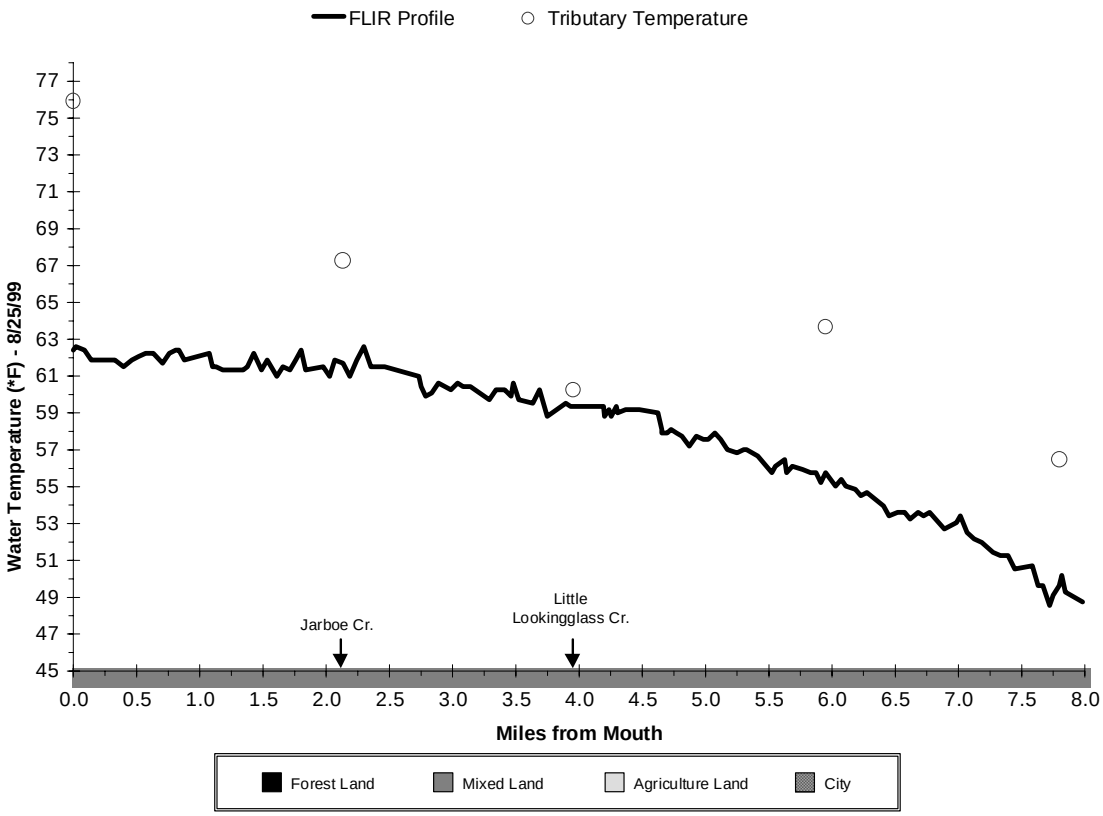

Indian Creek Temperature Pattern

FLIR temperature data was collected for Indian Creek on August 25, 1999 at approximately 4:00 PM. Observed water temperature less than 55°F occurred in 4.1 river-miles and 9.9 river-miles were less than 64°F (**Table A-7**). These cool water conditions occurred within the headwater regions of Indian Creek (**Figure A-13**). Rapid heating occurred over the most of Indian Creek as the tributary gained 29.3°F over a distance of 21.2 miles (averaging 1.4°F warming per mile). Tributary temperatures were similar to those of the mainstem and had little effect on the longitudinal temperature profile.

Table A-7. Water temperatures for Indian Creek on 8/25/99

Temperature (°F)	Distance (Miles)	Percent of Total	Mode of Thermal Mortality
Less than 55.0	4.1	19.2%	
55.0 to 59.5	3.0	14.2%	
59.5 to 64.0	3.2	15.2%	
64.0 to 68.5	3.7	17.6%	Sub-Lethal Limit
68.5 to 73.0	3.5	16.7%	
73.0 to 77.5	2.0	9.2%	
Greater than 77.5	1.7	8.0%	Incipient Lethal Limit
Thermally Stratified	0.0	0.0%	
Totals	21.2	100.0%	

Figure A-13. Indian Creek Longitudinal Water Temperature Profile
3:55 PM to 4:17 PM August, 25 1999

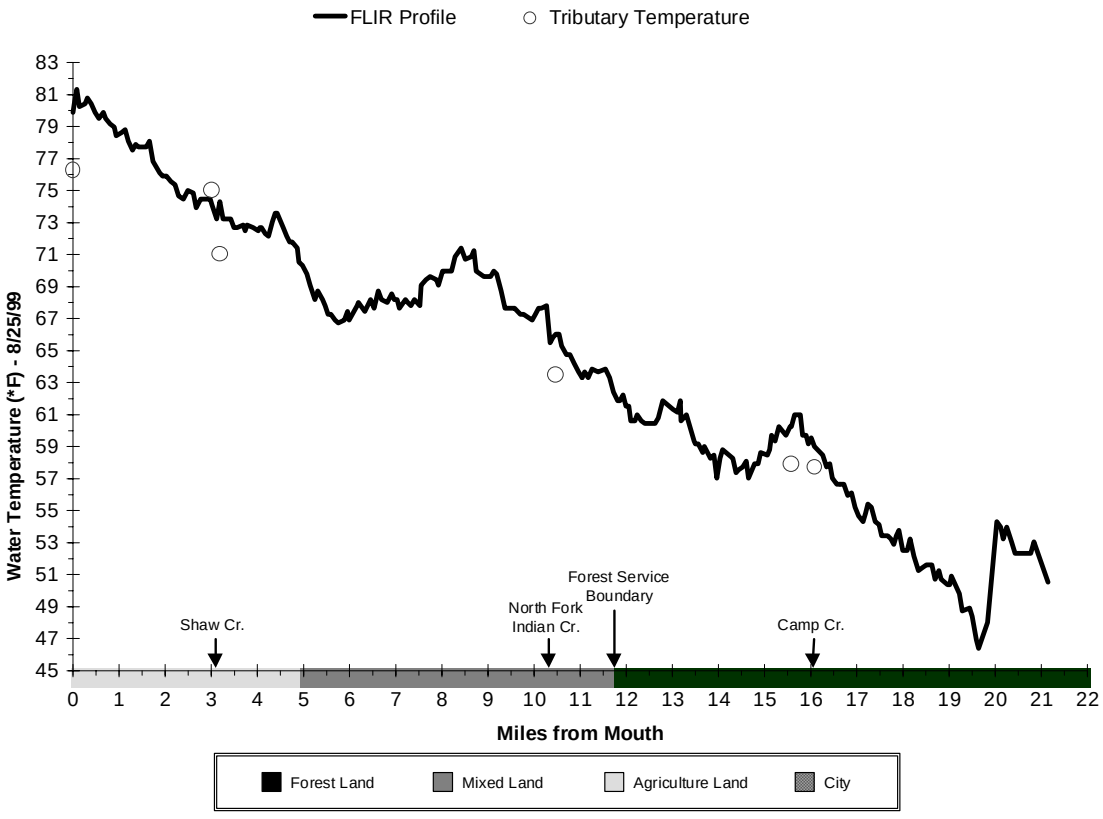

Willow Creek Temperature Pattern

FLIR temperature data was collected for Willow Creek between 4:32 PM and 4:48 PM on August 25, 1999. It was determined that Willow Creek was thermally stratified within the bottom 7.9 river-miles. For example, continuous temperature data (Onset Stowaway) collected at lower Courtney Road recorded a value 3.6°F less than the surface temperature measured by the FLIR. In addition, **Image A-2** provides an example of a thermally stratified condition in lower Willow Creek (Mill Creek confluence). A second continuous data collection point (DEQ Vemco) was located at the upper Courtney Lane Bridge crossing. This site is within a well-mixed reach and FLIR and continuous temperature closely match. In addition, FLIR imagery collected upstream of river mile 7.9 did not indicate thermal stratification. Table A-8 and Figure A-14 illustrate observed temperatures within Willow Creek.

Table A-8. Water temperatures for Willow Creek on 8/25/99

Temperature (°F)	Distance (Miles)	Percent of Total	Mode of Thermal Mortality
Less than 55.0	0.0	0.0%	
55.0 to 59.5	0.0	0.0%	
59.5 to 64.0	0.0	0.0%	
64.0 to 68.5	0.5	4.4%	Sub-Lethal Limit
68.5 to 73.0	1.9	18.2%	
73.0 to 77.5	0.0	0.0%	
Greater than 77.5	0.0	0.0%	Incipient Lethal Limit
Thermally Stratified	7.9	77.4%	
Totals	10.3	100.0%	

Image A-2. Thermal Stratification at Willow Creek and Mill Creek Confluence.
Temperature Scale on Right is in Celsius

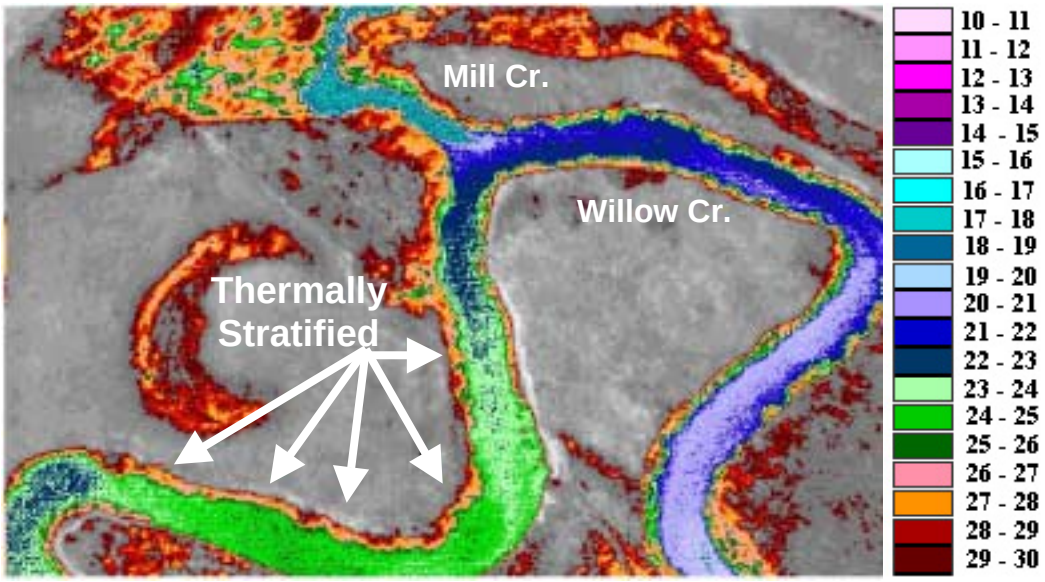

Figure A-14. Willow Creek Longitudinal Water Temperature Profile
4:32 PM to 4:48 PM August, 25 1999

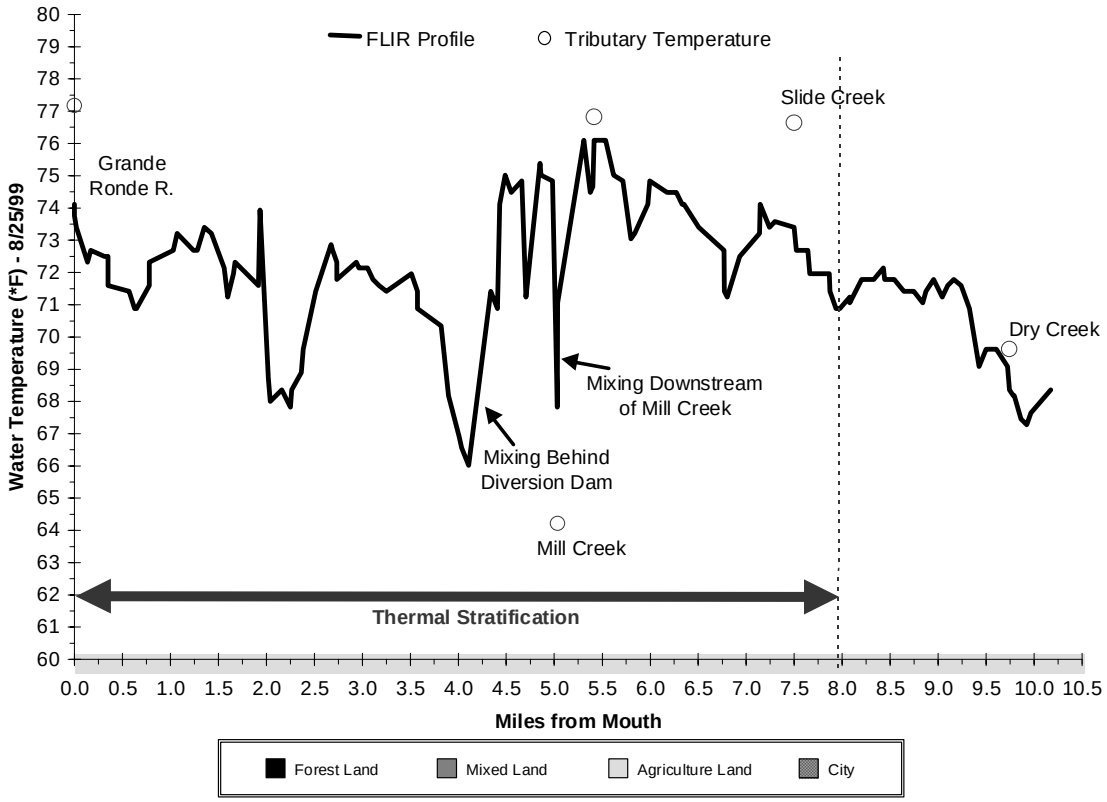

Meadow Creek Temperature Pattern

FLIR temperature data was collected for Meadow Creek on August 26, 1999 from 2:23 to 2:44 PM. The FLIR longitudinal profile shows little cold water refugia (5.7% of the stream length is less than 64°F) (**Table A-9**). Much of Meadow Creek falls in the sub-lethal temperature range (83.2% between 64.0°F and 77.5°F). Only, 2.1 stream miles (9.9%) have temperatures that are in the incipient lethal range. It is important to point out that 1.2% of Meadow Creek was stratified (**Image A-3**). In terms of thermal requirements for fish, little thermal habitat was suitable for salmonids in Meadow Creek during the August FLIR sampling period (**Figure A-15**).

Table A-9. Water temperatures in the Meadow Creek on 8/26/99

Temperature (°F)	Distance (Miles)	Percent of Total	Mode of Thermal Mortality
Less than 55.0	0.0	0.0%	
55.0 to 59.5	0.4	1.9%	
59.5 to 64.0	0.8	3.8%	
64.0 to 68.5	3.2	15.2%	Sub-Lethal Limit
68.5 to 73.0	6.0	27.8%	
73.0 to 77.5	8.6	40.2%	
Greater than 77.5	2.1	9.9%	Incipient Lethal Limit
Thermally Stratified	0.3	1.2%	
Totals	21.4	100.0%	

Image A-3. Thermal Stratification within Meadow Creek at Dam (RM 5.5).
Temperature Scale on Right is in Celsius

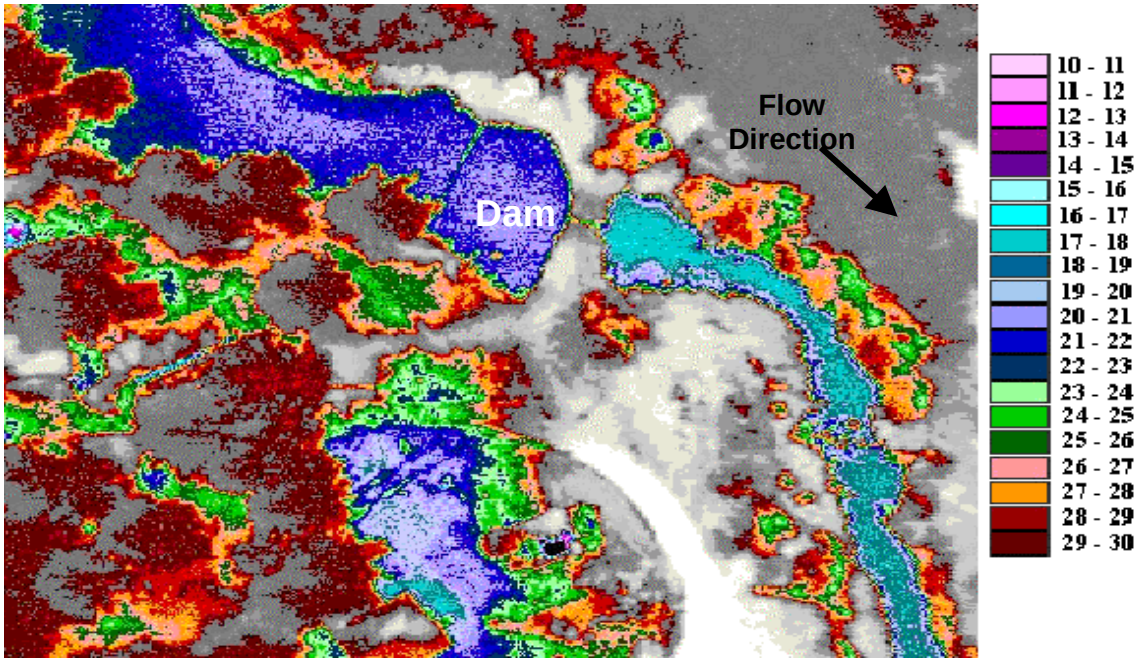

Figure A-15. Meadow Creek Longitudinal Water Temperature Profile
2:23 PM to 2:44 PM August, 26 1999

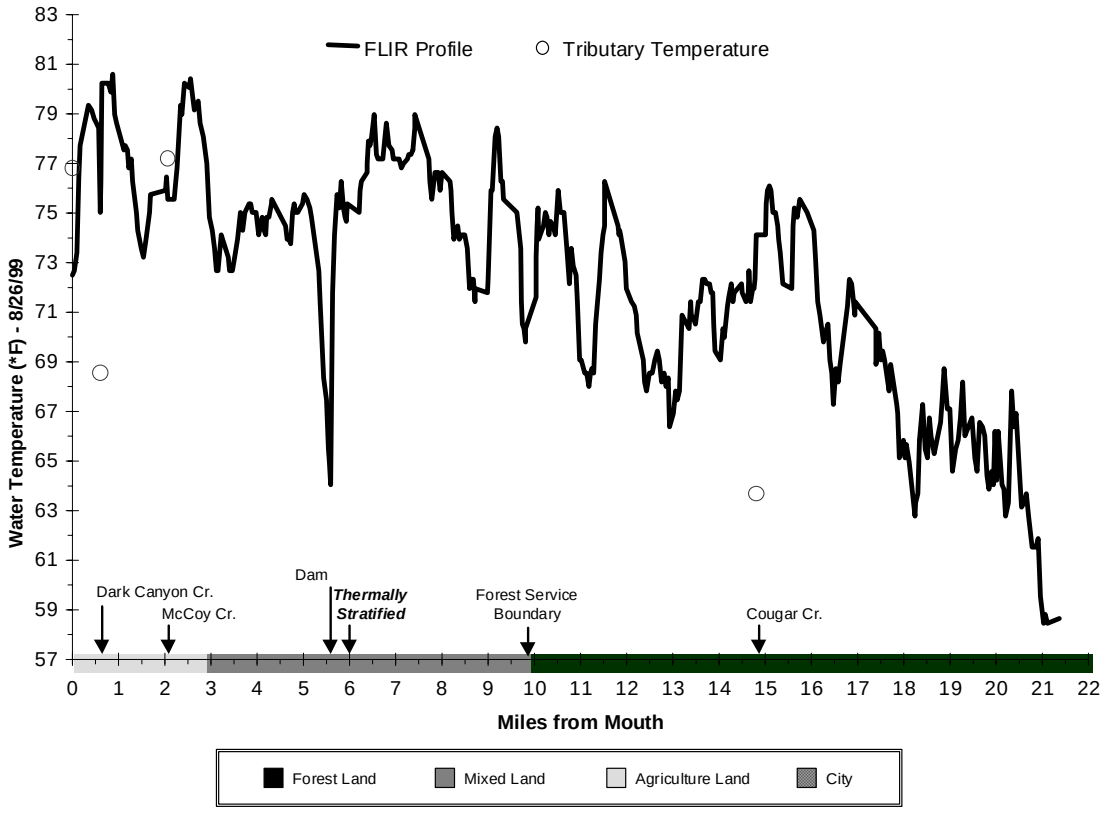

McCoy Creek Temperature Pattern

FLIR data was collected for McCoy Creek on August 26, 1999 from 3:00 to 3:09 PM. McCoy Creek heats rapidly into the sub-lethal and incipient lethal temperature ranges (**Figure A-16**). Temperatures fluctuate, but a clear warming trend is apparent. Little thermal habitat was sampled during the August 1999 FLIR sampling period. It is important to point out that 97.1% of the stream length had temperatures greater than 64°F (Table A-10).

Table A-10. Water temperatures in the McCoy Creek on 8/26/99

Temperature (°F)	Distance (Miles)	Percent of Total	Mode of Thermal Mortality
Less than 55.0	0.0	0.0%	
55.0 to 59.5	0.0	0.0%	
59.5 to 64.0	0.3	2.9%	
64.0 to 68.5	0.8	8.7%	Sub-Lethal Limit
68.5 to 73.0	2.7	29.0%	
73.0 to 77.5	3.7	40.2%	
Greater than 77.5	1.8	19.2%	Incipient Lethal Limit
Thermally Stratified	0.0	0.0%	
Totals	9.3	100.0%	

Figure A-16. McCoy Creek Longitudinal Water Temperature Profile
3:00 PM to 3:09 PM August, 26 1999

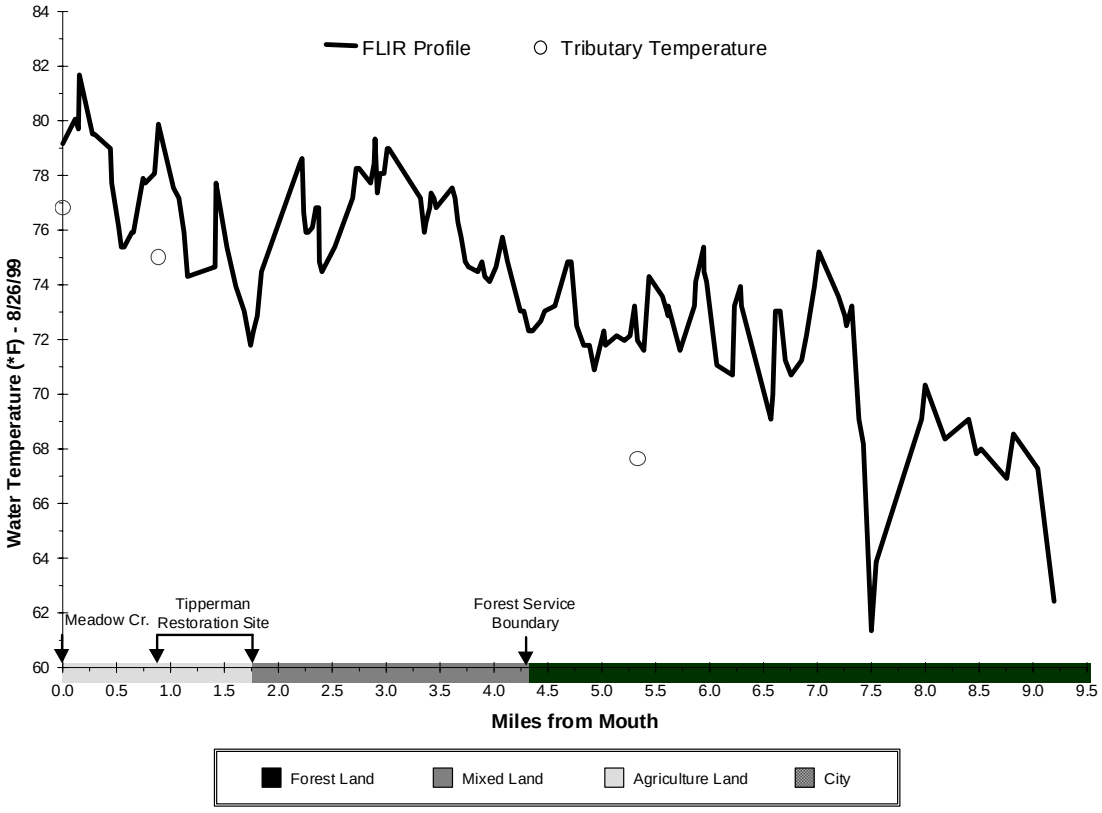

Beaver Creek Temperature Pattern

FLIR temperature data was collected from Beaver Creek on August 26, 1999 from between 2:00 and 2:11 PM. The flight ended downstream from the La Grande Reservoir. Of the stream miles within the Forest Service boundary, 97.1% is below 64°F (**Table A-11** and **Figure A-17**). Of the total stream miles flown, 52.7% were below 64°F, a majority of which occurred within public lands. (Only 5.8% of Beaver Creek traveling through private lands were below 64°F.)

Table A-11. Water temperatures in the Beaver Creek on 8/26/99

Temperature (°F)	Distance (Miles)	Percent of Total	Mode of Thermal Mortality
Less than 55.0	0.4	3.1%	
55.0 to 59.5	1.2	9.3%	
59.5 to 64.0	5.4	40.3%	
64.0 to 68.5	3.4	25.7%	Sub-Lethal Limit
68.5 to 73.0	2.9	21.5%	
73.0 to 77.5	0.0	0.0%	
Greater than 77.5	0.0	0.0%	Incipient Lethal Limit
Thermally Stratified	0.0	0.0%	
Totals	13.3	100.0%	

Figure A-17. Beaver Creek Longitudinal Water Temperature Profile
2:00 PM to 2:11 PM August, 26 1999

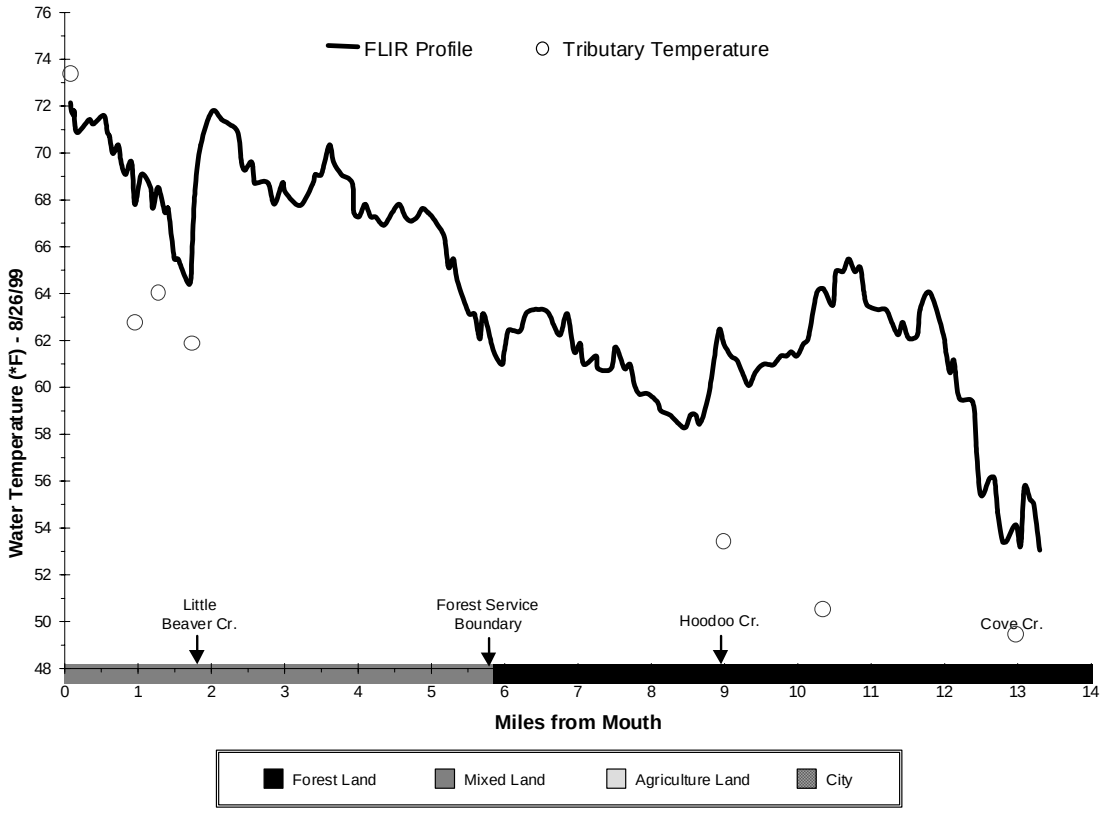

Fly Creek Temperature Pattern

FLIR data was collected for Fly Creek on August 26, 1999 from 3:45 to 3:57 PM. Of the 13.4 stream miles flown over Fly Creek, all of the FLIR derived temperatures were in the sub-lethal range (**Table A-12** and **Figure A-18**). It is important to point out that Fly Creek stream temperatures warm rapidly through Fly Meadow. It is also important to note that mixing from Little Fly Creek cools Fly Creek by 4°F, however Fly Creek temperatures warm rapidly back above 75°F. In addition, approximately 4-5°F cooling occurs in the Forest Service reach below Fly Meadow, but temperatures again warm to nearly 77°F near the confluence with the Grande Ronde River.

Table A-12. Water temperatures in the Fly Creek on 8/26/99

Temperature (°F)	Distance (Miles)	Percent of Total	Mode of Thermal Mortality
Less than 55.0	0.0	0.0%	
55.0 to 59.5	0.0	0.0%	
59.5 to 64.0	0.0	0.0%	
64.0 to 68.5	1.2	8.8%	Sub-Lethal Limit
68.5 to 73.0	5.6	42.0%	
73.0 to 77.5	6.6	49.3%	
Greater than 77.5	0.0	0.0%	Incipient Lethal Limit
Thermally Stratified	0.0	0.0%	
Totals	13.4	100.0%	

Figure A-18. Fly Creek Longitudinal Water Temperature Profile
3:45 PM to 3:57 PM August, 26 1999

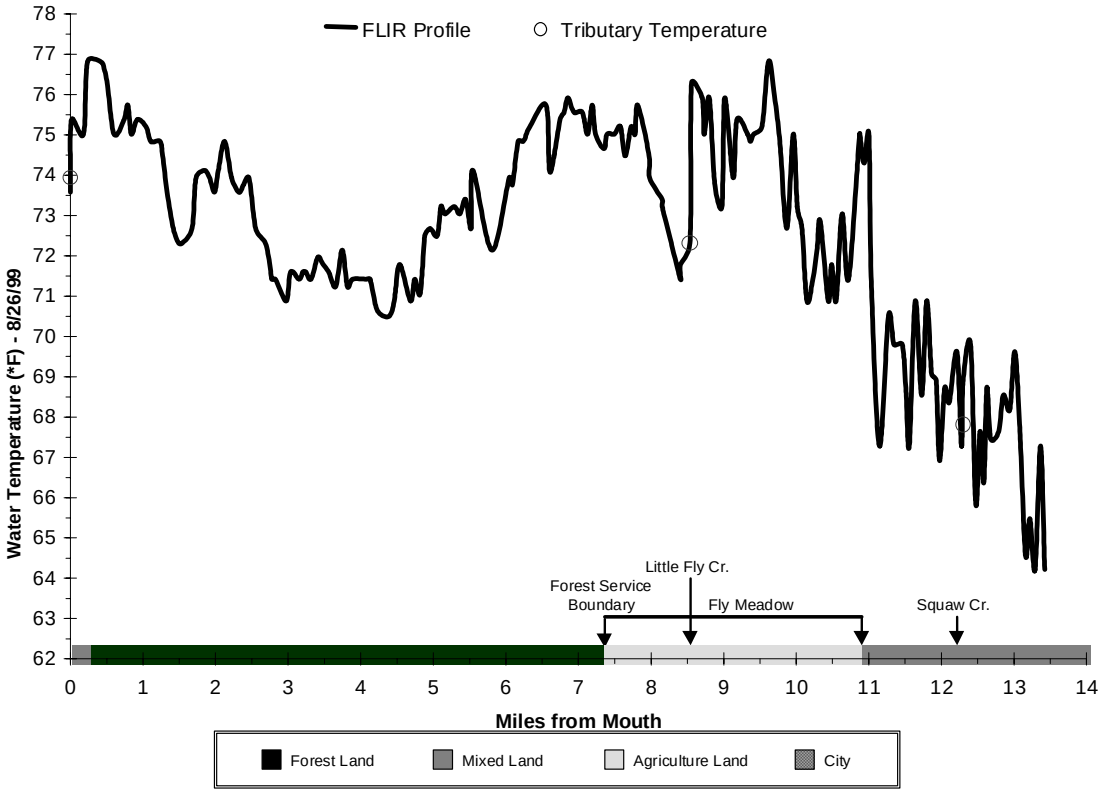

Sheep Creek Temperature Pattern

FLIR data was collected for Sheep Creek on August 26, 1999 from 4:11 to 4:21 PM. The upper 3.3 miles (30.6%) of Sheep Creek had temperatures less than 64°F. Rapid stream heating began one mile above the Forest Service boundary and continued throughout Vey Meadows until temperatures stabilized at 76°F (**Figure A-19**). In terms of percent of stream length FLIR sampled, 69.4% of Sheep Creek was within the sub-lethal temperature range (**Table A-13**).

Table A-13. Water temperatures in the Sheep Creek on 8/26/99

Temperature (°F)	Distance (Miles)	Percent of Total	Mode of Thermal Mortality
Less than 55.0	0.0	0.0%	
55.0 to 59.5	2.4	22.5%	
59.5 to 64.0	0.9	8.1%	
64.0 to 68.5	1.2	11.3%	Sub-Lethal Limit
68.5 to 73.0	1.4	13.4%	
73.0 to 77.5	4.7	44.7%	
Greater than 77.5	0.0	0.0%	Incipient Lethal Limit
Thermally Stratified	0.0	0.0%	
Totals	10.6	100.0%	

Figure A-19. Sheep Creek Longitudinal Water Temperature Profile
4:11 PM to 4:21 PM August, 26 1999

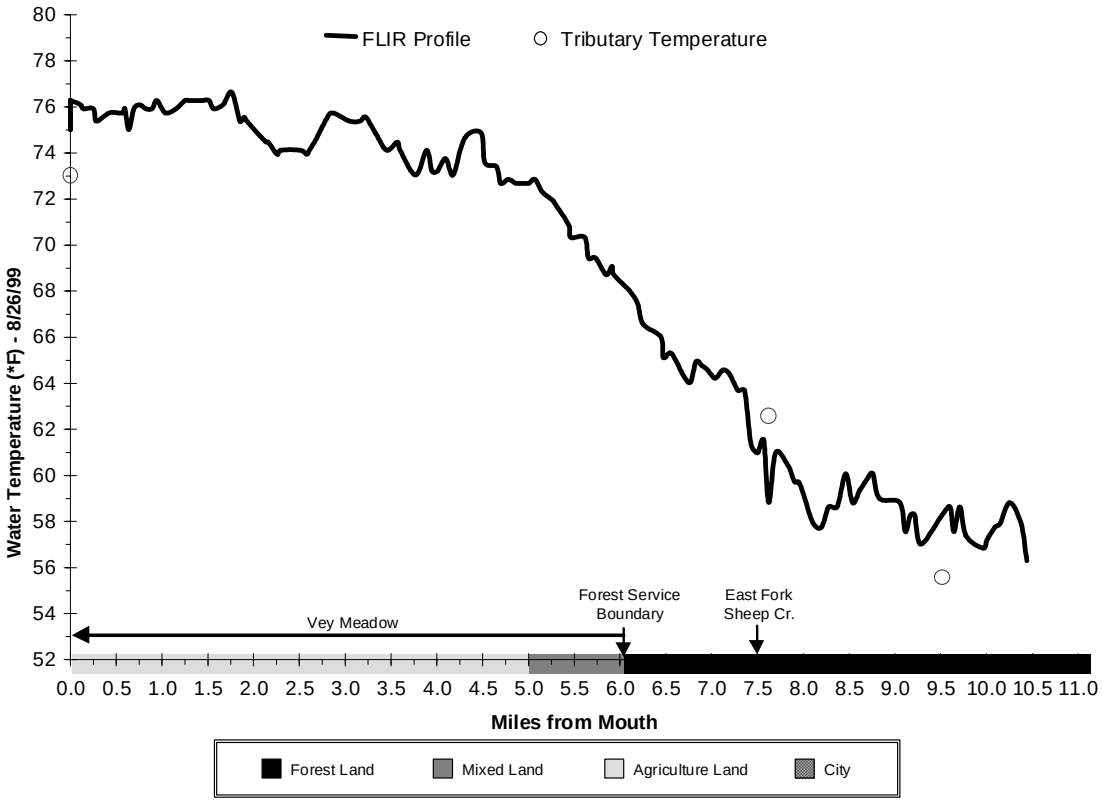

Limber Jim Creek Temperature Pattern

FLIR data was collected for Limber Jim Creek on August 26, 1999 from 4:29 to 4:34 PM. Of the 4.6 stream miles sampled for FLIR, 69.4% were below 64°F (**Table A-14**). Temperatures above the North Fork Limber Jim confluence were fairly stable and only gradual heating occurred. Limber Jim heated rapidly below the North Fork from 60°F to 71°F in less than 1.7 miles.

Table A-14. Water temperatures in the Limber Jim Creek on 8/26/99

Temperature (°F)	Distance (Miles)	Percent of Total	Mode of Thermal Mortality
Less than 55.0	0.0	0.0%	
55.0 to 59.5	1.5	33.2%	
59.5 to 64.0	1.7	36.2%	
64.0 to 68.5	0.4	7.9%	Sub-Lethal Limit
68.5 to 73.0	1.0	22.7%	
73 .0to 77.5	0.0	0.0%	
Greater than 77.5	0.0	0.0%	Incipient Lethal Limit
Thermally Stratified	0.0	0.0%	
Totals	4.6	100.0%	

Figure A-20. Limber Jim Creek Longitudinal Water Temperature Profile
4:29 PM to 4:34 PM August, 26 1999

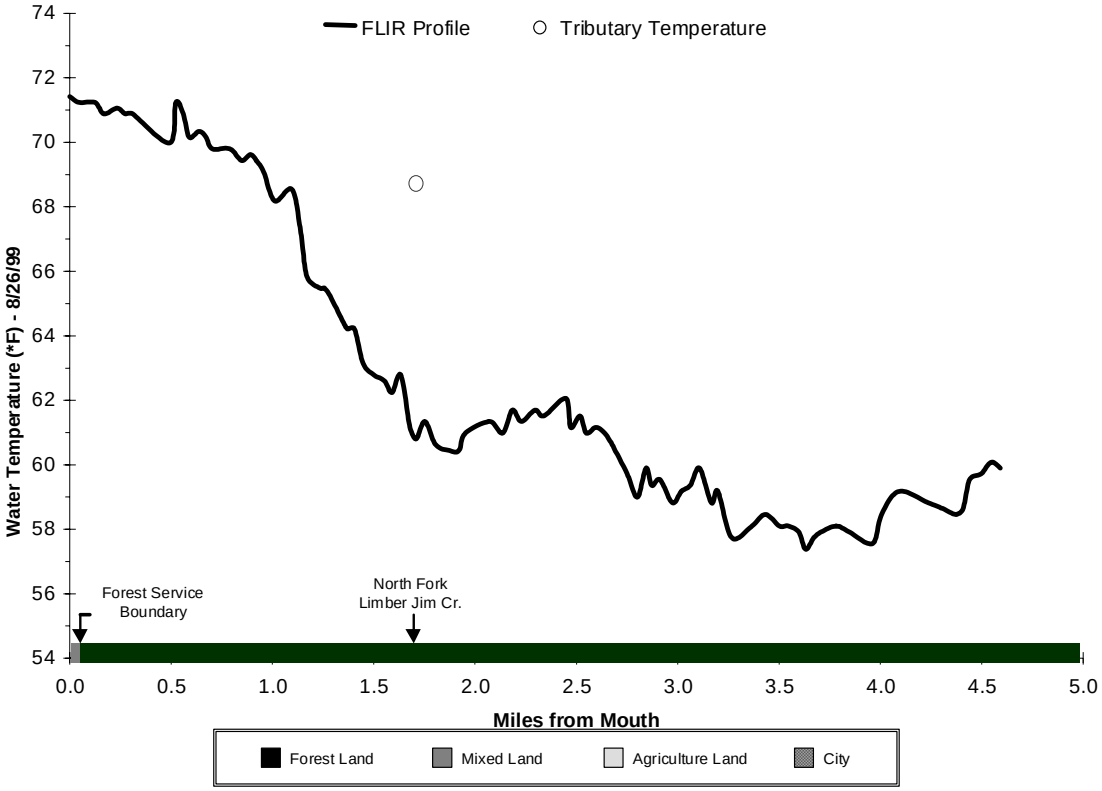

Source Assessment

Overview

Riparian vegetation, stream morphology, hydrology, climate, and geographic location influence stream temperature. While climate and geographic location are outside of human control, riparian condition, channel morphology and hydrology are affected by land use activities. Specifically, the elevated summertime stream temperatures attributed to anthropogenic sources in the Upper Grande Ronde sub-basin result from the following:

1. Riparian vegetation disturbance reduces stream surface shading via decreased riparian vegetation height, width and/or density, thus increasing the amount of solar radiation reaching the stream surface,
2. Channel widening (increased width to depth ratios) increases the stream surface area exposed to energy processes, namely solar radiation,
3. Reduced summertime saturated riparian soils that reduce the overall watershed ability to capture and slowly release stored water, and
4. Reduced summertime base flows may result from instream withdrawals.

Human activities that contribute to degraded water quality conditions in the Upper Grande Ronde sub-basin include timber harvest, as well as road, agriculture and rural and urban residential related riparian disturbances. The relationships between percent effective shade, channel morphology, hydrology and stream temperature are illustrated in **Figure A-21**.

Figure A-21. Stream Heating Processes in the Upper Grande Ronde Sub-basin.

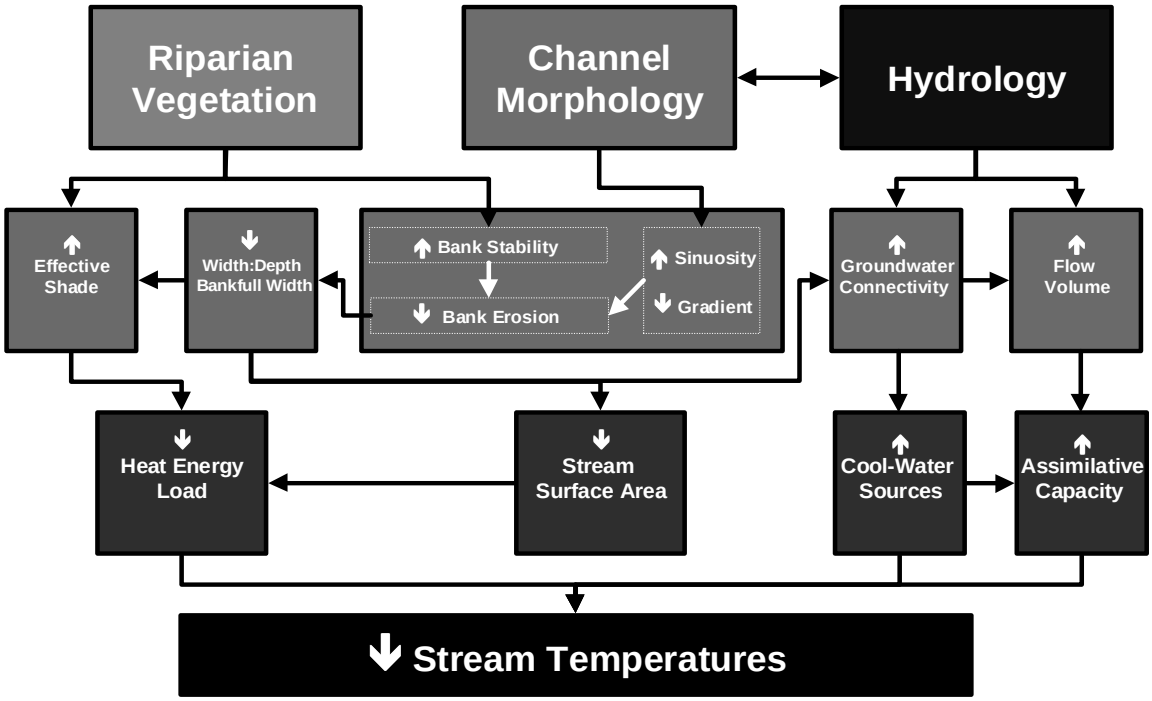

Riparian Vegetation Related to Stream Temperature

Stream Surface Shade

Stream surface shade is a function of several landscape and stream geometric relationships. Some of the factors that influence shade are listed in **Table A-15**. Geometric relationships important for understanding the mechanics of shade are displayed in **Figure A-22**. In the Northern Hemisphere, the earth tilts on its axis toward the sun during summer months, allowing longer day length and higher solar altitude, both of which are functions of solar declination (i.e., a measure of the earth's tilt toward the sun). Geographic position (i.e., latitude and longitude) fixes the stream to a position on the globe, while aspect provides the stream/riparian orientation. Riparian height, width and density describe the physical barriers between the stream and sun that can attenuate and scatter incoming solar radiation (i.e., produce shade). The solar position has a vertical component (i.e., altitude) and a horizontal component (i.e., azimuth) that are both functions of time/date (i.e., solar declination) and the earth's rotation (i.e., hour angle). While the interaction of these shade variables may seem complex, the math that describes them is relatively straightforward geometry, much of which was developed decades ago by the solar energy industry.

Table A-15. Factors that Influence Stream Surface Shade

Description	***Measure***
Season/Time	Date/Time
Stream Characteristics	Aspect, Bankfull Width
Geographic Position	Latitude, Longitude
Vegetative Characteristics	Buffer Height, Buffer Width, Buffer Density
Solar Position	Solar Altitude, Solar Azimuth

Percent effective shade is perhaps the most straightforward stream parameter to monitor/calculate and is easily translated into quantifiable water quality management and recovery objectives. **Figure A-23** demonstrates how effective shade is monitored and calculated. The measured solar load at the stream surface can easily be measured with a Solar Pathfinder© or estimated using mathematical shade simulation computer programs (Boyd, 1996 and Park, 1993).

Figure A-22. Geometric Relationships that Affect Stream Surface Shade

Solar Altitude and **Solar Azimuth** are two basic measurements of the sun's position. When a stream's orientation, geographic position, riparian condition and solar position are known, shading characteristic can be simulated.

Solar Altitude measures the vertical component of the sun's position
Solar Azimuth measures the horizontal component of the sun's position

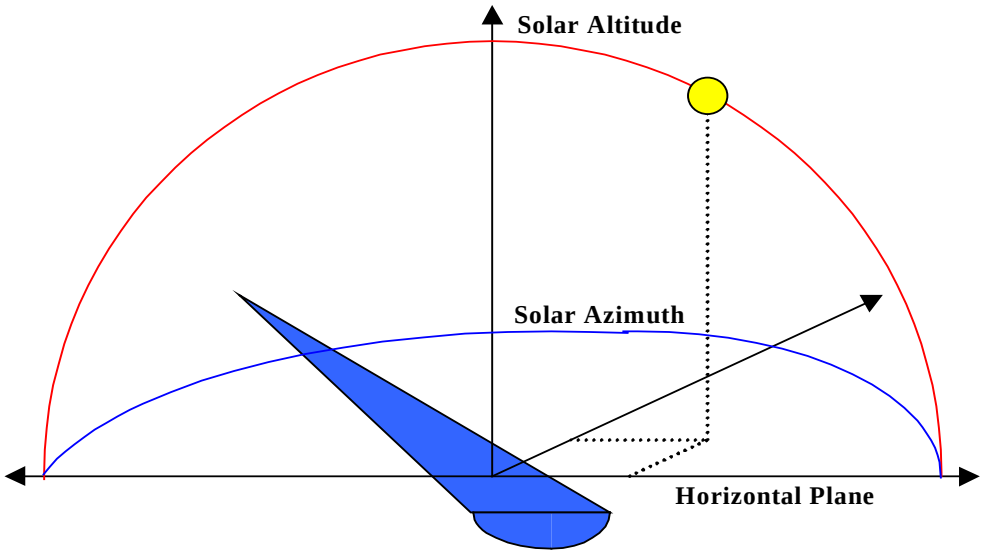

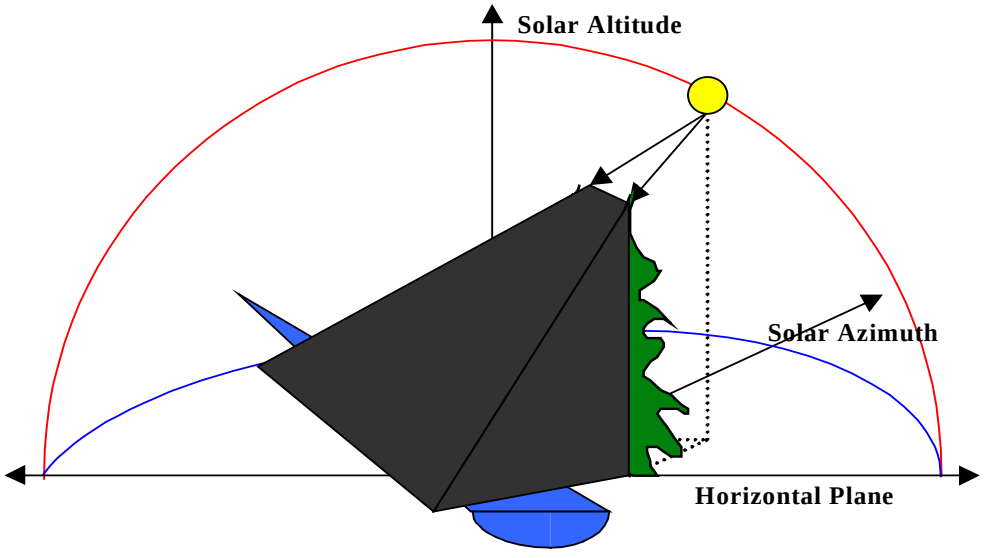

Figure A-23. Effective Shade – Defined

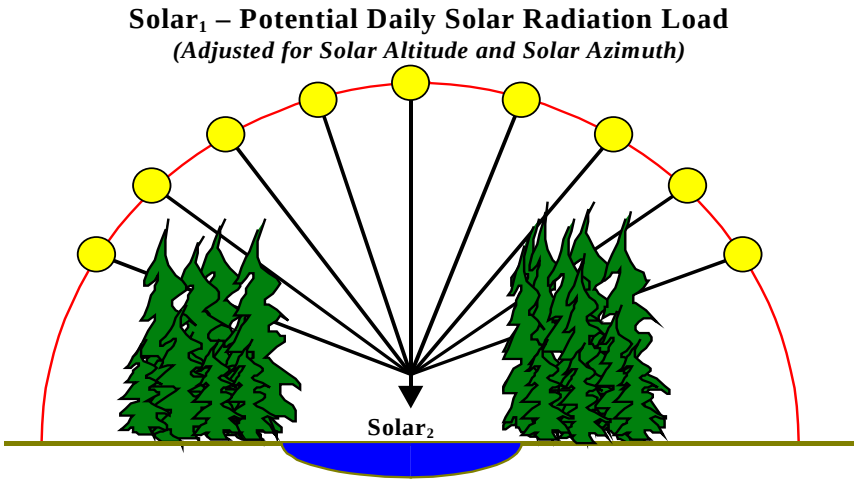

Effective Shade Defined:

$$\text{Effective Shade} = \frac{(\text{Solar}_1 - \text{Solar}_2)}{\text{Solar}_1}$$

Where,

$Solar_1$: Potential Daily Solar Radiation Load
$Solar_2$: Measured Daily Solar Radiation Load at Stream Surface

Thermal Microclimate

FLIR thermal imagery is used to facilitate visual observation of the effects that riparian vegetation, channel morphology, and hydrology have on the stream and surrounding environment. FLIR thermal imagery measures the temperature of the outermost portions of the bodies/objects in the image (i.e., ground, riparian vegetation, stream). **Image A-4** displays FLIR image and its corresponding video image collected in eastern Oregon. Cool surface temperatures within shadows cast by trees are apparent.

Image A-4. Surface Temperaures Within Shade in Northeastern Oregon (McIntosh, 1999).

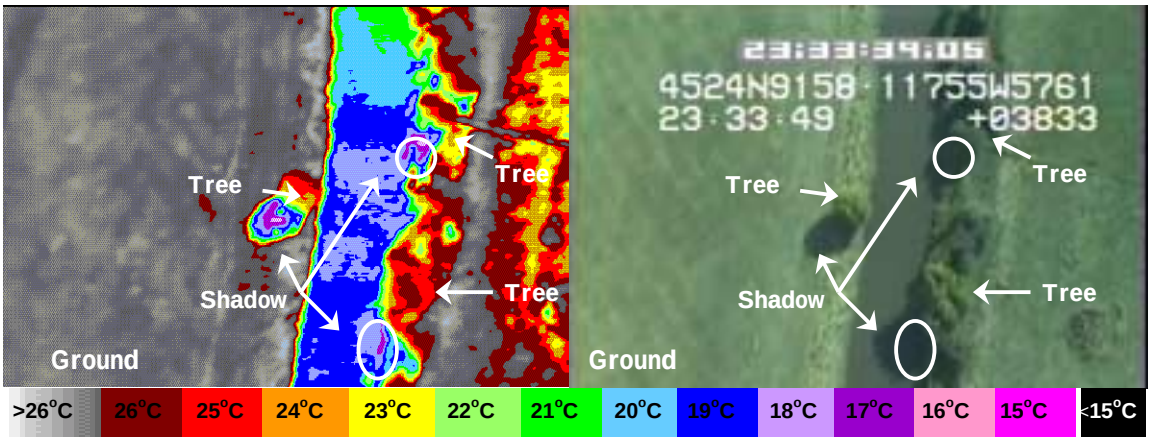

A study of the air temperature gradient between forest stands and adjacent openings has illustrated the significance of thermal microclimates (Geiger, 1965). This study revealed that shade, combined with increased humidity in forest stands, serves to keep air temperatures in the forested area cooler than in adjacent openings during the day. Conversely, at night the forest stand remains warmer than the adjacent opening, due to the greater heat capacity of the humid air and reduced rates of longwave energy loss.

Historic Riparian Vegetation Conditions

The Upper Grande Ronde sub-basin landscape has been drastically altered by human activities since the mid-1800's. Extensive grazing, cultivation, mining, timber harvest, and road development are examples of large-scale disturbances to the riparian vegetation. There is very little quantitative data available to describe the historical vegetation conditions; however, some qualitative descriptions are documented. Undoubtedly, riparian trees and shrubs historically were more abundant than today. The following excerpts from the Upper Grande Ronde Watershed Analysis (USFS, 1994) refer to the sub-basin's historical vegetative conditions:

> "*The UGRR drainage is about two-thirds forested with numerous natural openings. The [National Forest Service] land in the UGRR drainage, prior to widespread timber harvest, was about 80% forested, with numerous small acreages of scablands and meadows. Private ownerships are located at the lower elevations or around meadows. They are primarily on non-forested acreages.*" (Chapter III-66)
>
> "*Verbal accounts indicate that large-scale changes in vegetation occurred as early as the 1870's with the introduction of livestock. According to a local grazing permittee, the Grande Ronde River along Highway 244 used to be so thickly vegetated with cottonwoods and shrubs as to make travel along the river virtually impossible (Wade Sims, La Grande District Fisheries Biologist, pers. Comm., Sept. 1994). According to Bernal Hug's History of Union County (1961), while trying to move logs, which were being floated down Fly Creek, Beaver Creek, and the Grande Ronde, back in the water after being lodged on oxbows, 'there were so many bushes and obstructions for the logs to hang up on that the whole operation was a tedious job'."* (Chapter III-96)

The following are verbatim diary excerpts from Oregon Trail emigrants that describe the Grande Ronde sub-basin before extensive human impact (Evans, 1990):

> Capt. John C. Fremont; October 21, 1843: "*Some of the white spruces which I measured to-day were twelve feet in circumference, and one of the larches ten; but eight feet was the average circumference of those I measured along the road. I held in my hand a tape line as I walked along, in order to form some correct idea of the size of the timber. Their height appeared to be from 100 to 180, and perhaps 200 feet, and the trunks of the larches were sometimes 100 feet without a limb, but the white spruces were generally covered with branches nearly to their root…*"
>
> Rebecca Ketcham, September 6, 1853: "*We had a very fine view of the Grande Ronde after gaining the top of the high hill which led us out of it. This was beautiful indeed, with the river winding through it, all skirted with trees.*"

Finally, the first name for the Grande Ronde Valley was Kup-Kup-Pa, or "Place of the Cottonwood" (Gildemeister 1999).

Current Riparian Vegetation Condition

Through GIS analysis, Hines (1999) determined that riparian populations of black cottonwood (*Populus trichocarpa*) along the Grande Ronde River (near Pierce Lane) have declined in number, aerial extent, and average size (A loss of 45%, 82%, and 70%, respectively) from 1937 to 1987. The author concluded that the evidence suggested that land cover changes in the floodplains was a consequence of intense land-use practices in the upper Grande Ronde River sub-basin, interacting with such natural variations as climate and precipitation. As a result, the temporal requirement for establishing and replenishment of black cottonwood populations are not being met spatially (Hines, 1999).

The condition of the riparian vegetation varies considerably in the Grande Ronde sub-basin. The Grande Ronde Valley bottom has riparian vegetation types composed primarily of annuals (grassy vegetation). However, in some cases where crop cultivation extends to the active channel or where grazing pressure is high, little if any riparian vegetation exists along the Grande Ronde River within the Valley bottom (**Image A-5 and Image A-6**).

Above the City of La Grande, riparian vegetation consists mostly of conifers and hardwoods, with some meadows. **Image A-7** and **Image A-8** illustrate riparian conditions along the Grande Ronde River within the Blue Mountain Range. It is important to point out that less than six river miles separate the two locations illustrated in **Images A-7** and **A-8**.

Image A-9 illustrates riparian conditions within Vey Meadows, while **Image A-10** shows riparian conditions observed immediately upstream of Vey Meadows at the Forest Service boundary. Unlike Vey Meadows, the Grande Ronde River is flowing through a moderately constrained valley upstream of the Forest Service boundary. Riparian areas in the headwater reaches of the Grande Ronde River bear scars of past mining activities. There are numerous mine tailings within the riparian area of this portion of the Grande Ronde River (**Images A-11** and **A-12**). There is also a road in the riparian area (upper left corner of **Image A-12**). Mine tailings and roads within the riparian zone reduce potential vegetation establishment.

Image A-5. Grande Ronde River Downstream Catherine Creek Confluence in August, 1999.

Image A-6. Grande Ronde River within the State Ditch in August, 1999.

Image A-7. Grande Ronde River Downstream of the Fly Creek Confluence (≈ 1 mile). [Ponderosa Pine Heights: 75' to 100']

Image A-8. Grande Ronde River Upstream of the Fly Creek Confluence (≈ 4.5 miles). [Ponderosa Pine Heights: 75' to 100']

Image A-9. Grande Ronde River within Vey Meadows.

Image A-10. Grande Ronde River Upstream Vey Meadows (Forest Service Boundary). [Tree Heights: 90'-100', few 130']

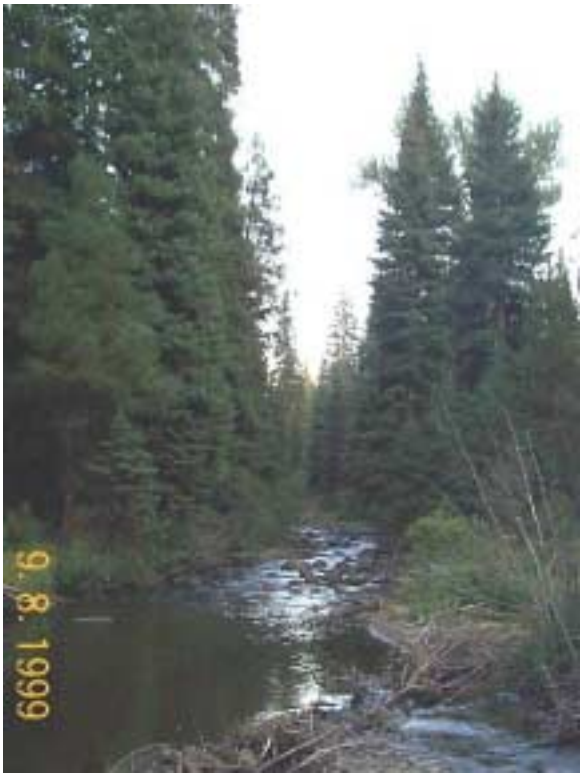

Image A-11. Grande Ronde River Upstream Clear Creek Confluence (Headwaters)
[Tree Height: 30'-40']

Image A-12. Grande Ronde River Upstream Clear Creek Confluence (Headwaters).

The United States Environmental Protection Agency (USEPA, 1993) created a high-resolution riparian vegetation map of the Upper Grande Ronde River and its tributaries. A 2,000-foot wide corridor centered on the river was digitally mapped using aerial photograph interpretation and Landsat thermal satellite imagery. Individual riparian communities, based on dominant species, height, and canopy density were identified and delineated as polygons. Riparian classification was based upon the principles of "Wetlands and Deepwater Habitats Classification System" (Cowardin et al., 1979), which was modified to cover uplands as well as wetlands. Riparian vegetation classifications, based on this analysis, are spatially presented in **Figure A-24**.

Figure A-24. Riparian Vegetation Classification within the Upper Grande Ronde Sub-basin (USEPA, 1993)

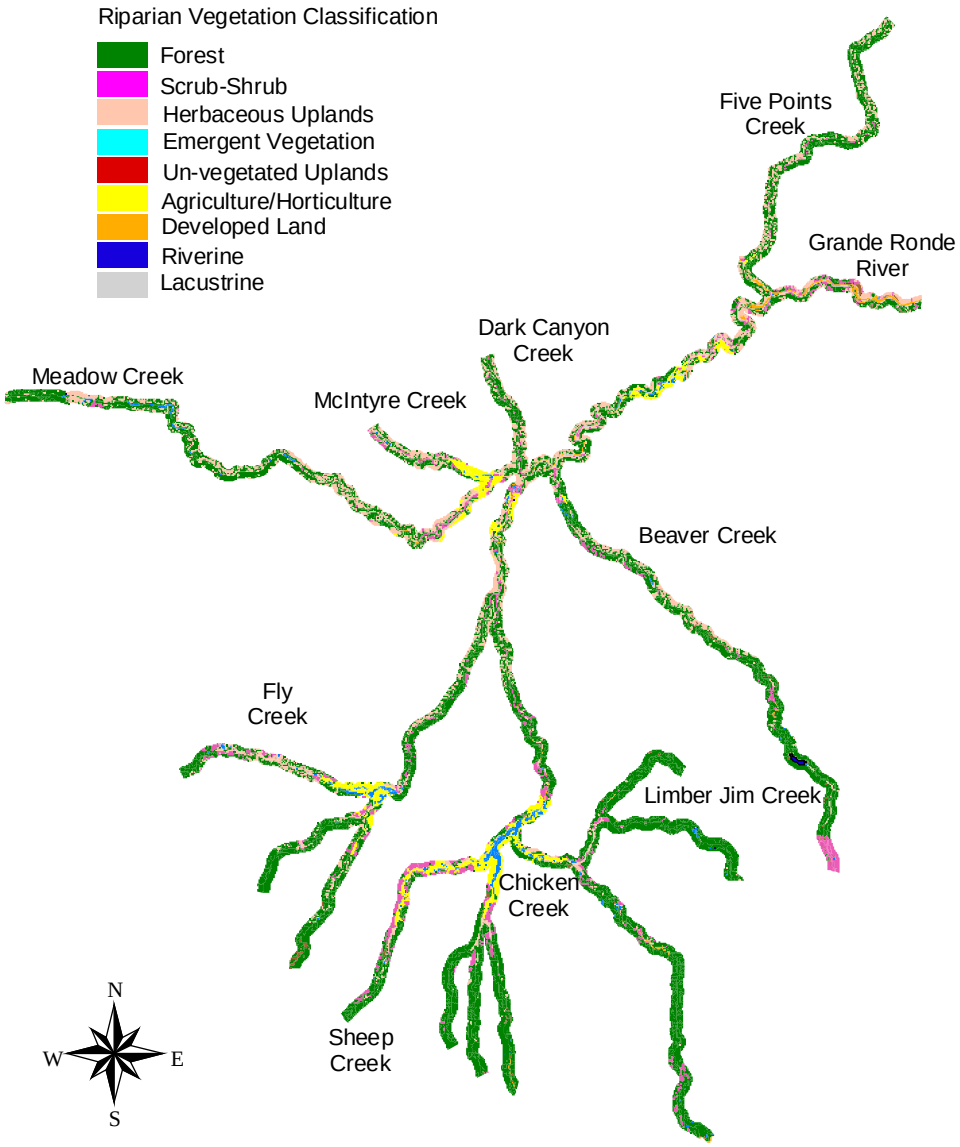

Low shade levels result from a combination of lack of streambank vegetation and/or wide stream channels. **Figure A-25** presents effective shade levels and **Figure A-26** displays vegetation heights along the Grande Ronde mainstem. It is apparent that in many cases, low shade levels result from lack of tall streambank vegetation. However, many areas that do have tall streambank vegetation have low shade levels. In these cases, channel widths are too great to effectively shade. An example of wide channels reducing shade levels in the Grande Ronde River is located between the River Mile 97 and Rondowa (RM 82).

Effective shade levels experienced on the Grande Ronde mainstem range between 0% and 91% Averaged over three miles lengths effective levels range between 0% and 50%. Shading levels are highest on forest service lands above and below Vey Meadows. Vey Meadows has low shade levels, as do private lands from the lower Forest Service boundary to the confluence with the Wallowa River.

Potential Riparian Vegetation Conditions

Terms Used:

- *Composite Dimension*: The average potential maximum height of tree species occurring within a given physiographic unit.
- *Fluvial Surface*: The various land surfaces associated with the riparian zone such as active and inactive floodplains, active channel terraces, alluvial bars, streambanks, and overflow channels.
- *Physiographic Units*: Crowe and Clausnitzer (1997) simplified sub-regions developed by Clarke and Bryce (1997) to physiographic units comprised of similar wetland/riparian plant associations (**Figure A-27**).
- *Plant Association*: “An assemblage of native vegetation in equilibrium with the environment on a specific fluvial surface” (Kovalchik 1987). Environmental changes occurring at the growing area will result in changes to the plant assemblage.
- *Riparian Vegetation*: Vegetation that grows within the valley of, and is hydrologically influenced by, a stream or river.
- *Rosgen Stream Types*: Stream types classified using the Rosgen stream typing classification system (Rosgen, 1996) are based upon valley morphology, channel form, and substrate.
- *Valley Grad.*: “Valley Gradient”; the percent slope of the valley, which can be calculated by dividing the change in elevation by the valley length.
- *Valley Morph*.: “Valley Morphology”; refers to the general shape of the river valley.
- *Wetland*: An area having on of the three following attributes: (1) at least periodically the substrate is dominated by facultative or obligate hydrophytes; (2) the substrate is predominantly hydric soil; (3) the substrate is non-soil and is either saturated with or covered by shallow water at some time during the growing season (Clausnitzer and Crowe, 1997).

Figure A-25. Longitudinal Grande Ronde River Effective Shade Levels

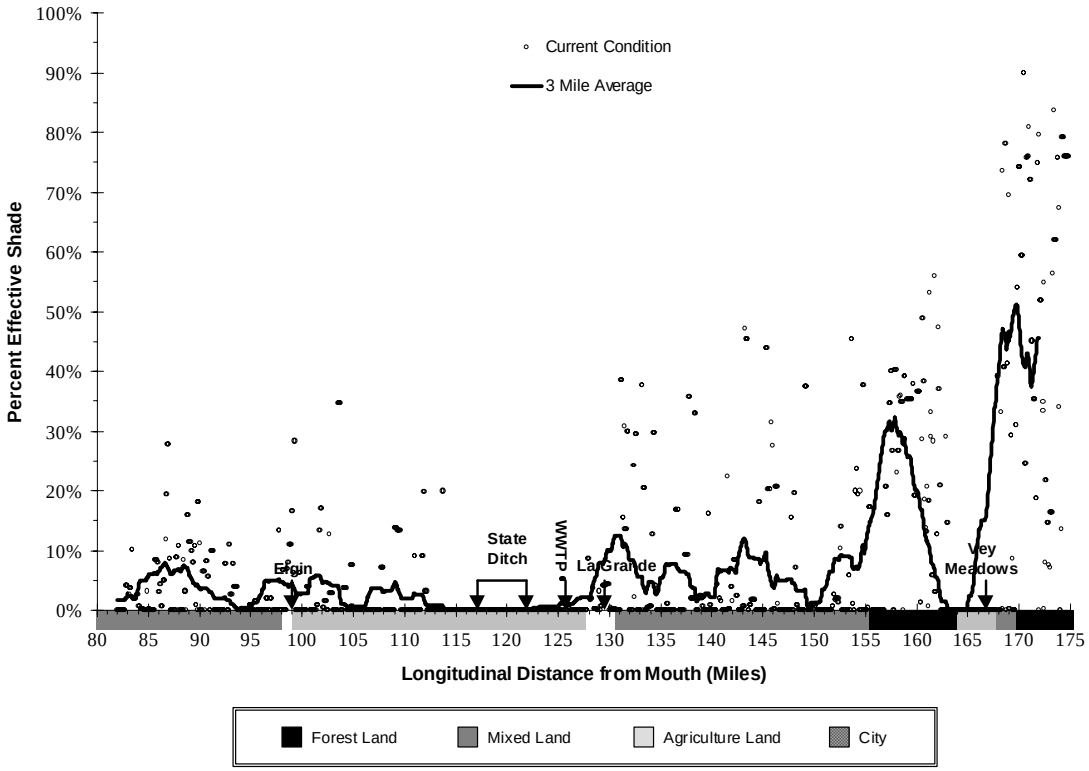

Figure A-26. Longitudinal Grande Ronde River Riparian Vegetation Height

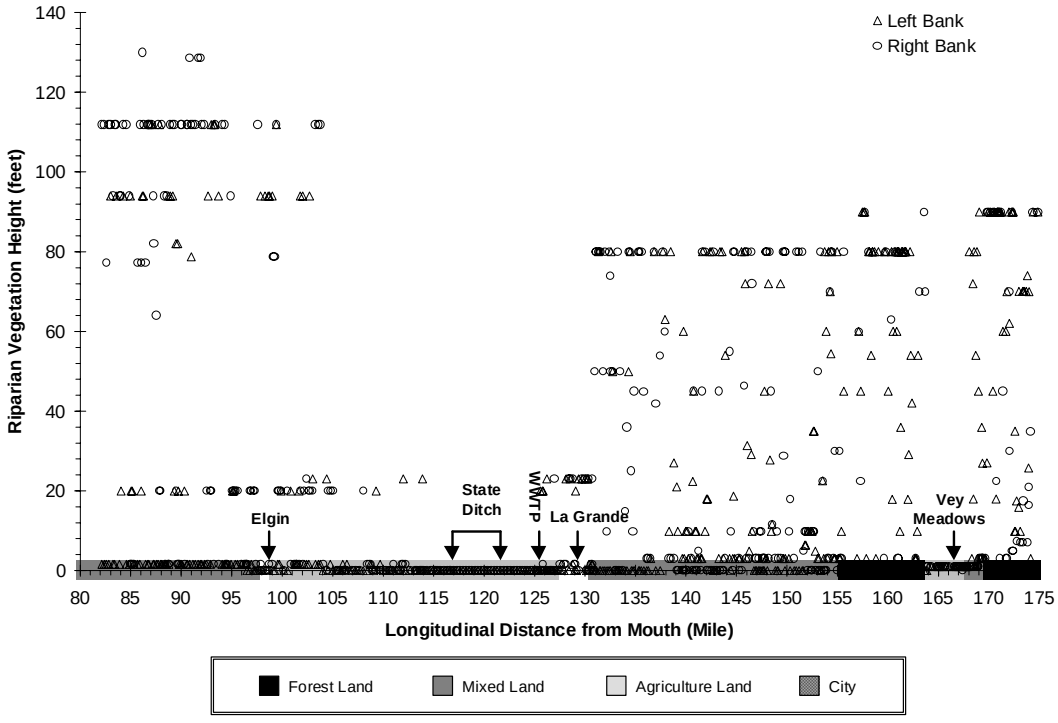

Figure A-27. Physiographic Units of the Upper Grande Ronde Sub-basin (Clausnitzer and Crowe, 1997)

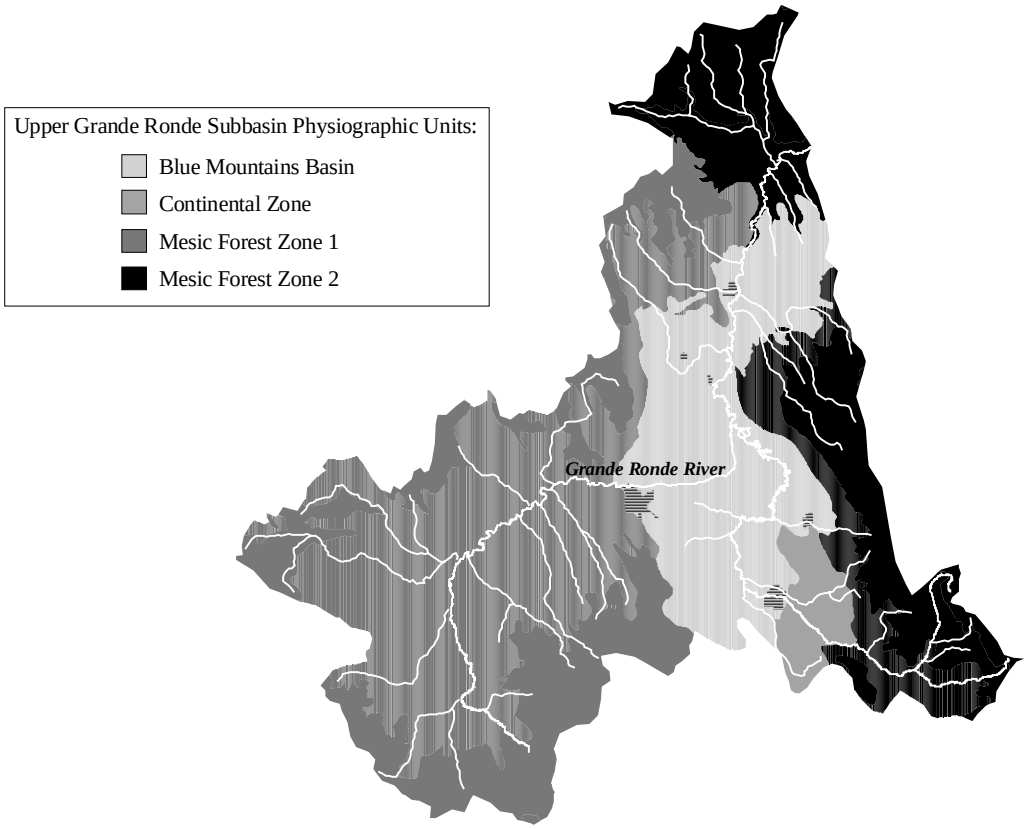

Species Characterization

This section describes some of the dominant riparian species native to the greater Blue Mountain region, as documented by the United States Department of Agriculture Forest Service in "Mid-Montane Wetland Plant Associations of the Malheur, Umatilla and Wallowa-Whitman National Forests" (Clausnitzer and Crowe, 1997). Where available, mature height (H) and mature diameter at breast height (DBH) are provided.

Engelmann Spruce (Picea engelmannii)

H: 80-100 feet

DBH: 1.5-2.5 feet

Comments: Dominant with Subalpine Fir in subalpine zone up to timberline; also with other conifers. Prefers long cold winters and short cool summers. Can stand high water tables, but only if aerated (like in a floodplain as opposed to wet meadows). Requires moderately deep, loamy sands and silts, well-drained soils.

Ponderosa Pine (*Pinus ponderosa*)

H: 60-130 feet

DBH: 2.5-4 feet

Comments: Widespread. Commonly, only dominant tree species; occurs with shrubs, grasses, sedges, or herbaceous understory. Occupies warmer and dryer sites than other tree-plant associations mentioned in Clausnitzer and Crowe (1997). Good fire resistance due to high branches, thick bark, deep roots, and high moisture content of foliage. Low livestock palatability.

Lodgepole Pine (*Pinus contorta*)

H: 20-80 feet

DBH: 1-3 feet

Comments: There are three geographic varieties. They typically occur in cold air drainages where frost occurs in the interior Blue Mountains. Requires less water than Engelmann spruce and subalpine fir. It has low palatability to ungulates/livestock, except sheep may browse the branch ends.

Western Larch (*Larix occidentalis*)

H: 80 to 150 feet

DBH: 1.5 to 3 feet

Comments: Very large deciduous tree (needle-leaved) on mountain slopes and valleys on porous, gravelly, sandy, and loamy soils; with other conifers. Often follows or survives fires.

Subalpine Fir (*Abies lasiocarpa*)

H: *

DBH: 10-20 inches at 150-200 years of age

Comments: Grows in cold, humid climates. Very shade tolerant. Often codominant with Engelmann spruce on cool, moist floodplains. Most late seral riparian stands are mixed age due to fire, insects, disease, windthrow, and flood events.

Grand Fir (*Abies grandis*)

H: 115-150 feet

DBH: *

Comments: Blue Mountains where temperatures average 43-50°F. Elevations 1500-6000 feet. Very shade tolerant. More fire resistant than subalpine fir, Engelmann spruce, and lodgepole pine, but less resistant than western larch, ponderosa pine, and Douglas fir.

Douglas Fir (*Pseudotsuga menziesii*)

H: 100-120 feet at 200-300 years of age (can reach 160 feet)

DBH: 15-40 inches (can reach 60 inches dbh)

Comments: Wide variety of climatic conditions. More fire resistant than Engelmann spruce and true firs, but less resistant than ponderosa pine and western larch. Low palatability to livestock.

Quaking Aspen (*Populus tremuloides*)

H: 66-82 feet

DBH: 7-12 inches dbh

Comments: Intolerant to excessive heat and shade. Grows on Alfisols, Inceptisols, Andisols, and Mollisols. Intolerant to acidic and sandy soils. Typically grow in clonal colonies – lateral root propagation.

Red Alder (*Alnus rubra*)

H: 100-130 feet at maturity

DBH: *

Comments: Grows in humid climates characterized by cool, wet winters and warm, dry summers. Found in the Blue Mountains in the Walla Walla Ranger District (Umatilla NF).

Black Cottonwood (*Populus trichocarpa*)

H: 30-55 feet at sexual maturity (7-10 years of age), max height up to 120 feet.

DBH: 5-8 inches dbh

Comments: Grows in a variety of climates, from relatively arid to humid. In the Blue Mountains, typically found at 3500-4000 feet. Full sunlight required for germination. Black cottonwood rooted or unrooted cuttings can usually be successfully planted. Very flood tolerant, thus an alluvial bar colonizer. Mature stand density is 270-730 trees per acre. Lives 100-200 years. Occur in association with Pacific willow on alluvial deposits. Also grows well in unsaturated floodplains. Overuse of cottonwood populations by livestock is a common problem in the Blue Mountain Province. Enhances fish habitat by stabilizing stream banks and by providing shade and large woody debris.

Willow Spp. (*Salix spp.*)

H: *

DBH: *

Comments: Three general ecological categories, (1) "cold" group includes undergreen, Eastwood, and Tweedy's, (2) "general" group includes Geyer, Booth, Lemmon, Bebb, and occasionally the rigid willow, and (3) "alluvial bar" group includes rigid willow, Pacific, and coyote willow. All can propagate vegetatively from broken root or stem pieces.

Mountain Alder/Sitka Alder (*Alnus incana/Alnus sinuata*)

H: Mountain = 30-40 feet, Sitka = 10-15 feet

DBH: *

Comments: Probably the most abundant and widespread riparian shrub on National Forest lands in the Blue Mountain province. Sitka Alder fills the niche in higher elevations in some areas.

Shrub Types (Dominant Species in Shrub Communities)

Currants (*Ribes spp.*) -Narrow V-shaped, steep canyons in Northern Blue Mountains.

Red-osier Dogwood (*Cornus stolonifera*): Generally narrow, V-shaped canyons with 2-10% gradient. Average 8 feet tall.

Black Hawthorn (*Crataegus douglasii*): Low to moderate elevations. Infrequently flooded sites, water table 2-5 feet in summer. Appear to be disturbance induced communities.

Mountain Big Sagebrush (*Artemisia tridentata ssp.*): In broad trough shaped or flat valleys. Moderately dense to dense shrub canopy 3 feet tall over an herbaceous understory. Adjacent upland vegetation includes: terraces – low sagebrush; side slopes – big sagebrush, Idaho fescue, and ponderosa pine.

Vegetation Communities by Physiographic Units

Tables A-16, A-17, and **A-18** list the various plant associations that have been found to grow within the different physiographic units (Clausnitzer and Crowe, 1997). Each physiographic unit has been further broken down by valley slope and elevation. Plant associations are listed according the fluvial surface that they have been identified on. Finally, the corresponding Rosgen stream types (Rosgen 1996) are shown in the last column.

Table A-16. Continental Zone and Blue Mountain Zone (from Clausnitzer and Crowe, 1997)

Valley Morph.	Valley Grad.	Elevation (feet)	Fluvial Surface	Soil Grain Size / Moisture Content	Plant Associations	Rosgen Stream Type
Flat Trough Shaped	<2%	3,000 - 6,000	Alluvial Bars	Sand/Gravel/Cobble	Creeping spikerush Common horsetail Coyote willow Rigid willow Black cottonwood/Pacific willow	-- B2/B3/B4/C4 B3/C3/C4/D3 C3/B3 C3/C4/D3
			Floodplain	Silt Saturated Soils	Aquatic sedge Bladder sedge Inflated sedge	C3/C4/C5/E4/E5/E6 C3/C4/E3/E4/E6/F6 --
				Silt Partially Saturated Soils	Wooly sedge Tufted hairgrass Silver sagebrush/Tufted hairgrass Shrubby cinquefoil/Tufted hairgrass	C3/C4/E4/E6 C4/C6/E6 E/F E4/E6
				Silt Unsaturated Soils	Quaking aspen/Common snowberry Ponderosa pine/Common snowberry	F3/F6 B3/B4B5/C3/C4/E3/F4
				Gravel/sand/Silt/Clay Saturated Soils	Willow/Bladder sedge Willow/Aquatic sedge Mountain alder/Bladder sedge	C5/C6/E4/E5/E6 C4/C5/E4/E5/E6/F6 --
				Gravel/sand/Silt/Clay Partially Saturated Soils	Willow/Woolly sedge	E3/E4/E6/C4/F4/F6
				Gravel/sand/Silt/Clay Unsaturated Soils	N/A	--
			Terraces	All	Quaking Aspen/Common Snowberry Black Cottonwood/Common Snowberry Ponderosa Pine/Common Snowberry Douglas Fir/Common Snowberry	F3/F6 B2/B3/C4/D3 B3/B4/B5/C3/C4/E3/F4 B3/C2/C3/F4
V-Shaped	2% to 4%	3,000 - 6,000	Alluvial Bars	Sand/Gravel/Cobble	Common horsetail	B2/B3/B4/C4
			Floodplain	All	Mountain alder/Red-osier dogwood/Mesic Forb Mountain alder/Common snowberry Mountain alder/Common horsetail Mountain alder/Tall mannagrass Red-osier dogwood	B2/B3/B4 A3/B2/B3/B4/C4 B2/B3/C3/E5 A3/A4/A5/B2/B3/B4 A2/A4/A5/B2/B3
			Terraces	All	Ponderosa pine/Common snowberry Douglas fir/Common snowberry	B3/B4/B5/C3/C4/E3/F4 B3/C2/C3/F4
	>4%	3,000 - 6,000	Streambank	Sand/Gravel/Cobble	Mountain alder/Mesic forbs Mountain alder/Tall mannagrass	A3/A4/B3/B4/C4 A3/A4/A5/B2/B3/B4

Table A-17. Mesic Forest Zone 1 (from Clausnitzer and Crowe, 1997)

Valley Morph.	Valley Grad.	Elevation (feet)	Fluvial Surface	Soil Grain Size / Moisture Content	Plant Associations	Rosgen Stream Type
Broad Valleys	<1%	2,500 - 4,800	Alluvial Bars	Sand/Gravel/Cobble	Torrent sedge Common horsetail Coyote willow Rigid willow Black/Cottonwood/Pacific willow	-- B2/B3/B4/C4 B3/C3/C4/D3 C3/B3 C3/C4/D3
			Floodplain	All	Small-fruit bulrush Mountain alder/Red-osier dogwood/Mesic forb Mountain alder/Dewey's sedge Mountain alder/Bladder sedge Red-osier dogwood Willow/Mesic forb Black cottonwood/Mountain alder/Red-osier dogwood Quacking aspen/Common snowberry Quaking aspen/Mesic forb	B3/B4/C3/C4/E6 B2/B3/B4 B2/B3/B4/C3 C4/C5/E5/E6 A2/A4/A5/B2/B3 -- B3/B4/C3/C5 F3/F6 --
			Terraces	All	Black cottonwood/Common snowberry Quaking aspen/Common snowberry Ponderosa pine/Common snowberry Douglas fir/Common snowberry Grand fir/Common snowberry	B2/B3/C4/D3 F3/F6 B3/B4/B5/C3/C4/E3/F4 B3/C2/C3/F4 --
		4,000 - 7,500	Streambank	All	Mountain alder/Currant	A3/A4/B3/B4/C4
			Floodplain	Saturated Soils	Sedge Bladder sedge Inflated sedge Densely-tufted sedge Holm's sedge Few-flowered spikerush	C3/C4/C5/E4/E5/E6 C3/C4/E3/E4/E6/F6 -- C4 B3/B4/E5/E6 --
				Partially Saturated Soils	Bluejoint reedgrass Tufted hairgrass Sheldon's sedge Swamp onion Lodgepole pine/Aquatic sedge	C3/C4/E4/E5/E6 C4/C6/E6 -- -- E4
				Unsaturated Soils	Lodgepole pine/Tufted hairgrass	E5
			Terraces	All	Lodgepole pine/Tufted hairgrass	E5

Table A-17. (Continued) Mesic Forest Zone 1 (from Clausnitzer and Crowe, 1997)

Valley Morph.	Valley Grad.	Elevation (feet)	Fluvial Surface	Soil Grain Size / Moisture Content	Plant Associations	Rosgen Stream Type
V-Shaped	2%-4%	3,000 - 4,800	Alluvial Bars	Sand/Gravel/Cobble	Arrowleaf groundsel Tall mannagrass Common horsetail	A3/B5/C4 B2/B3/B4/C4 B2/B3/B4/C4
			Floodplain and Terrace	Sand/Gravel/Cobble	Mountain alder/Red-osier dogwood/Mesic forbs Mountain alder/Common horsetail Mountain alder/Ladyfern Mountain alder/Tall mannagrass Mountain alder/Dewey's sedge Sitka alder/Drooping woodreed Grand fir/Rocky mountain maple Grand fir/Ladyfern	B2/B3/B4 B2/B3/C3/E5 B3/B4/B5/A3/C3/E6 A3/A4/A5/B2/B3/B4 B2/B3/B4/C3 A2/A3/B3 A2a/A4/B2/B3/B4/C3 B3/B4
	>4%	4,500 - 7,000	Streambank	Sand/Gravel/Cobble	Mountain alder/Currants/Mesic forbs Mountain alder/Ladyfern Subalpine fir/Arrowleaf groundsel Engelmann spruce/Arrowleaf groundsel	A3/A4/B3/B4 B3/B4/B5/A3 A4/B4/B4c A2/C3

Table A-18. Mesic Forest Zone 2 (from Clausnitzer and Crowe, 1997)

Valley Morph.	Valley Grad.	Elevation (feet)	Fluvial Surface	Soil Grain Size / Moisture Content	Plant Associations	Rosgen Stream Type
Broad Valley	<1%	<4,800	Alluvial bar	Sand/Gravel/Cobble	Common horsetail Coyote willow Rigid willow Black cottonwood/Pacific willow Red alder/Alluvial bar	B2/B3/B4/C4 B3/C3/C4/D3 C3/B3 C3/C4/D3 B3
			Floodplain	Sand/Gravel/Cobble	Mountain alder-Red-osier dogwood/Mesic Forb Mountain alder/Dewey's sedge Red-osier dogwood Black Hawthorn Black Cottonwood/Mountain alder/Red-osier dogwood Black Cottonwood/ Rocky Mountain maple Quaking aspen/Common snowberry Quaking aspen/Mesic Forb Red alder/Pacific ninebark Grand fir/Common snowberry – Floodplain Grand fir/Rocky Mountain maple – Floodplain	B2/B3/B4 B2/B3/B4/C3 A2/A4/A5/B2/B3 B3/B4/C3/G3/F4 B3/B4/C3/C5 A2/B2/C3/C4 F3/F6 -- B2/B3/B4 -- A2a/A4/B2/B3/B4/C3
			Terraces	Sand/Gravel/Cobble	Black hawthorn Black cottonwood/Common snowberry Ponderosa pine/Common snowberry – Floodplain Douglas fir/Common snowberry – Floodplain Grand fir/Common snowberry – Floodplain Grand fir/Rocky Mountain maple – Floodplain	B3/B4/C3/G3/F4 B2/B3/C4/D3 B3/B4/B5/C3/C4/E3/F4 B3/C2/C3/F4 -- A2a/A4/B2/B3/B4/C3
		>4,800	Streambank	Silt/Sand	Mountain alder-Currants/Mesic Forb	A3/A4/B3/B4/C4
			Floodplains	Silt/Sand Saturated Soils	Sedges/rushes	E
				Silt/Sand Partially Saturated Soils	Sedges/rushes/lodgepole pine	E
				Silt/Sand Unsaturated soils	Lodgepole pine/Tufted hairgrass	E
			Terraces	Silt/Sand	Lodgepole pine/Tufted hairgrass	E

Table A-18. (Continued) Mesic Forest Zone 2 (from Clausnitzer and Crowe, 1997)

Valley Morph.	Valley Grad.	Elevation (feet)	Fluvial Surface	Soil Grain Size / Moisture Content	Plant Associations	Rosgen Stream Type
V-Shaped	2-4%	3,000 - 4,800	Alluvial bars	All	Arrowleaf groundsel	A3/B5/C4
					Tall mannagrass	B2/B3/B4/C4
					Common horsetail	B2/B3/B4/C4
			Floodplain	All	Mountain alder-Red-osier dogwood/Mesic Forb	B2/B3/B4
					Mountain alder/Common horsetail	B2/B3/C3/E5
					Mountain alder/Ladyfern	B3/B4/B5/A3/C3/E6
					Mountain alder/Dewey's sedge	B2/B3/B4/C3
					Mountain alder/Tall mannagrass	A3/A4/A5/B2/B3/B4
					Sitka alder/Ladyfern	A2/A3/A4/B2/B3/B4
					Sitka alder/Drooping woodreed	A2/A3/B3
					Sitka alder/Mesic Forb	B3
					Black cottonwood/Rocky Mountain maple	A2/B2/C3/C4
					Engelmann spruce/Ladyfern	A3/B3/C2/C4
					Engelmann spruce/Arrowleaf groundsel	A2/C3
					Douglas fir/Rocky Mountain maple-Mallow ninebark-Floodplain	A2a/A3/A5/C3/C4
					Grand fir/Rocky Mountain maple-Floodplain	A2a/A4/B2/B3/B4/C3
					Grand fir/Oakfern	A2/A3/B3/B4/F4
			Terraces	All	Grand fir/Rocky Mountain maple - Floodplain	A2a/A4/B2/B3/B4/C3
	>4%	4,500 - 7,000	Stream banks	All	Arrowleaf groundsel	A3/B5/C4
					Currants/Tall mannagrass	A3/A4/B3
					Currants/Mesic Forb	A4/A5/C3/C4
					Mountain alder-Currants/Mesic Forb	A3/A4/B3/B4/C4
					Mountain alder/Tall mannagrass	A3/A4/A5/B2/B3/B4
					Sitka alder/Ladyfern	A2/A3/A4/B2/B3/B4
					Sitka alder/Drooping woodreed	A2/A3/B3
					Engelmann spruce/Ladyfern	A3/B3/C2/C4
					Subalpine fir/Ladyfern	A4/A6/B3

Composite Vegetation Dimensions by Physiographic Unit

Woody riparian species native to the Upper Grande Ronde sub-basin, and their respective potential heights are listed in **Table A-19** (Clausnitzer and Crowe, 1997). Potential mature vegetation densities have been assumed to be 80%.

Table A-19. Composite Vegetation Dimensions By Physiographic Unit

Physiographic Unit	Elevation (feet)	Potential Terrace/Streambank Overstory Vegetation	Height[1] (feet)	Assumed Density
Continental Zone and Blue Mountain Sub-basin Zone	All	Quaking Aspen Black cottonwood Ponderosa Pine Douglas fir Mountain alder **Composite Dimension**	70 100 125 140 40 **95**	**80%**
Mesic Forest Zone 1	<4,800	Quaking Aspen Black cottonwood Ponderosa Pine Douglas fir Grand fir **Composite Dimension**	70 100 125 140 125 **112**	**80%**
	>4,800	Lodgepole pine Subalpine fir Engelmann spruce **Composite Dimension**	50 40 80 **57**	**80%**
Mesic Forest Zone 2	<4,800	Black cottonwood Ponderosa pine Douglas fir Grand fir Engelmann spruce **Composite Dimension**	100 125 140 125 80 **114**	**80%**
	>4,800	Lodgepole pine Subalpine fir Engelmann spruce **Composite Dimension**	50 40 80 **57**	**80%**

[1] Vegetation heights from Clausnitzer and Crowe, 1997

Black Cottonwood Potential in the Grande Ronde Valley Bottom

The Oregon Department of Agriculture (ODA) has suggested potential heights for black cottonwoods (*Populus trichocarpa*) along the Grande Ronde River within agricultural areas (**Table A-20**). Assumptions were based on *Silvics of North American Trees*[2] and a soils map of the Grande Ronde valley. Potential black cottonwood height depends upon riparian soil characteristics, thus ODA has given three site classifications based upon existing soils:

1. Category 1,
2. Category 2,
3. Category 3.

It is recognized that regeneration of black cottonwoods in the Grande Ronde valley is not likely to occur without artificial planting, weeding, and watering for the first two years.

Table A-20. Potential Black Cottonwood Heights in the Grande Ronde River Valley

Location	Site Classification	Percentage of Bank	Potential Height (ft)
Island City to Head of State Ditch	1	35%	140
	2	50%	97
	3	15%	70
	Average Potential Black Cottonwood Height⇒		108
State Ditch	1	25%	140
	2	12.5%	97
	3	62.5%	70
	Average Potential Black Cottonwood Height⇒		91
Bottom of State Ditch to Imbler	1	20%	140
	2	50%	97
	3	30%	70
	Average Potential Black Cottonwood Height⇒		98
Imbler to Rhinehart	1	3%	140
	2	85%	97
	3	12%	70
	Average Potential Black Cottonwood Height⇒		95

[2] Burns, R. M. and B. H. Honkala (1990). Silvics of North American Trees. Vol2, Hardwoods. Washington, D.C., U.S. Department of Agriculture.

Channel Morphology Related to Stream Temperature

Channel Width

Changes in channel morphology (namely channel widening) impact stream temperatures. As a stream widens, the surface area exposed to radiant sources and ambient air temperature increases, resulting in increased energy exchange between the stream and its environment (Boyd, 1996). Further, wide channels are likely to have decreased levels of shade due to simple geometric relationships between riparian height and channel width. Conversely, narrow channels are more likely to experience higher levels of shade. An additional benefit inherent to narrower/deeper channel morphology is a higher frequency of pools that contribute to aquatic habitat or cold water refugia.

The width to depth ratio is a fundamental measure of channel morphology. High width to depth ratios (greater than 10.0) imply wide shallow channels, while low width to depth ratios (less than 10.0) suggest that the channel is narrow and deep. The PACFISH target for width to depth ratio is 10.0 (USFS, 1995). In terms of reducing stream surface exposure to radiant energy sources, it is generally favorable for stream channels to be narrow and deep (low width to depth ratios).

Stream Bank Stability and Riparian Vegetation

Stream bank erosion recovery processes require the simultaneous occurrence of two elements that induce stream bank building: protect stream banks from kinetic energy (bank particle cohesion) and reduce kinetic energy (stream bank/flood plain roughness). High levels of stream bank cohesion tend to protect the stream bank from erosive kinetic energy associated with flowing water. Stream bank erosion reflects looseness of bank soil, rock and organic particles. The opposite condition is cohesion of stream bank soil, rock and organic particles. Vegetation strengthens particle cohesion by increasing rooting strength that helps bind soil and add structure to the stream bank. Different riparian vegetation communities (annual, perennial, deciduous, mixed and conifer dominated) offer a variety of rooting strengths to stream banks. It is a general observation that healthy/intact indigenous riparian vegetation communities will add preferable stream bank cohesion over bare soil/ground conditions.

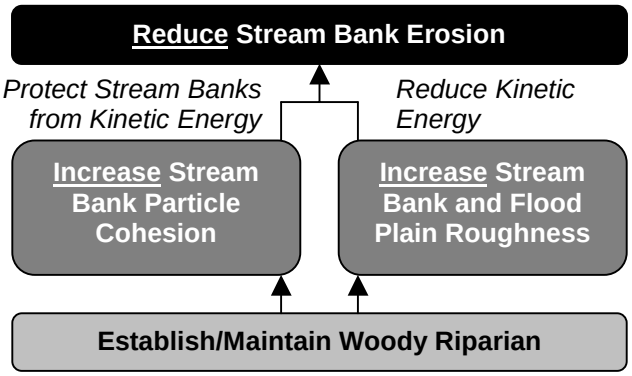

Physical relationships that relate to decreasing/preventing stream bank erosion can be summarized as:

1. Rough surfaces decrease local flow velocity,
2. Reduced local velocity lowers shear stress acting on the stream bank,
3. Lower shear stress acting on the stream bank will be less likely to detach and entrain stream bank particles.

In an effort to control stream bank erosion processes, the focus then becomes to retain high stream bank and flood plain roughness via riparian vegetation. The species composition and condition of the riparian vegetation determines natural stream bank roughness. Values of roughness (Manning's n) correspond to various riparian conditions (**Figure A-28**). In essence, the roughness coefficients help explain the relationship between riparian vegetation types and active stream bank erosion:

- Highest stream bank erosion rates correspond with annual/perennial riparian vegetation types that have a low Manning's n (roughness coefficient)
- Low stream bank erosion rates correspond with woody riparian vegetation types that have a high Manning's n (roughness coefficient).

Figure A-28. Manning's n (Roughness Coefficient) Related to Riparian Vegetation.

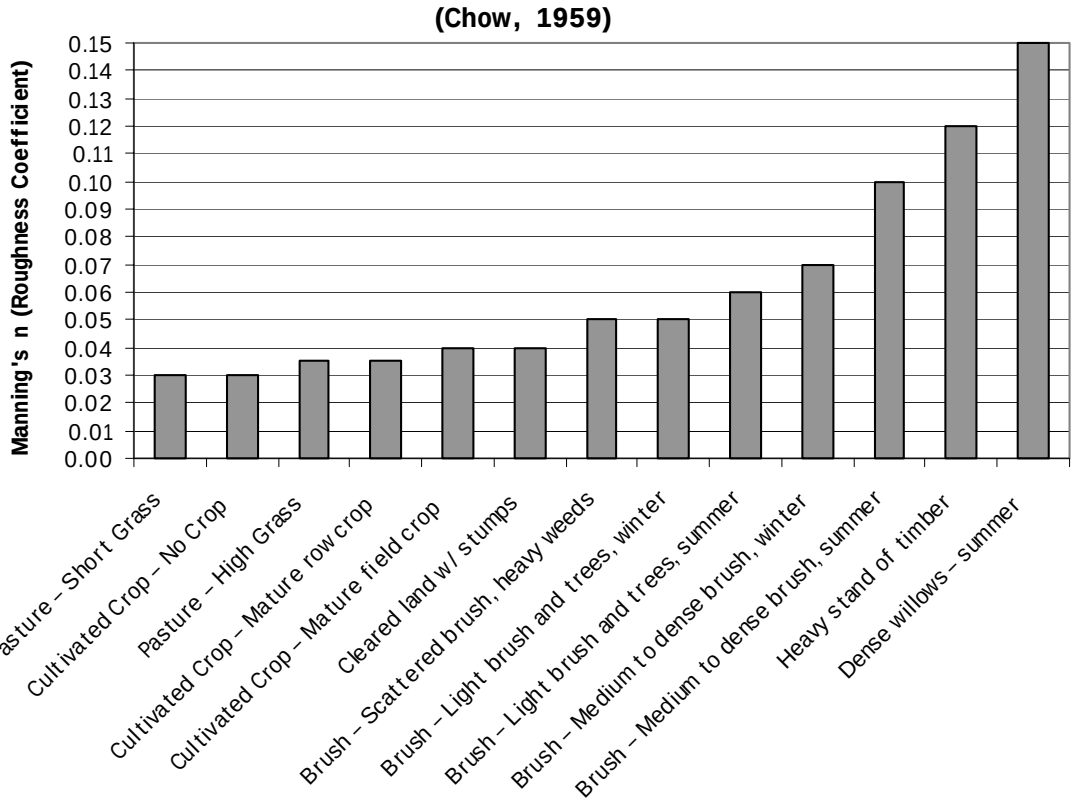

Sinuosity, Gradient and Stream Temperature

River sinuosity (defined as the ratio of channel length/valley length) indicates how a river has adjusted its slope (gradient) to that of its valley. The degree of sinuosity is related to channel dimensions, sediment load, streamflow, and the bed and bank materials. Rosgen (1996) notes that when river sinuosity is decreased, local reach slopes are increased and instability generally results. Straighter river channels have steeper gradients and hence higher flow velocities. Increased flow velocity exerts more force on the banks, accelerating erosion and stream widening. Subsequently, a lower potential effective shade condition (due to a wider channel) allows more direct solar radiation to reach the stream surface. Research has shown that natural rivers attempt to maintain a dynamic and continuing balance between sediment loads and the energy available from streamflow so that the river neither degrades nor aggrades.

Unique features in the Grande Ronde Valley must be considered when evaluating water quality. The Valley form is flat and wide, offering an unconstrained area for low velocity channel development with significant sediment deposition. As a result, a large floodplain has developed where soils are much deeper than in other parts of the subbasin. Accordingly, a stable channel configuration in the Grande Ronde Valley would be expected to have high sinuosity (Khan, 1971). The Grande Ronde River and most of the tributaries in the Grande Ronde Valley have been channelized to some extent and most riparian vegetation has been removed (James Webster, Personal Communications, 1999). The land has been highly developed for agriculture and

livestock management, which are now the predominant land uses in the Grande Ronde Valley. The State Ditch reduced channel length through the Grande Ronde Valley by almost 37 miles and provides an example of the results of channel straightening. With this combination of valley and channel form within the Grande Ronde Valley, the potential for erosion and down cutting is high when banks are destabilized through land management activities and/or streams are artificially straightened. It has been noted that bank stability and sediment problems occur throughout the Grande Ronde River throughout the valley, particularly along the State Ditch (NRCS/USFS/Union SWCD, 1997).

Sedimentation

Streambed material classification defines *fines* as sand, silt and organic material that have a grain size of 6.4 mm or less. Sediments may affect the spawning success of salmonids. Sedimentation of spawning gravel has been shown to significantly impair the success of juvenile emergence from gravel *redds*. Sedimentation may affect survival through entombment of juvenile or through reduction of intergravel dissolved oxygen delivery.

Studies have shown that fry emergence is seriously compromised as fine sediments are introduced into spawning gravel (Tappel and Bjornn, 1993). When fine grain sized substrate cover spawning gravel (*redds*) anadromous *sac-fry* (larval fish) may emerge prematurely. *Sac-fry* are often forced out of gravel before they have absorbed their yolk sacs as a fine sediments fill the interstitial pore spaces of the *redd*, resulting in a lack of oxygen (Tappel and Bjornn, 1993). Low survival rates accompany *sac-fry* that have been forced to prematurely emerge from the *redd* (**Figure A-29**).

Figure A-29. Percentage Emergence of Sac Fry from Newly Fertilized Eggs in Gravel/Sand Mixtures - Fine sediment was granitic sand with particles less than 6.4 mm (Bjornn 1974).

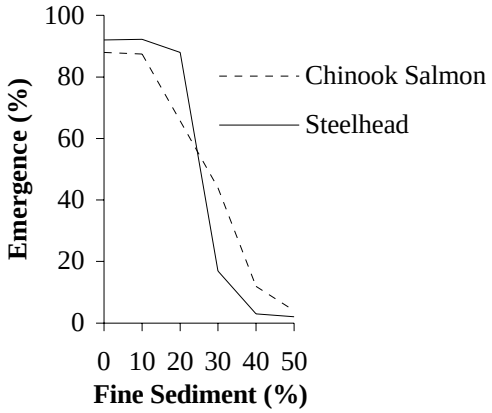

Increases in bed sediments, affected by landscape and bank mass failures, are often accompanied by channel widening and braiding resulting in increased bank erosion and decreased pool riffle amplitude. Reduced channel complexity may be associated with reduced habitat complexity for aquatic species (salmonids and food sources such as macroinvertebrate communities).

Beschta et al. (1981) concluded that bedload processes are extremely important in shaping the character and quality of stream habitats. Sedimentation of the stream substrate, particularly the gravel used for spawning, produces significant detrimental effects on salmonid resources (Iwamoto et al., 1978). Everest et al (1987) observed that watershed characteristics, as well as the erosion and bedload processes, will affect the level of risk to salmonids by accelerated sedimentation. Fine sediments can act directly on the fish by (Newcombe and McDonald 1991): 1) Killing salmonids or reducing growth or reducing disease resistance; 2) Interfering with the

development of eggs and larvae; 3) Modifying natural movements and migration of salmonids, or 4) Reducing the abundance of food organisms.

High fine sediment distributions in the Upper Grande Ronde sub-basin correlate strongly with non-woody riparian vegetation (i.e., annuals and perennials) (**Figure A-30**). Annual riparian vegetation types have median percent fine sediment distributions approaching 100%. Perennial riparian vegetation types have a median percent fine level of 58%. Woody riparian vegetation classifications correlate to lower fine sediment distributions (median values less than 20% fine sediment). Established/Mature deciduous/mixed/conifer riparian vegetation correlate to the lowest median percent fine value (16% of the stream bed substrate).

Figure A-30. Stream Bed Percent Fines Related to Various Riparian Vegetation Types *(ODFW data, 1996) [PACFISH targets for fine sediment is 20% (USFS, 1995)]*

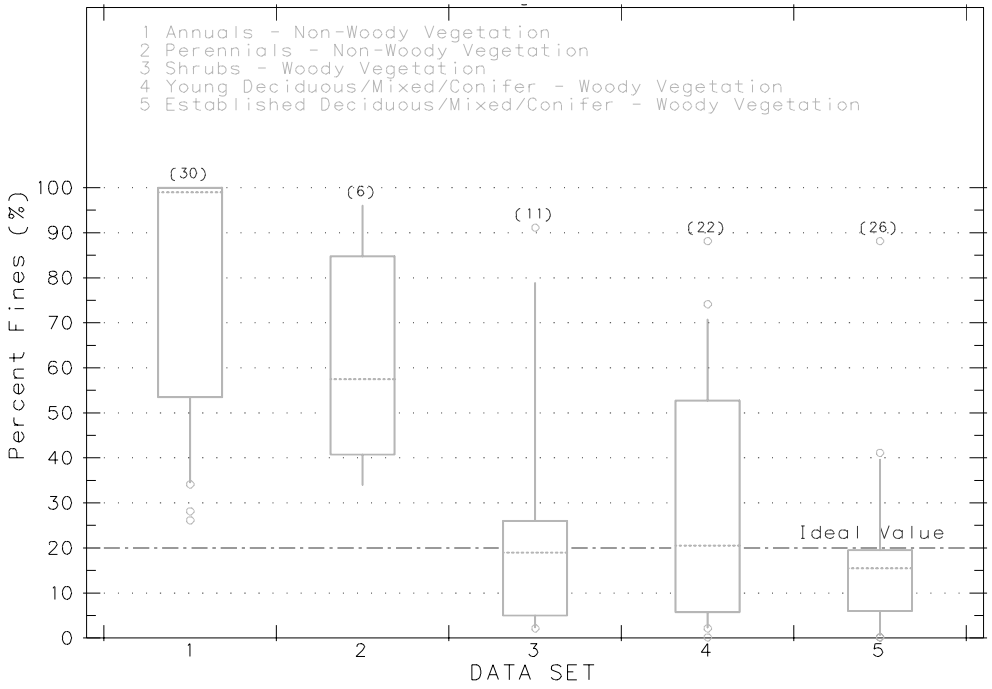

Referring back to **Figure A-30**, 15% of fine sediment distributed over *redds* is an upper limit before serious *sac-fry* impairment occurs. The widespread high distribution of fine sediments constitutes worrisome impacts to egg incubation and *sac-fry* emergence/survival. Serious detriment to sac-fry may be occurring in all streams with dominant annual and perennial riparian vegetation communities. Non-woody riparian vegetation communities correlate to fines sediment distributions that would prevent nearly all *sac-fry* emergence. Simply stated, these survey reaches are degraded to a level that reduces salmonid reproductive fitness to near zero levels. Further, much of the woody riparian communities are afflicted with high levels of fine sediments. The data suggest that sources of sediment, beyond sources related to riparian vegetation, are affecting the sediment distributions in the Grande Ronde River and tributaries.

Streambed substrate gravel occurrence is lowest where riparian vegetation communities are annual and perennial plant species (median gravel distribution of 21%) (**Figure A-31**). Woody riparian vegetation corresponds to higher gravel streambed substrate. The data show that established deciduous/mixed/conifer riparian vegetation types correlate with higher median gravel substrate (32%).

Figure A-31. Stream Bed Percent Gravel Related to Various Riparian Vegetation Types *(ODFW data, 1996) [PACFISH target for fine sediment is 20% (USFS, 1995)]*

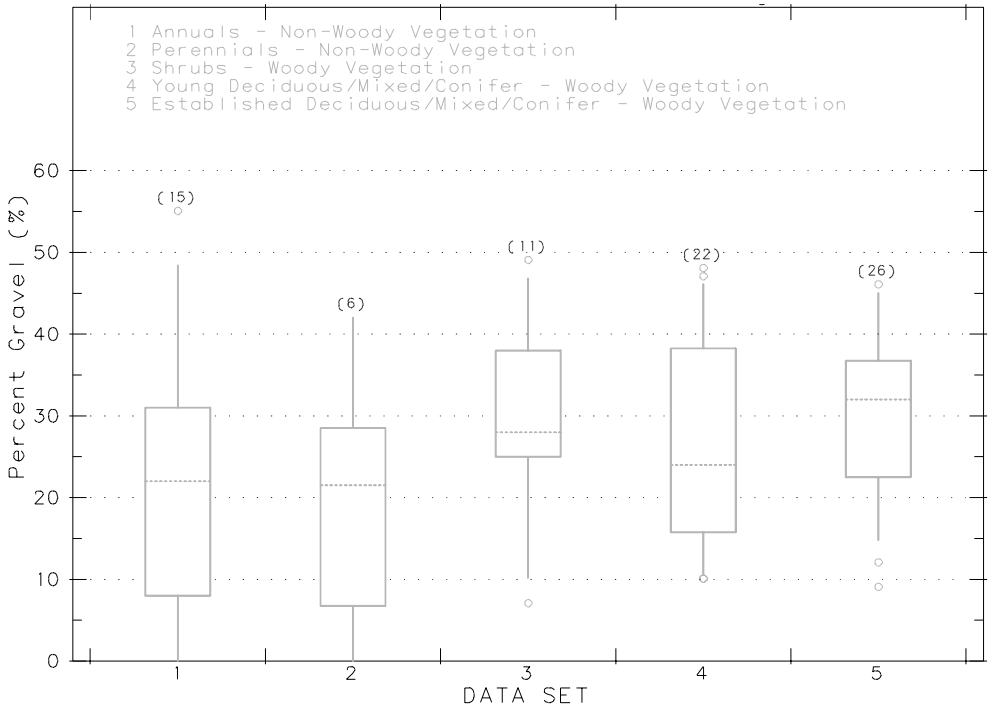

Streams with distributions of fine substrate must ultimately experience a decrease in fine sediment introduction into the water column before channel morphologic recovery can occur. Sediment sources, both upslope and instream, are elevated in some portions of the Upper Grande Ronde sub-basin. Before lasting improvements in channel substrate can take place, these sources must be reduced, in some cases, dramatically. Further, if the stream channel, riparian zone and/or upslope landscape is in a degraded state, the same high flow events that transport sediments out of the stream channel can introduce large quantities of fine sediment.

Sediment, once introduced into the stream channel, either becomes deposited in the bed substrate, deposits along banks or remains suspended in the water column (i.e., transported downstream). Fine sediment deposited in the stream bed material must be re-suspended during high flow events and transported downstream or deposited in the flood plain/stream bank areas bordering the stream channel. These processes occur during hydrologic events that are relatively infrequent. Major sediment moving events have return periods measured in decades. In conclusion, the condition of the stream channel and upslope landscape will create drastically different consequences in terms of sedimentation during high flow events:

Resilient/Healthy System: *Prevent large introductions of fine sediment from upslope or riparian areas, maintain stream bank stability, encourage deposition in the flood plain and bank building processes, introduce disturbed riparian vegetation (large woody debris into the active channel) and allow the resuspension and transportation of existing stream bed fine substrate in the downstream direction.*

Degrading/Impaired System: *Allow large introductions of fine sediment from upslope or riparian areas, experience moderate to high rates of active stream bank erosion, allow erosion in the flood plain and bank retreating processes, is unable to introduce disturbed riparian vegetation (large woody debris into the active channel) and resuspended/transported stream bed fine substrate is replaced by incoming fine sediment sources.*

Hydrology Related to Stream Temperature

Flow Volume

Runoff in the Upper Grande Ronde sub-basin is primarily derived from snowmelt, with peaks typically occurring in the spring. Late summer low flows are common for many streams in the Upper Grande Ronde sub-basin due to low summer precipitation combined with extensive water withdrawals for irrigation. The lowest mainstem flows occur in late September and early October (ODEQ, 1995-a). Low flows are of particular concern along the mainstem of the Grande Ronde Valley, with water rights over-appropriated, resulting in insufficient flow to support anadromous and resident fish stocks, meet water quality standards, or provide for recreational opportunities (ODEQ, 1995-a). **Figure A-32** shows Grande Ronde River flows measured during the last two weeks of August 1999. Irrigation withdrawals noticeably reduce the stream flow within the Grande Ronde Valley.

Figure A-32. Late August 1999 Grande Ronde River and Tributary Discharge

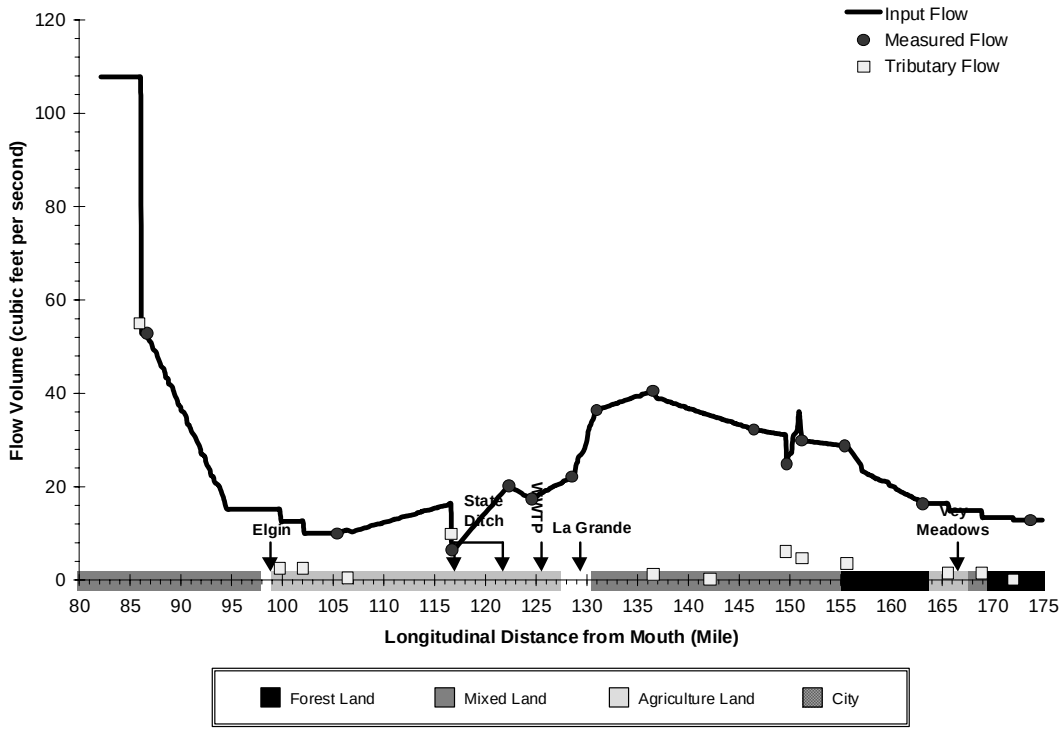

Stream temperature is generally inversely related to flow volume. As flows decrease, stream temperature tends to increase, if energy processes remain unchanged (Boyd, 1996). Very low water volumes observed in **Image A-13a** are confined within a bedrock channel with no available effective riparian shading, and bedrock temperatures are extremely elevated. Accordingly, water temperatures within this river reach are in 81-82°F range (27-28°C). **Image A-13b** illustrates the temperature and flow regime within the river less than one mile upstream from the low flow volume location. Water temperatures are approximately 3-6°C cooler at the high volume location.

Images A-13a and **13b**. Flow Volume and River Temperature[3]

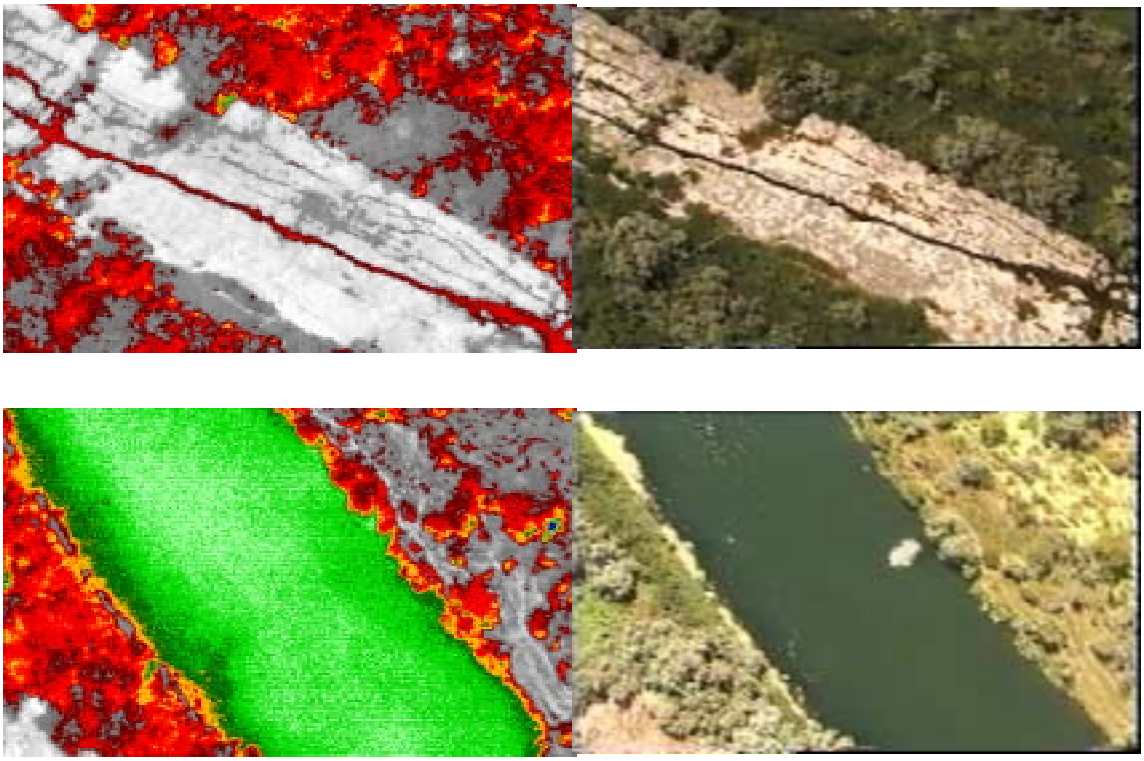

Floodplain Connectivity and Groundwater

Groundwater inflow has a cooling effect on summertime stream temperatures. Subsurface water is insulated from surface heating processes and most often groundwater temperatures fluctuate little and are cool (45°F to 55 F). Many land use activities that disturb riparian vegetation and associated flood plain areas affect the connectivity between river and groundwater sources. Groundwater inflow not only cools summertime stream temperatures, but also augments summertime flows. Reductions or elimination of groundwater inflow will have a warming effect on the river.

FLIR thermal imagery detects groundwater contributions as cooler plumes within the instream temperatures. **Image A-14** shows distinct seeps that deliver groundwater. Areas of cooler soils saturated with groundwater are marked with circles. (Cooler surface temperatures resulting from riparian shading are present on this image and is marked by an arrow.) It is important to note that river temperatures reduce by approximately 3.6 F through this reach (i.e., 24 C to 22 C), indicating that groundwater connectivity within this river reach is reducing stream temperatures.

The ability of riparian soils to capture, store and slowly release groundwater is largely a function of the level of riparian disturbance and geology. Riparian disturbance can separate the connectivity of the groundwater and the stream, and occurs when a permeability barrier prevents normal flood plain functions. **Image A-15** illustrates an area where the riparian area that is not connected to the river. Any cooling effect from the riparian zone on the left bank is not influencing river temperature.

---

[3] FLIR Image Temperature Scale (°C)

>50	30-50	29	28	27	26	25	24	23	22	21	20	19	18	17	16	15	<15

Floodplain drainage efficiency has increased throughout the Grande Ronde Valley as a result of river channel down-cutting into alluvial material within channelized sections (James Webster, Personal Communications, 1999). The construction of flood abatement structures (i.e., levees, berms and dikes) and additional wetland drainage has potentially contributed to increased drainage efficiency of the watershed and effectively disconnected the channel from the floodplain.

Image A-14.Connectivity Between Groundwater and a River in Northeastern Oregon[4]

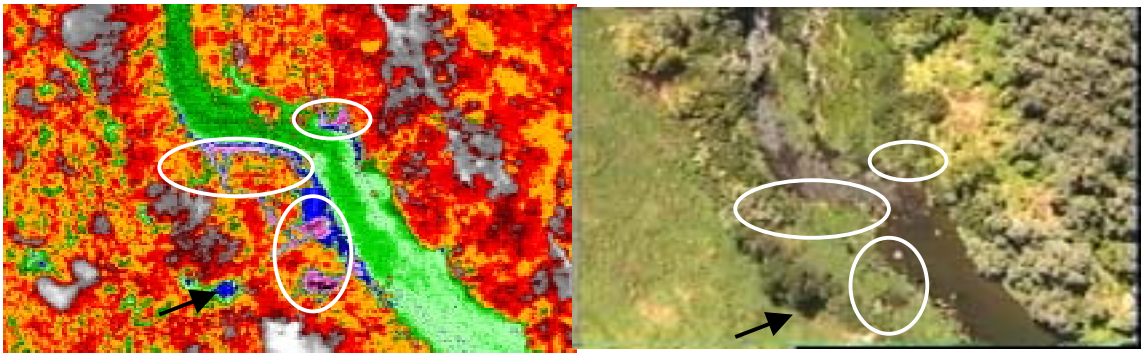

Image A-15. Non-Connectivity Between Groundwater and a River in Northeastern Oregon.

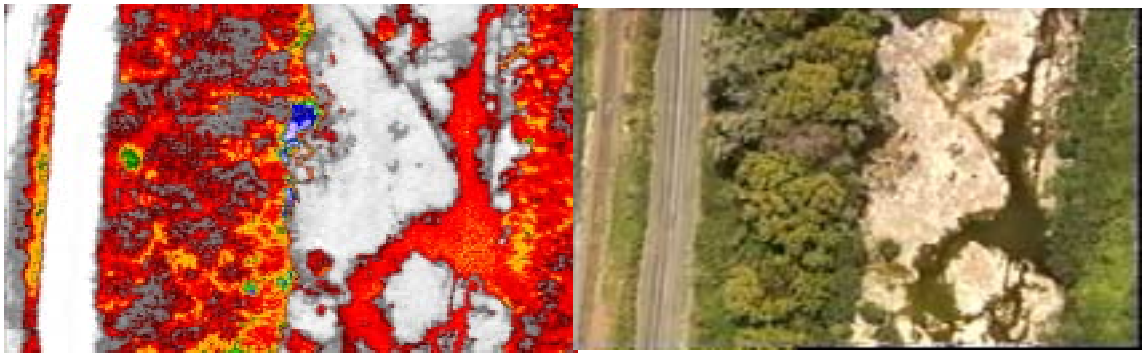

[4] **FLIR Image Temperature Scale (°C)**

>50	30-50	29	28	27	26	25	24	23	22	21	20	19	18	17	16	15	<15

Analytical Framework

Data Acquisition

Data collected and refined for this TMDL effort has allowed the development of temperature simulation methodology that is both spatially continuous and spans full day lengths (diurnal). Detailed spatial data sets have been developed for the riparian, channel morphology and hydrology parameters (from Tanner Gulch RM 202.4 to the Wallowa River confluence RM 82):

Data Source Descriptions

Existing Vegetation Above La Grande: The United States Environmental Protection Agency (USEPA) created a high-resolution riparian vegetation map of the Upper Grande Ronde River and its tributaries in 1993. A 2,000 foot-wide corridor centered on the river was digitally mapped using photointerpretation and Landsat thermal satellite imagery interpretation. Individual riparian communities, based on dominant species, height, and canopy density were identified and delineated as polygons. Riparian classification was based upon the principles of "Wetlands and Deepwater Habitats Classification System" (Cowardin et al., 1979) and extends the Cowardin classification system to cover uplands as well as wetlands. All coverage was verified using Digital Orthophoto Quads (DOQs).

Existing Vegetation Below La Grande: The Oregon Department of Forestry (ODF) contracted Pacific Meridian to delineate Landsat thermal satellite imagery according to vegetation species, size, and canopy density in 1997. The pixel size of this data is 25 meters. Tree sizes were presented as diameter at breast height (DBH) ranges. The mid-range DBH was used to calculate approximate heights for each species. All coverage was verified using Digital Orthophoto Quads (DOQs).

Digital Elevation Models (DEM): 30-meter DEMs are available for the entire state of Oregon through the State Service Center for Geographic Information Systems (SSCGIS).

Digital Orthophoto Quarter Quads (DOQQs): DOQQs for the Upper Grande Ronde sub-basin are available from the United States Geologic Survey. (Areas for which DOQQs are not available are typically covered with DOQs.)

Digital Orthophoto Quads (DOQs): DOQs for the Upper Grande Ronde sub-basin are available through the State Service Center for Geographic Information Systems (SSCGIS). (Areas for which DOQs are not available are typically covered with DOQQs.)

GIS Data Developed for Temperature Model Input

1. Mainstem River and Tributary locations are mapped from digital orthophoto quads (DOQs) sampled in 1994 (see **Image A-16**).
2. Near Stream Vegetation Groupings are derived from Landsat data classified at a 25-meter pixel size that attains an accuracy of 80% (BLM, 1998). Vegetation groupings are by type, height and density (see **Images A-17 and A-18**).
3. Channel Widths are measured from DOQs for all simulated reaches where channels are greater than 10 meters (see **Image A-19**).

4. Stream Reach Elevation and Gradient for each simulation reach are derived from DEMs. Stream lengths used for gradient calculations are measured from the stream length data at a 1:5,000 scale (see **Image A-20**).
5. Maximum Topographic Shade Angles (East, South, West) are calculated at each reach break using a TopoAngle Tool developed by DEQ that samples Digital Elevation Model (DEM) 30 meter pixel grid data (see **Image A-21**).
6. Sinuosity is calculated from stream length overlaying valley morphology slope that is derived from DEM data at 1:5,000 scale (see **Image A-22**).

Spatial Data Developed for Temperature Model Input

All data is longitudinally referenced in the model allowing spatial and/or continuous inputs to apply to certain zones or specific river segments. Longitudinal distance nodes differentiate input data for reach segments. Reach segmentation is based on homogeneity in either riparian vegetation or hydrology or stream aspect.

Channel/Valley Morphology Parameters

- Longitudinal Distance (river miles): Defines the modeled reaches for which spatial input parameters are referenced. Distances are derived from DEQ 1:5,000 river layer digitized from Digital Orthophoto Quads (DOQs) and measured in the upstream direction from the confluence with the Wallowa River (Rondowa).
- Elevation (feet): Measured from DEM at upstream and downstream reach boundaries and averaged (see **Figure A-33**).
- Gradient (%): The difference between the upstream and downstream elevations divided by the reach length (see **Figure A-33**).
- Bedrock (%): The percent of streambed material that has a diameter of 25 cm or greater. Values are derived from stream survey data or assumed where data is limited (see **Figure A-34**).
- Aspect (decimal degrees from North): Measured from DEQ 1:5,000 rivers layer and rounded to the nearest 15^{o} (see **Figure A-35**).
- Bankfull Channel Width (feet): Measured from 1:1,500 DOQs (see **Figure A-36**). It is the distance between near stream shade-producing vegetation or active channel banks where near stream shade-producing vegetation is non-existent.
- Channel Incision (feet): Depth of the active channel below riparian terrace or floodplain. Assumed to be zero due to lack of data, except La Grande through State Ditch river sections (see **Figure A-37**).
- Topographic Shade Angle (decimal degrees): The angle made between the stream surface and the highest topographic features to the west, east and south as calculated from DEM at for each stream reach (see **Figure A-38**).

Riparian Parameters

- Riparian Height (feet): Derived from Landsat imagery and averaged along reach length (see **Figure A-39**).
- Canopy Density (%): Derived from canopy density via aerial photo interpretations, Landsat imagery and densiometer measurements (see **Figure A-40**).
- Riparian Overhang (feet): Distance of riparian vegetation intrusion over bankfull channel. Assumed to be zero for entire simulation distance due to lack of data.

Hydrology Parameters

- Flow Volume (cubic feet per second): Measured by DEQ with standard USGS protocols and interpolated between flow measurement sites (see **Figure A-41**).
- Flow Velocity (feet per second): Derived from Manning's equation and Leopold power functions calibrated to measured flow velocity data (see **Figure A-42**).
- Wetted Width (feet): Derived from Manning's equation and Leopold power functions calibrated to measured wetted width data (see **Figure A-36**).
- Average Depth (feet): Derived from Manning's equation and Leopold power functions calibrated to measured average depth data. Calculated based on assuming that channel shape is rectangular (see **Figure A-43**).
- Reynolds Number: Derived from Reynolds Equation and used to test for turbulent flow (see **Figure A-44**).
- FLIR Temperature Data (^{o}F): FLIR temperatures measured from Rondowa to Tanner Gulch on August 20, 1999 (see **Figure A-45)**.

Continuous Input Parameters

- Wind Speed (miles per hour): Hourly values measured at La Grande airport (see **Figure A-46**).
- Relative Humidity (%): Hourly values measured by DEQ (see **Figure A-47**).
- Air Temperature (^{o}F): Hourly values measured by DEQ (see **Figure A-48**).
- Tributary Temperature (^{o}F): Hourly values measured by DEQ (see **Figures A-49** and **A-50**).
- Upstream Boundary Condition (^{o}F): Hourly values measured by DEQ upstream of Clear Cr. at reach #1. Note that only the upstream boundary is used for simulation purposes. Additional diel temperature data are used for model validation (see **Figures A-51**).

Image A-16. Mainstem River and Tributary Mapping from DOQs
(Red stars indicate model reach breaks)

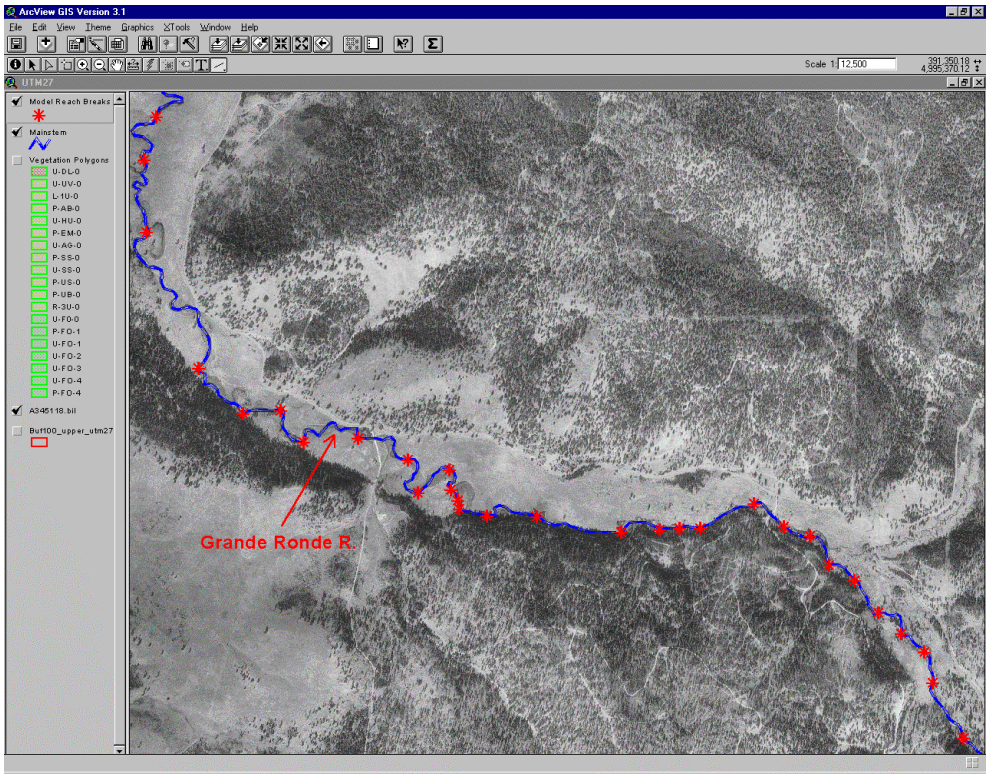

Image A-17. Landsat Polygons Overlaying DOQ for Visual Inspection Displayed at 1:5,000.
(Green lines indicate vegetation polygon boundaries.)

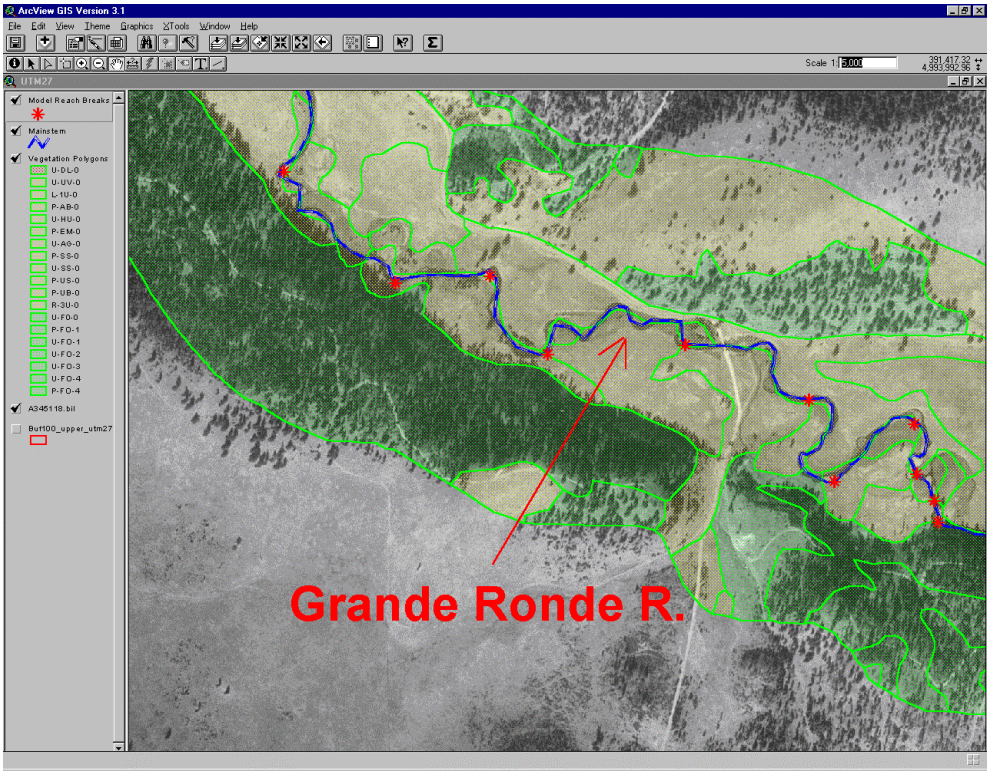

Image A-18. Landsat Grids Overlaying DOQ for Visual Inspection Displayed at 1:5,000.
(Green lines indicate vegetation polygon boundaries.)

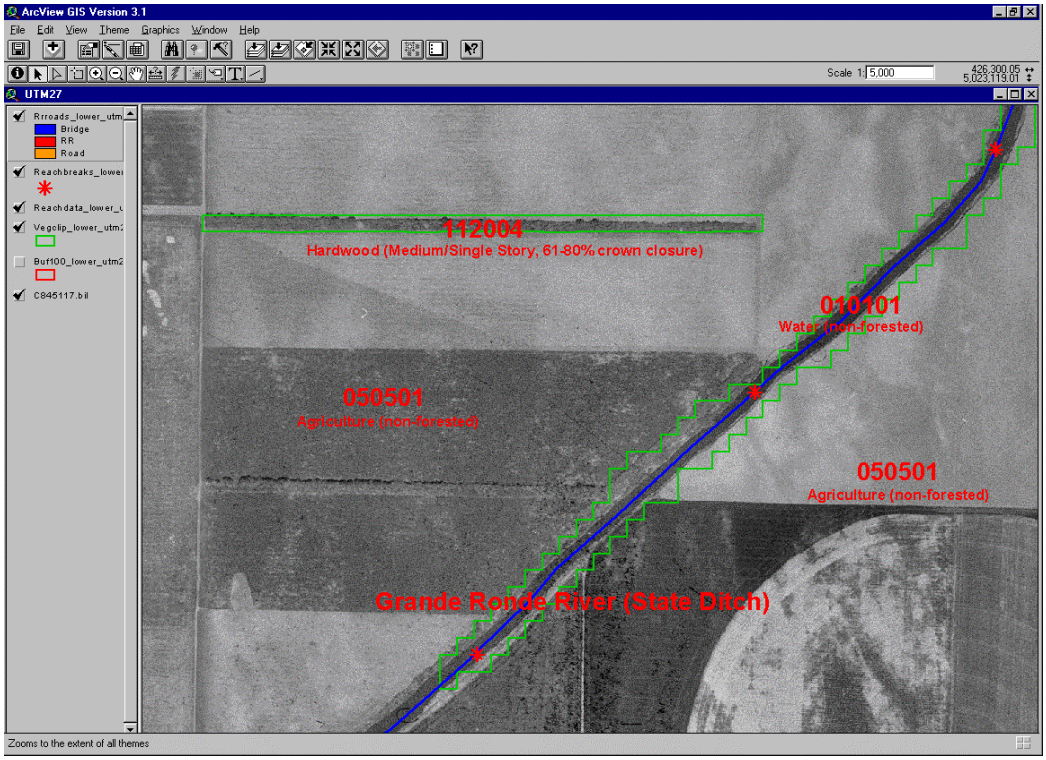

Image A-19. Channel Width Measured from DOQs (1:1,500 scale).

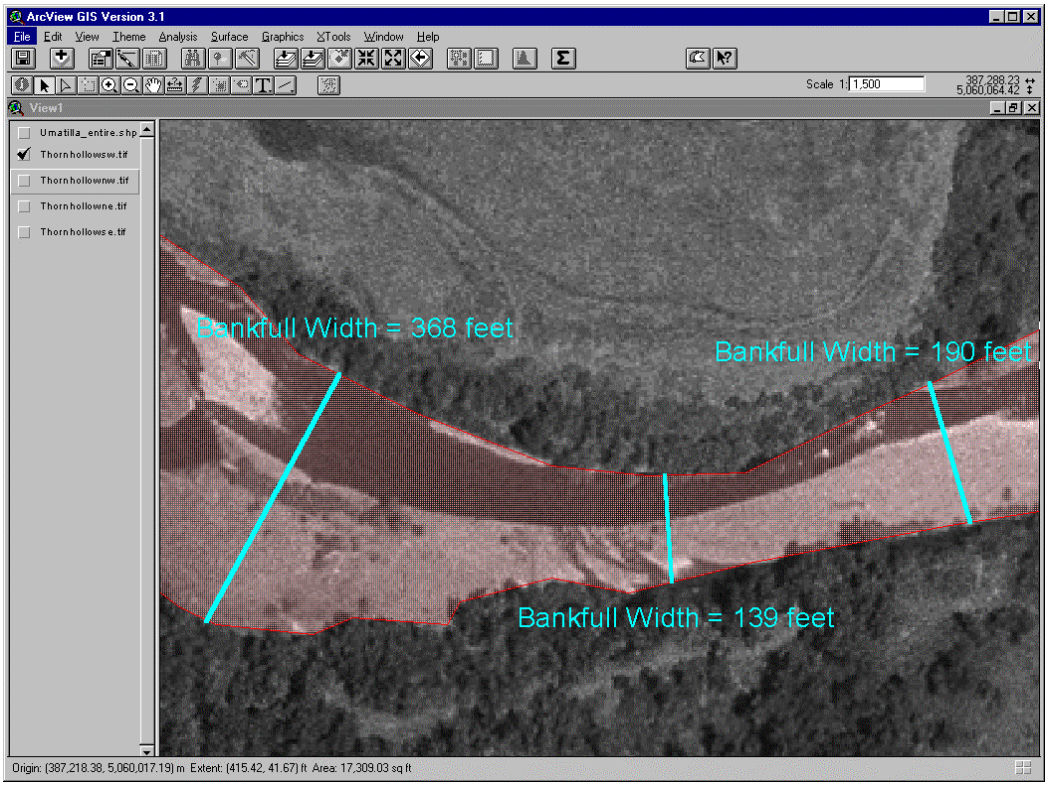

Image A-20. Shaded Relief Where Grande Ronde River Enters Grande Ronde Valley.

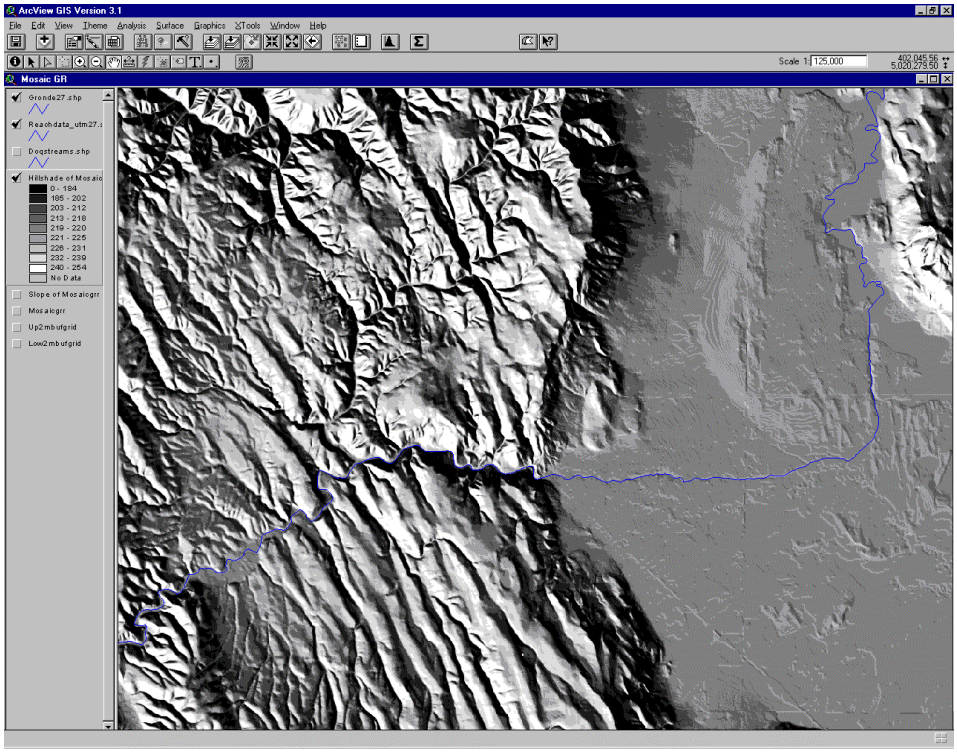

Image A-21. Maximum Topographic Shade Angles. **Red** circles indicate reach breaks, and corresponding maximum topographic shade angles.

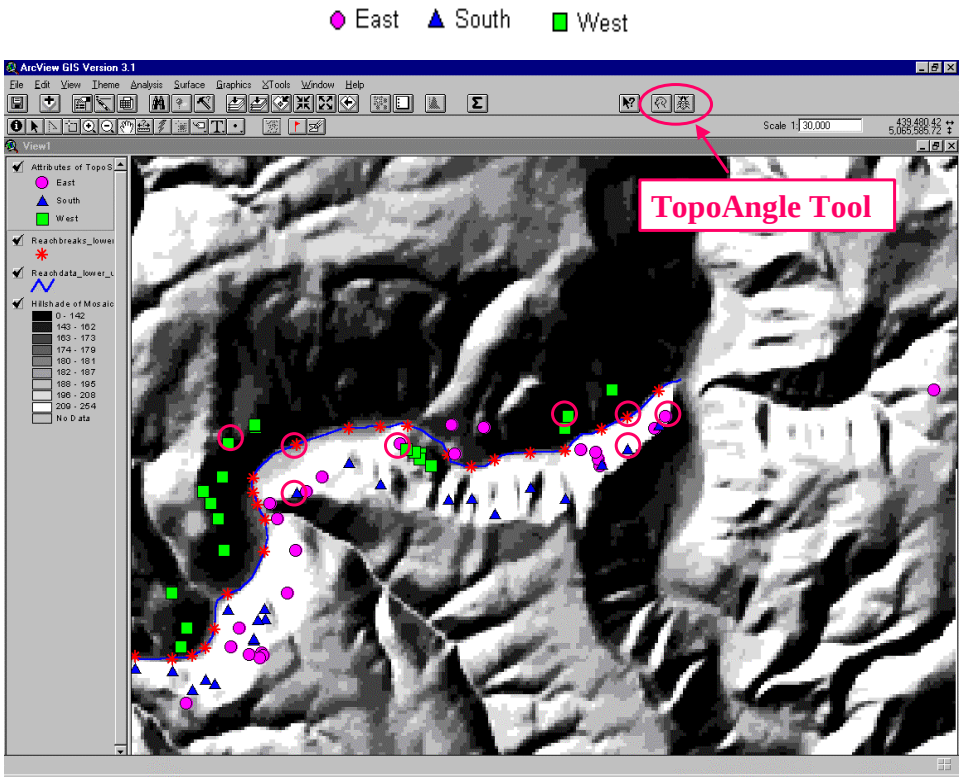

Image A-22. Stream Data & Surface Slope Derived from DEM Used for Sinuosity Measurements

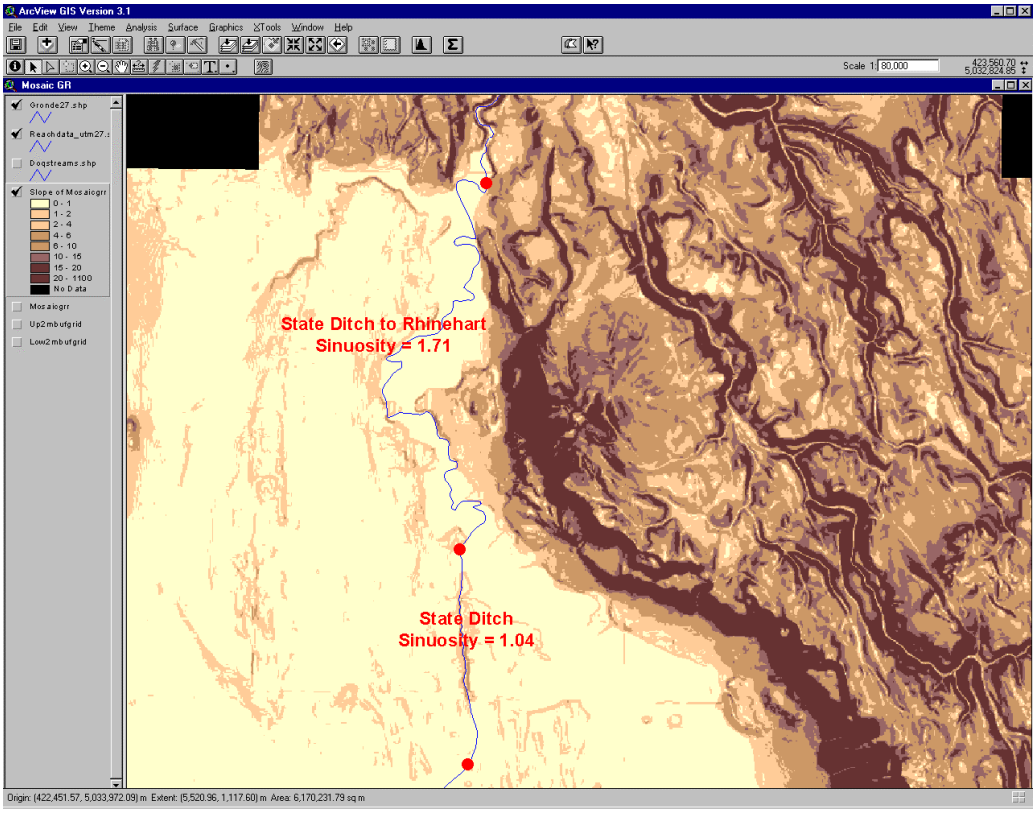

Figure A-33. Longitudinal Grande Ronde River Elevation and Gradient

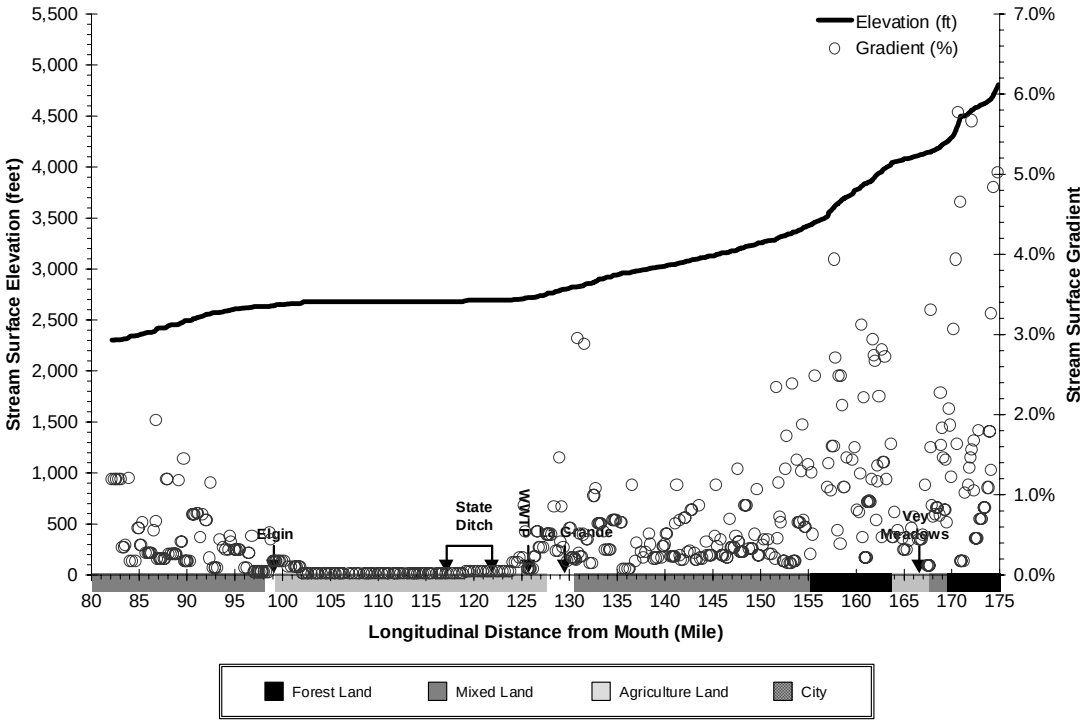

Figure A-34. Longitudinal Grande Ronde River Percent Bedrock

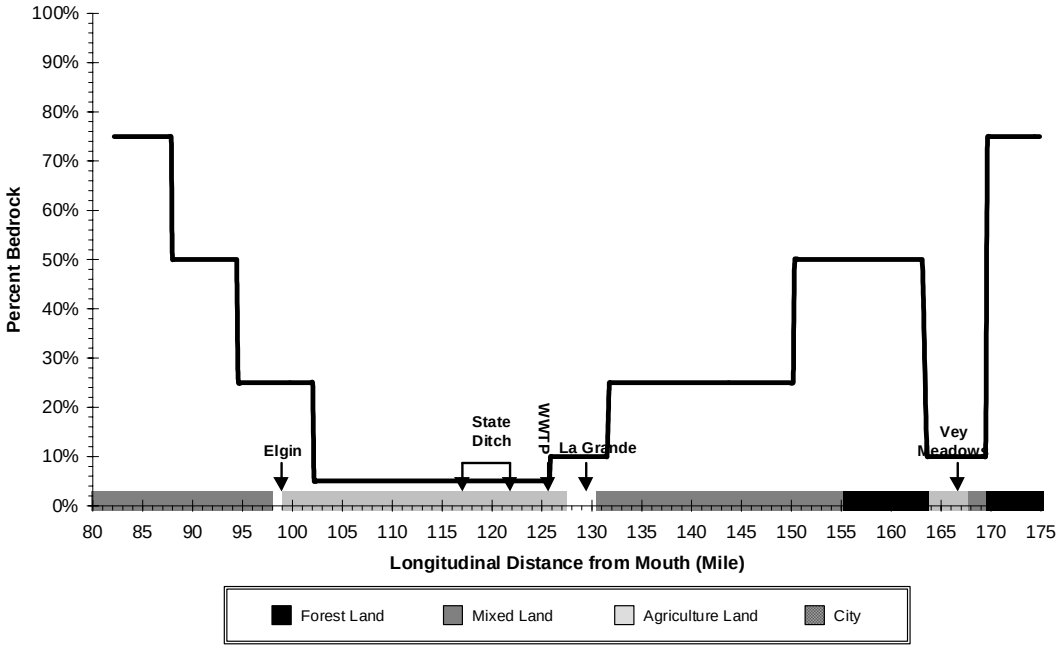

Figure A-35. Longitudinal Grande Ronde River Aspect (Degrees from North)

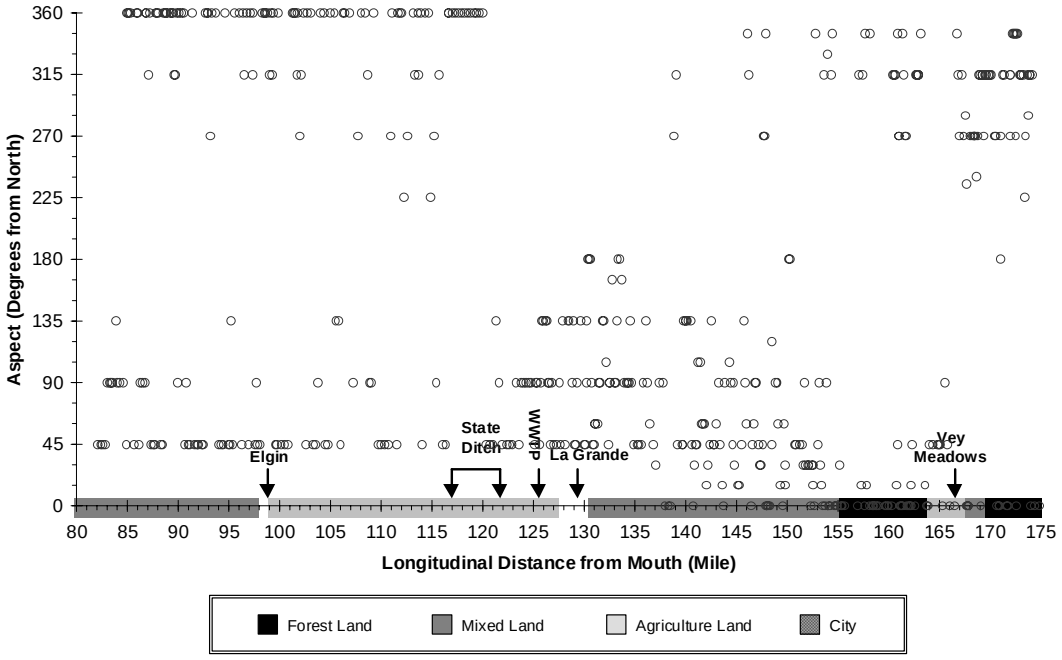

Figure A-36. Longitudinal Grande Ronde River Width (Channel and Wetted)

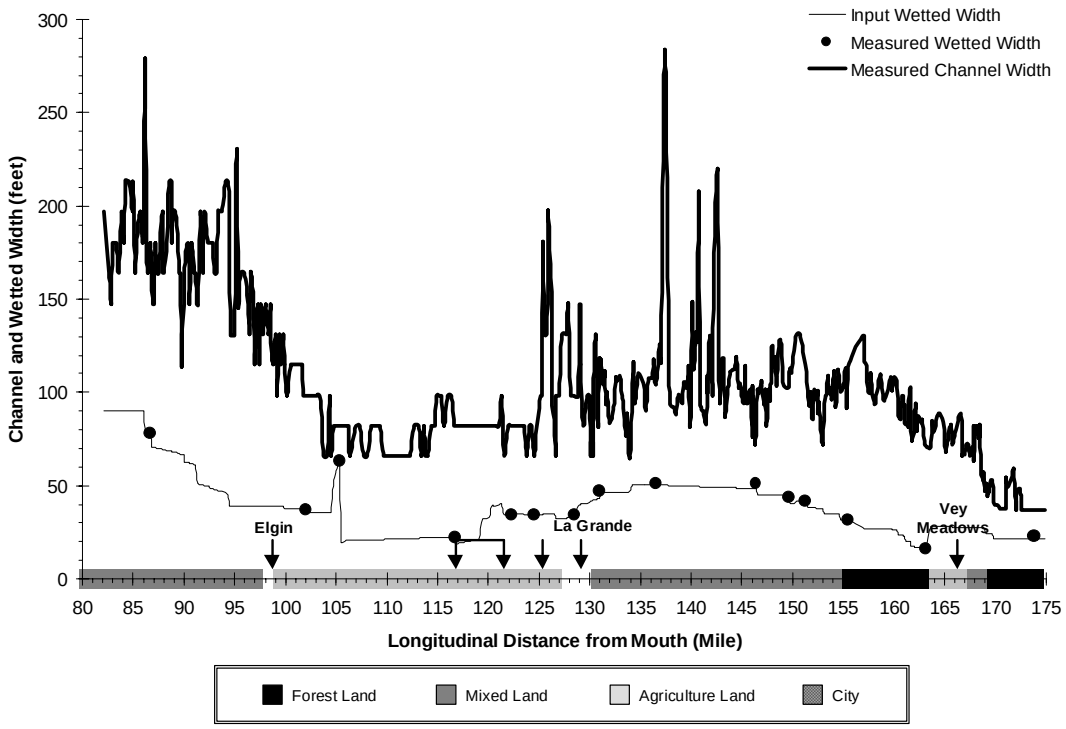

Figure A-37. Longitudinal Grande Ronde River Channel Incision

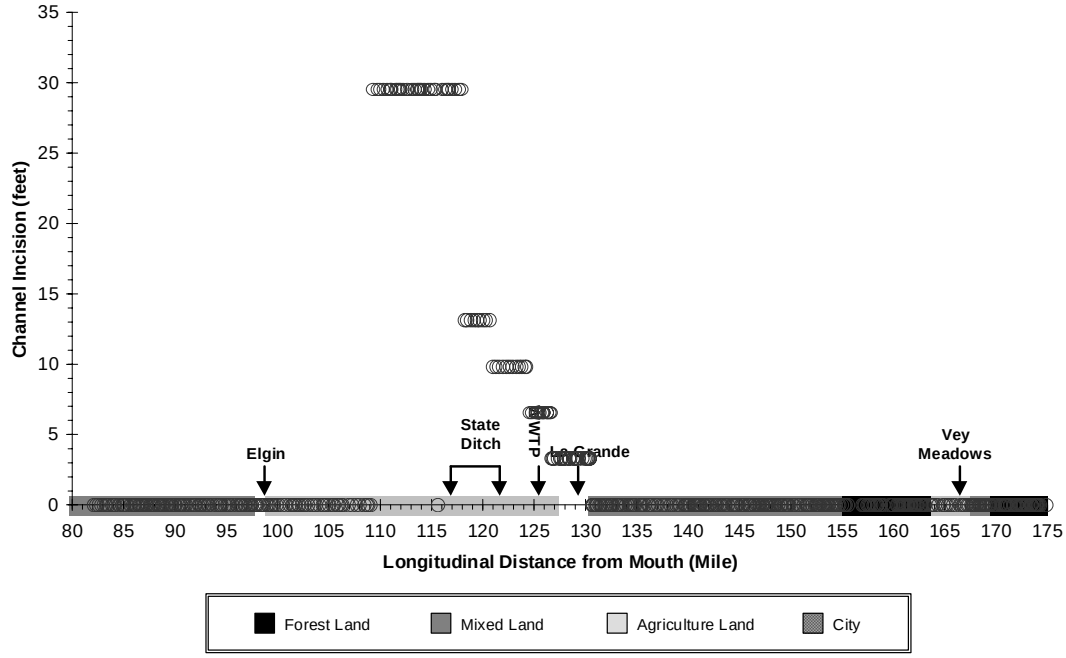

Figure A-38. Longitudinal Grande Ronde River Topographic Shade Angles

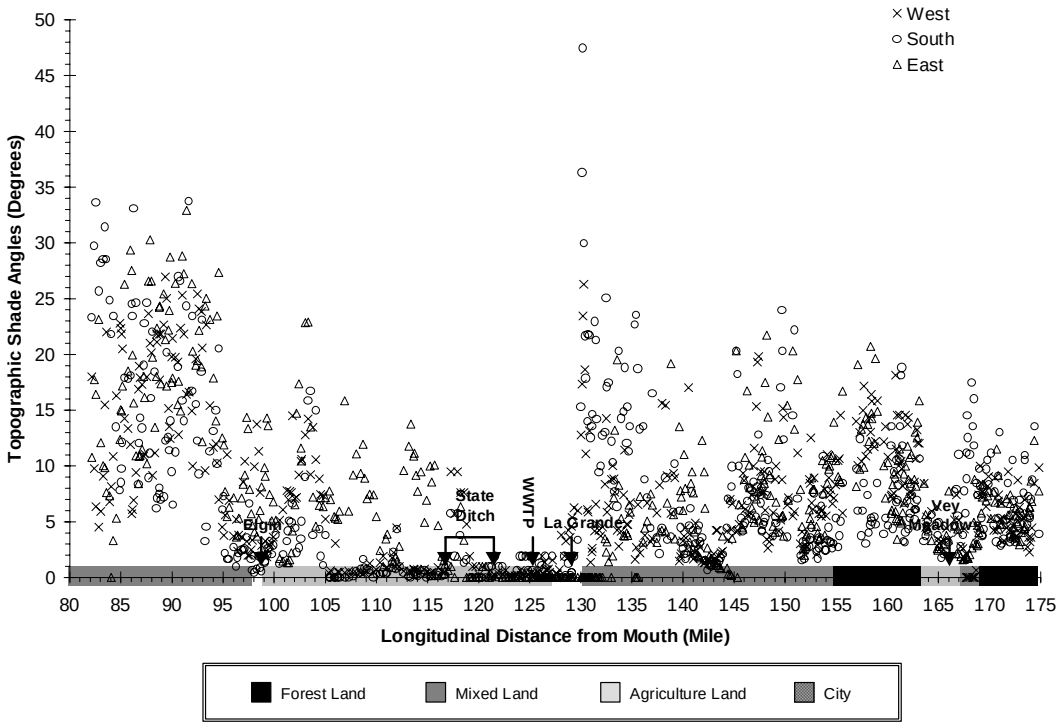

Figure A-39. Longitudinal Grande Ronde River Riparian Vegetation Height

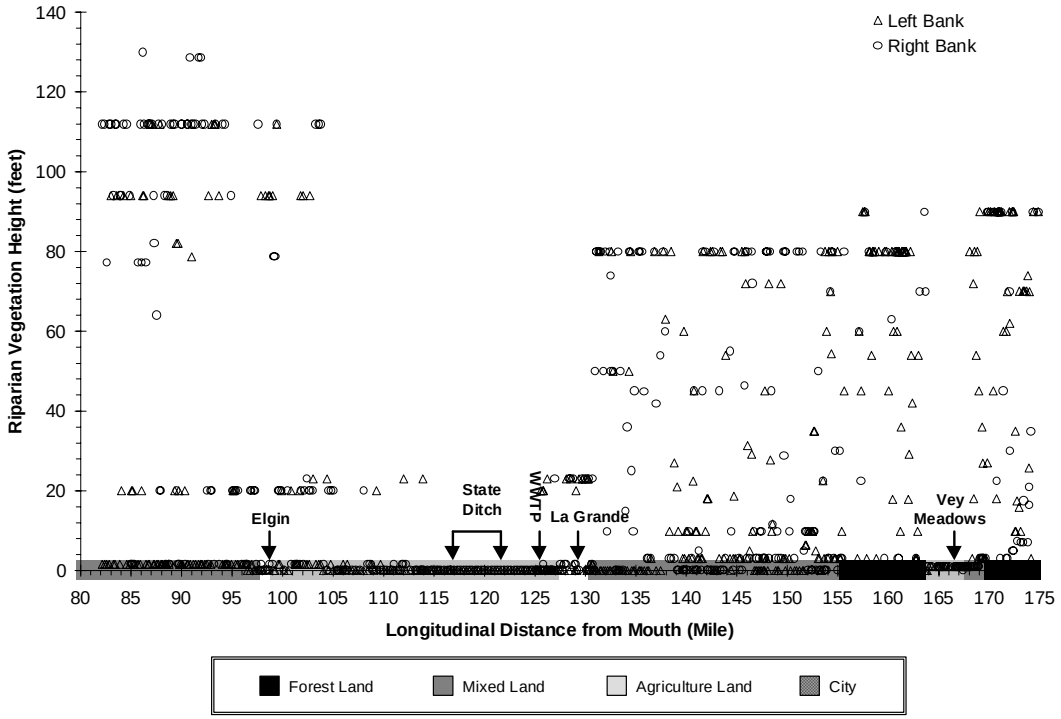

Figure A-40. Longitudinal Grande Ronde River Riparian Vegetation Density

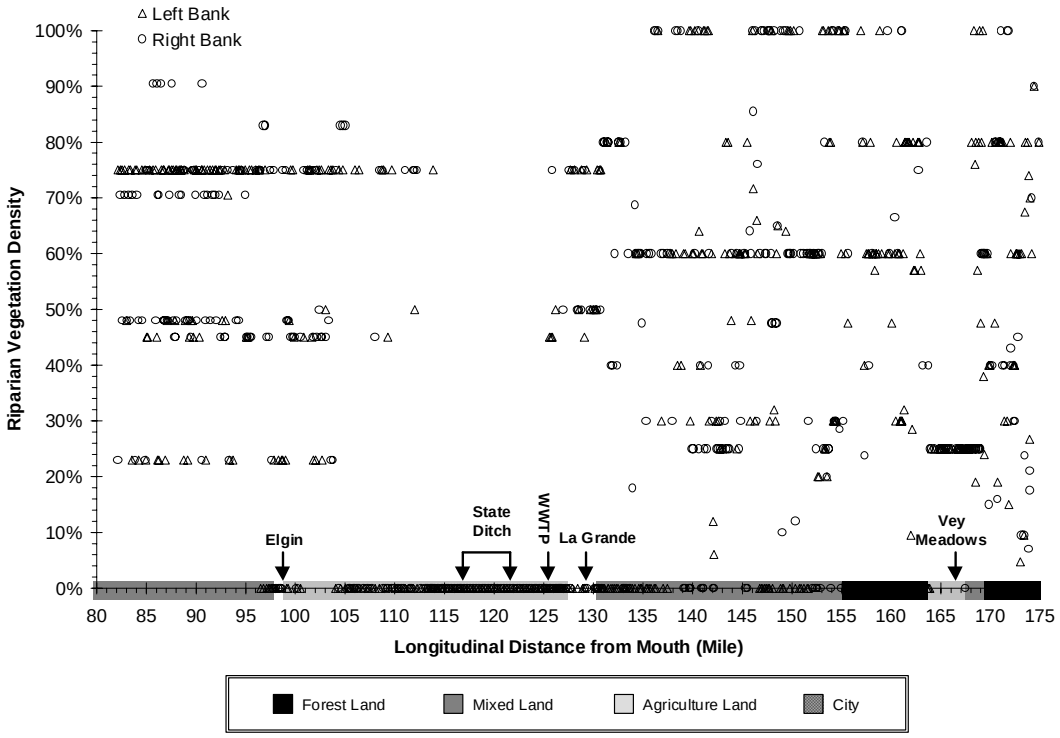

Figure A-41. Longitudinal Grande Ronde River Flow Volume

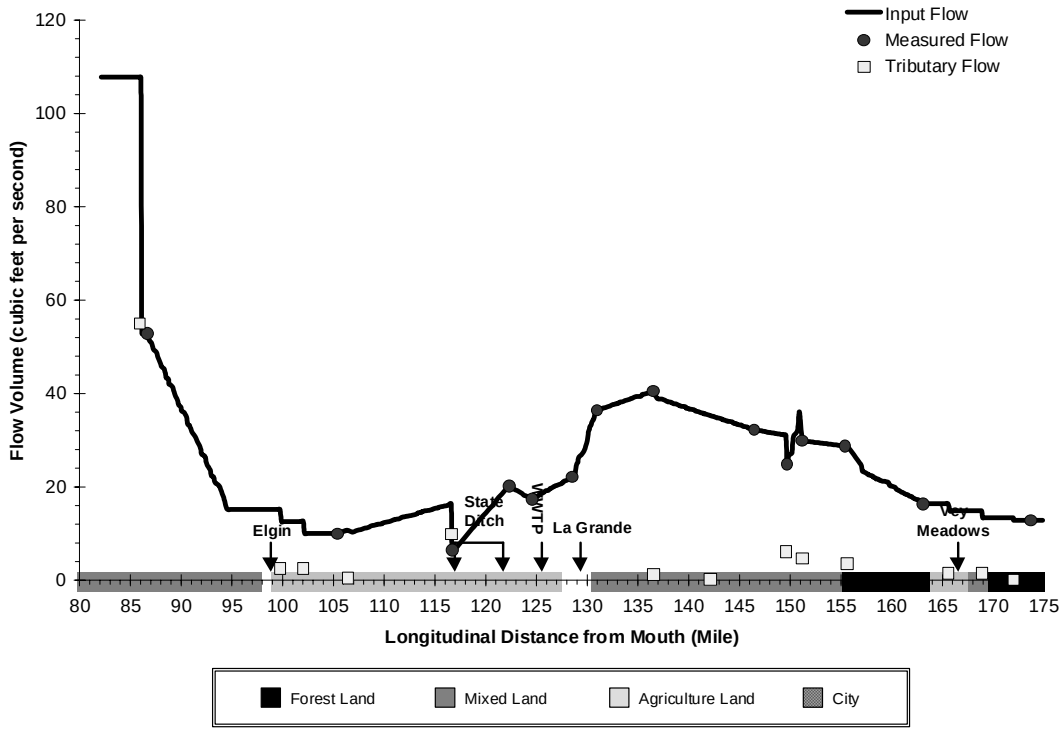

Figure A-42. Longitudinal Grande Ronde River Flow Velocity

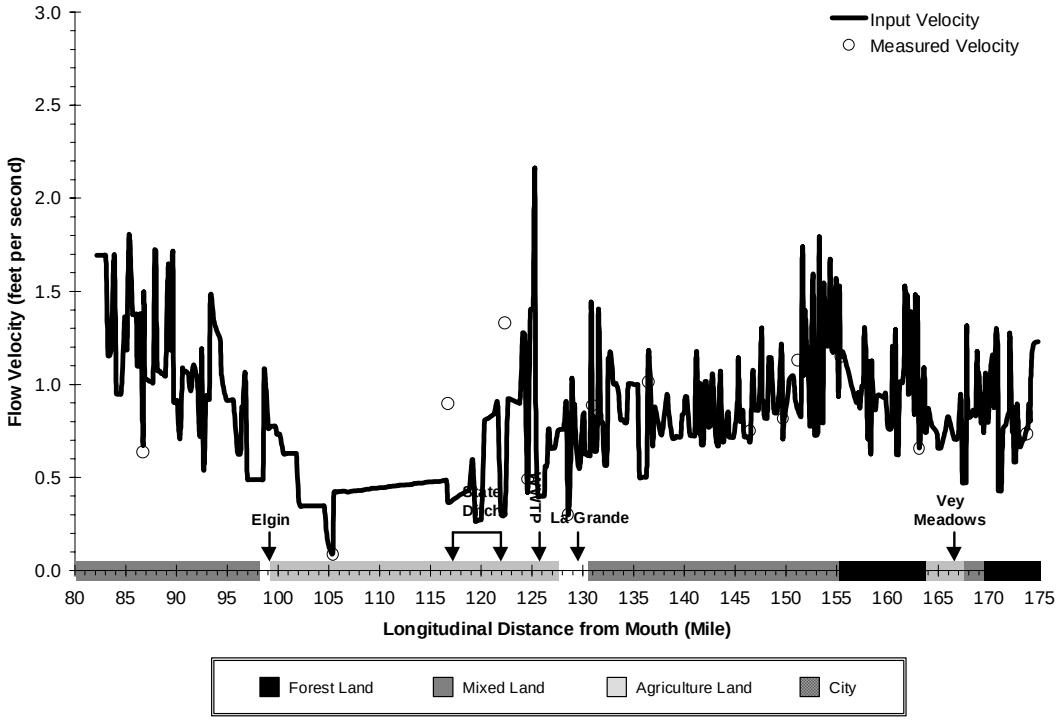

Figure A-43. Longitudinal Grande Ronde River Average Depth

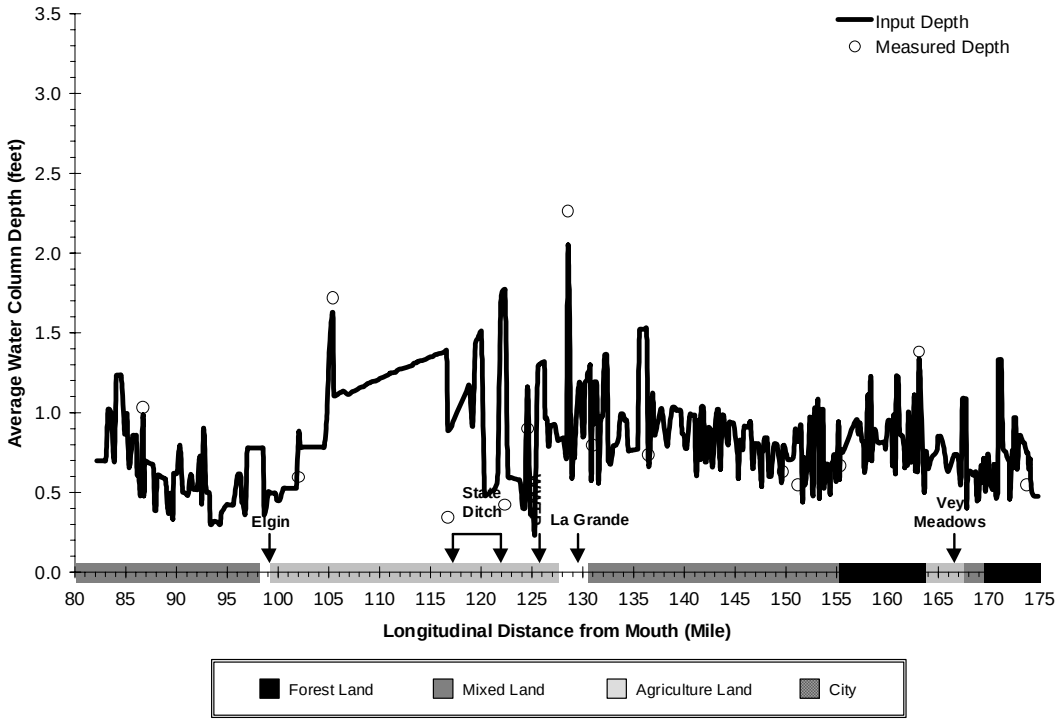

Figure A-44. Longitudinal Grande Ronde River Reynolds Number
(Values Greater than 2000 Indicate Turbulent Flow/Mixing)

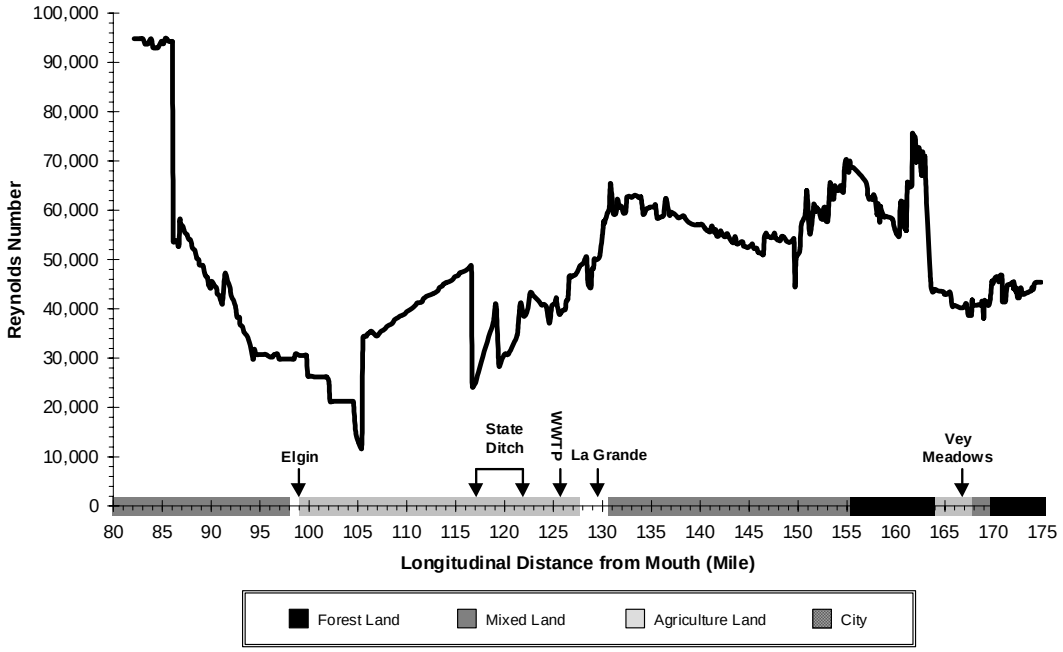

Figure A-45. FLIR Derived Longitudinal Temperature Profile

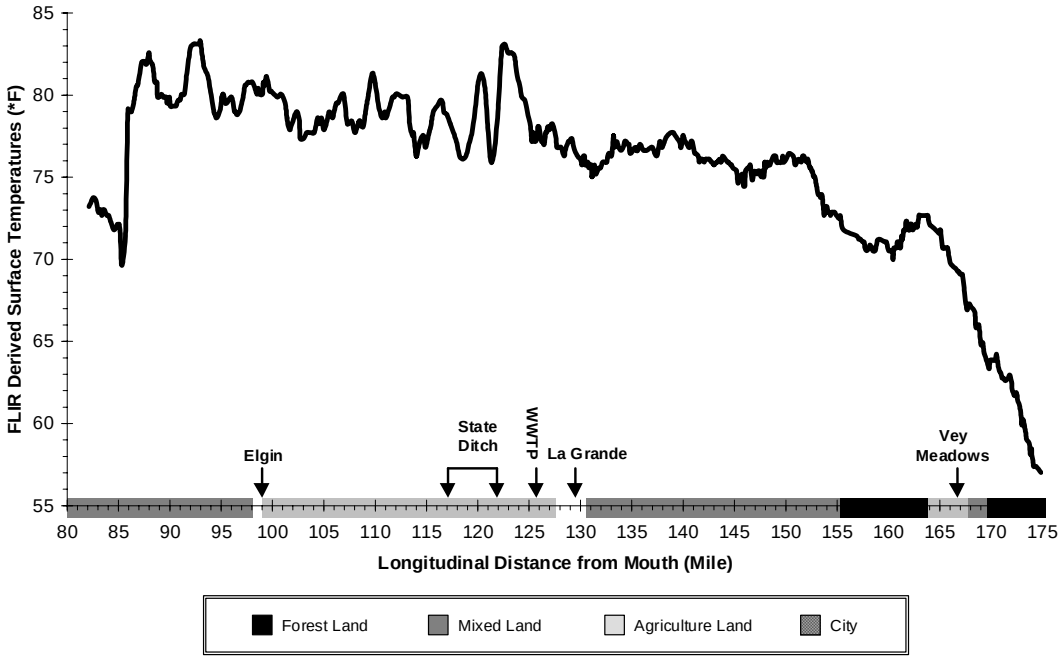

Figure A-46. Diel Wind Speed (La Grande Airport)

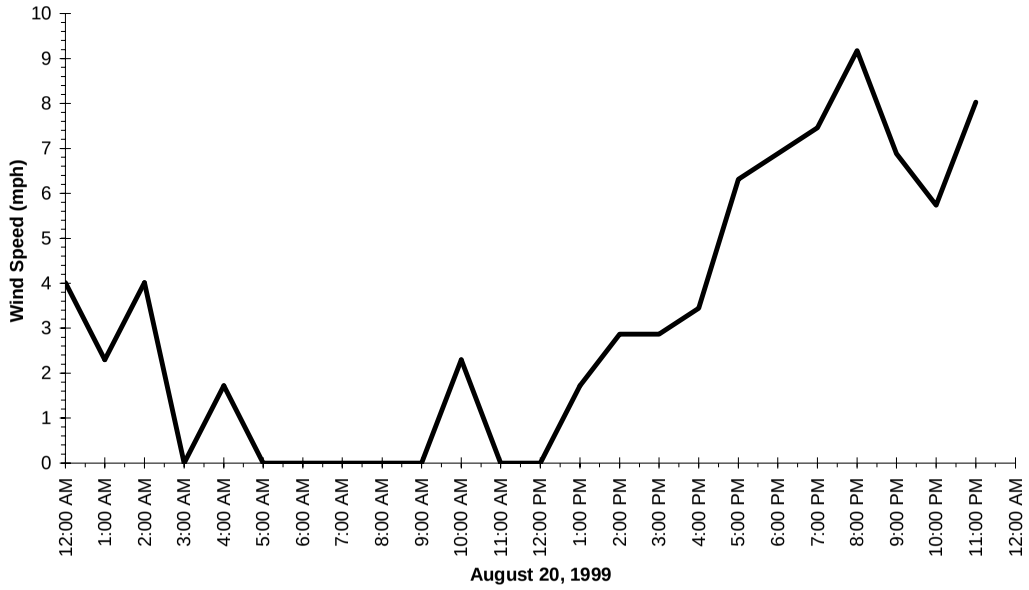

Figure A-47. Diel Relative Humidity

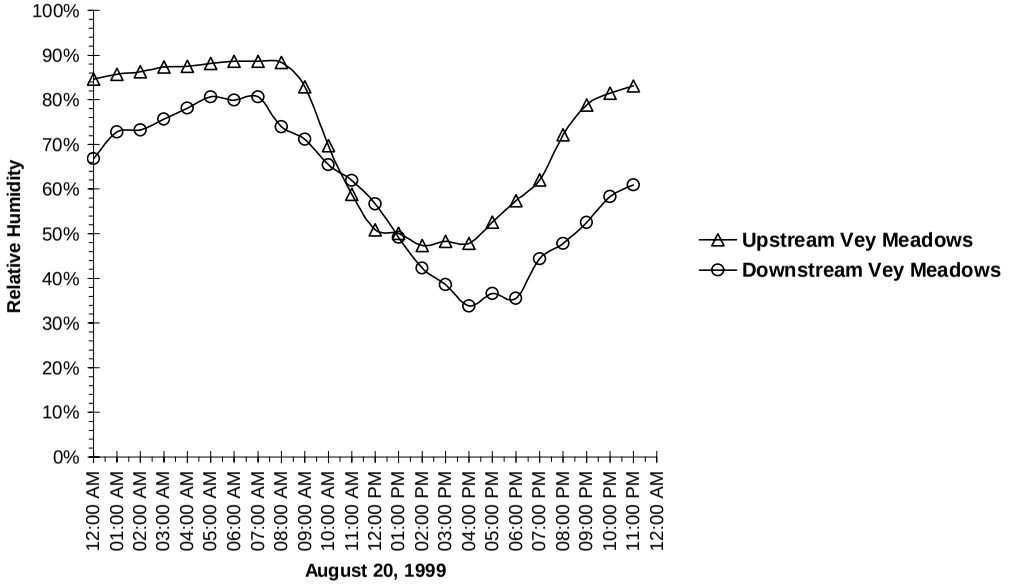

Figure A-48. Diel Air Temperature

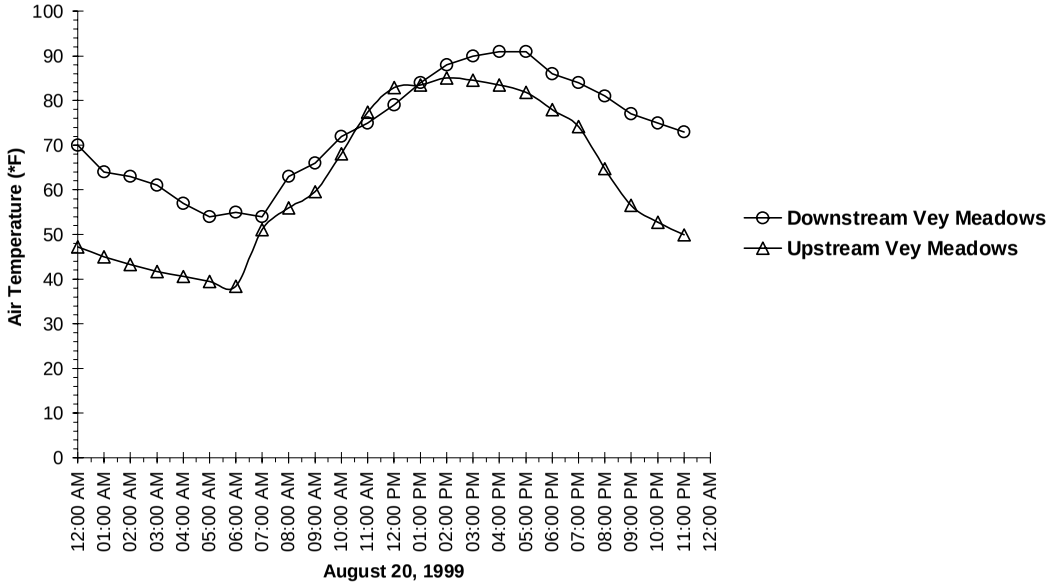

Figure A-49. Diel Tributary Temperatures

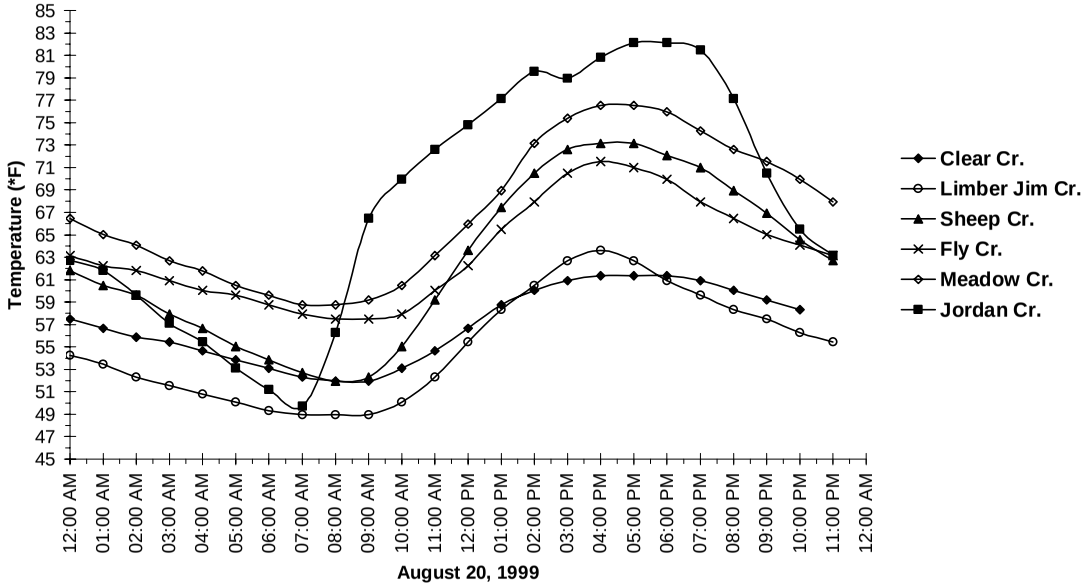

Figure A-50. Diel Tributary Temperatures

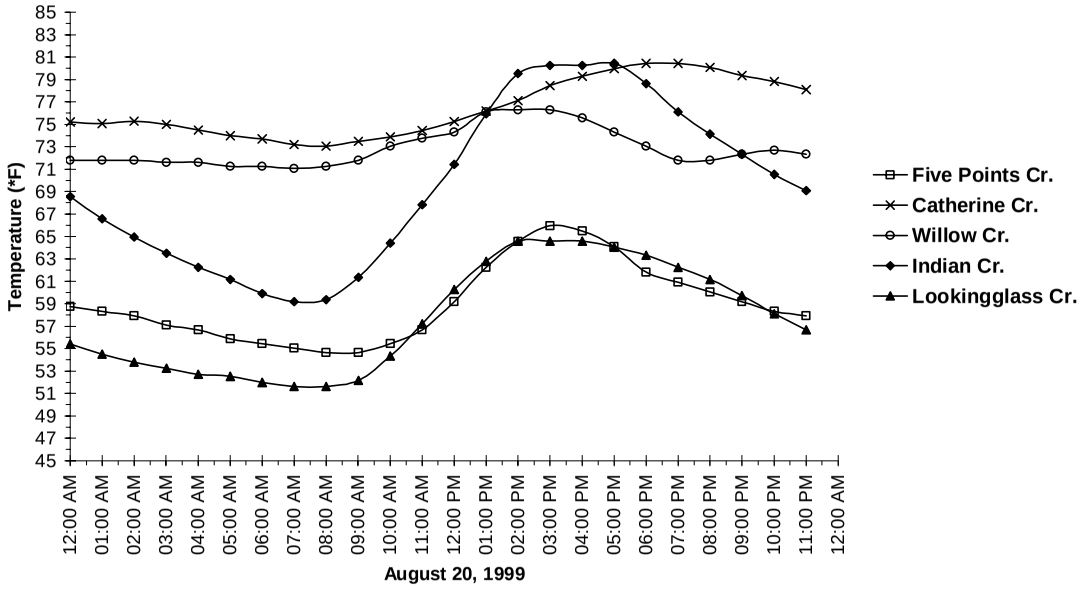

Figure A-51. Grande Ronde River Upstream Boundary Condition

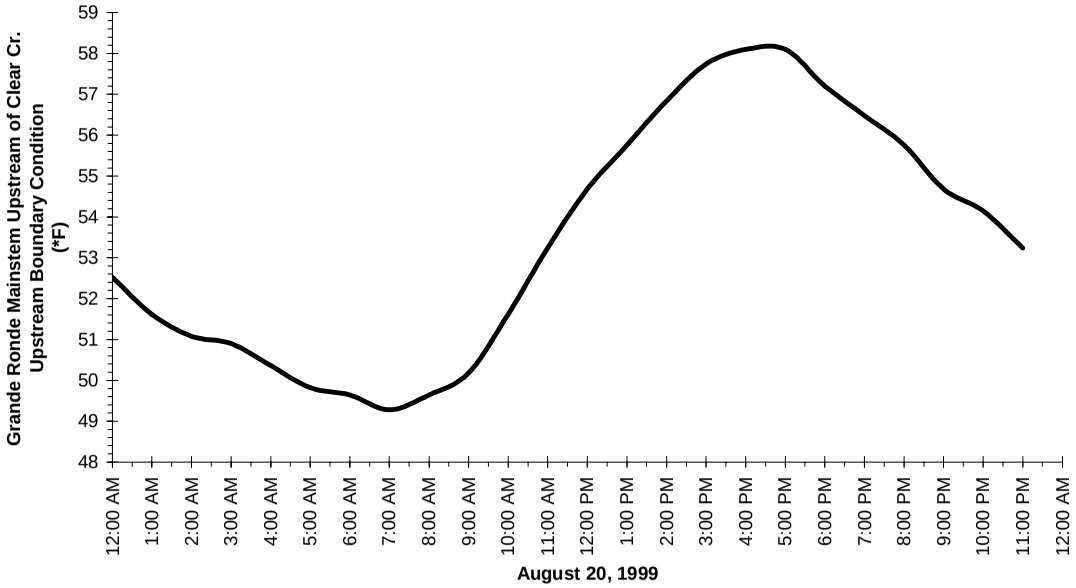

Model Development

Conceptual Model

At any particular instant of time, a defined stream reach is capable of sustaining a particular water column temperature. Stream temperature change that results within a defined reach is explained rather simply. The temperature of a parcel of water traversing a stream/river reach enters the reach with a given temperature. If that temperature is greater than the energy balance is capable of supporting, the temperature will decrease. If that temperature is less than energy balance is capable of supporting, the temperature will increase. Stream temperature change within a defined reach, is induced by the energy balance between the parcel of water and the surrounding environment and transport of the parcel through the reach.

Figure A-52. Temperature Model Flow Chart

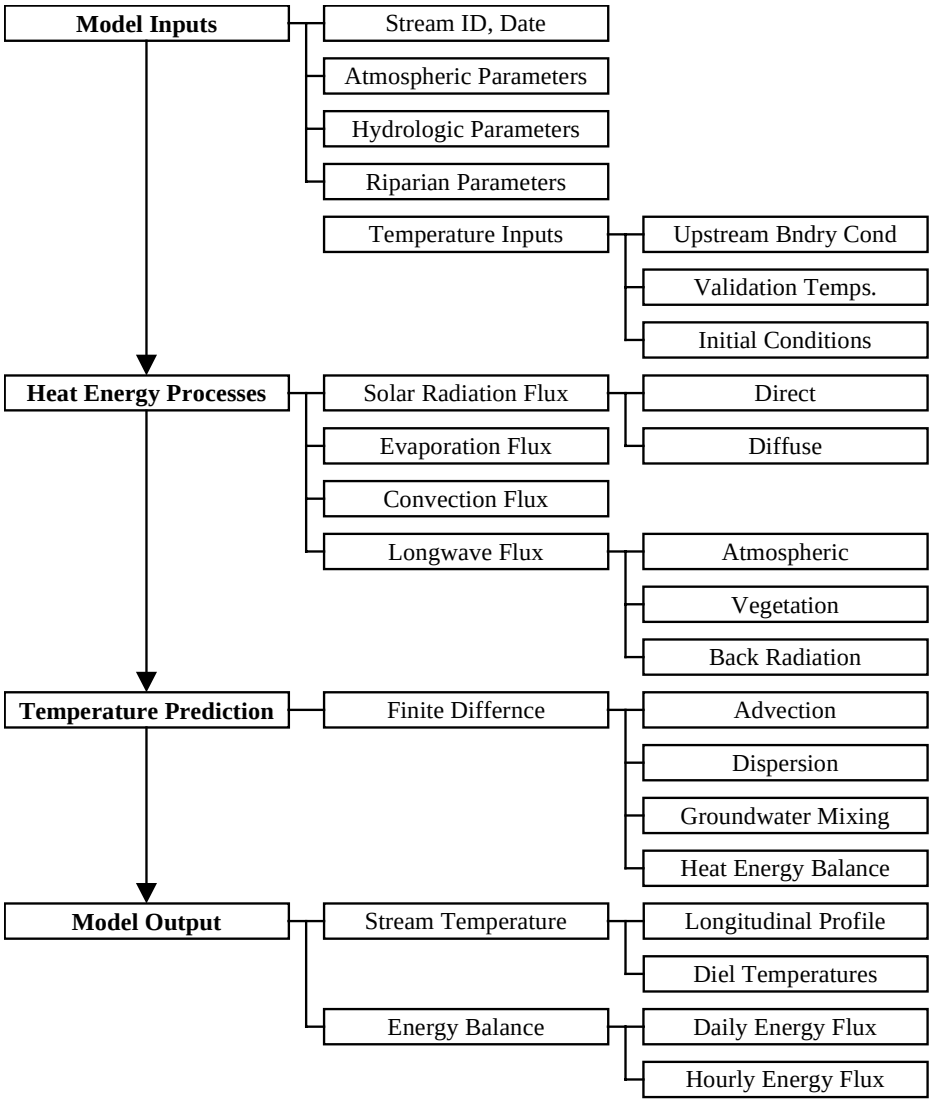

It takes time for the water parcel to traverse the longitudinal distance of the defined reach, during which the energy processes drive stream temperature change. At any particular instant of time, water that enters the upstream portion of the reach is never exactly the temperature that is supported by the defined reach. And, as the water is transferred downstream, heat energy and hydraulic process that are variable with time and space interact with the water parcel and induce water temperature change. The described modeling scenario is a simplification, however, understanding the basic processes in which stream temperatures change occurs over the course of a defined reach and period of time is essential. The general progression of the model is outlined in the model flow chart, **Figure A-52**.

Governing Equations

Heat Energy Processes

Water temperature change is a function of the change in heat energy contained in a discrete volume. It follows that large volume streams are less responsive to temperature change, and conversely, low flow streams will exhibit greater temperature sensitivity.

Water has a relatively high heat capacity ($c_w = 10^3$ cal kg^{-1} K^{-1}) (Satterlund and Adams 1992). Conceptually, water is a heat sink. Heat energy that is gained by the stream is retained and only slowly released back to the surrounding environment, represented by the cooling flux ($\Phi_{cooling}$). Heating periods occur when the net energy flux (Φ_{total}) is positive: ($\Phi_{heating} > \Phi_{cooling}$).

Equation A-1. Heat Energy Continuity,

$$\Phi_{total} = \Phi_{heating} - \Phi_{cooling}$$

In general, the net energy flux experienced by all stream/river systems follows two cycles: a seasonal cycle and a diurnal cycle. In the Pacific Northwest, the seasonal net energy cycle experiences a maximum positive flux during summer months (July and August), while the minimum seasonal flux occurs in winter months (December and January). The diurnal net energy cycle experiences a daily maximum flux that occurs at or near the sun's zenith angle, while the daily minimum flux often occurs during the late night or the early morning. It should be noted, however, that meteorological conditions are variable. Cloud cover and precipitation seriously alter the energy relationship between the stream and its environment.

The net heat energy flux (Φ_{total}) consists of several individual thermodynamic energy flux components, as depicted in **Figure A-53**, namely: solar radiation (Φ_{solar}), long-wave radiation ($\Phi_{longwave}$), conduction ($\Phi_{conduction}$), groundwater exchange ($\Phi_{groundwater}$) and evaporation ($\Phi_{evaporation}$).

Equation A-2. Net Heat Energy Continuity,

$$\Phi_{total} = \Phi_{solar} + \Phi_{longwave} + \Phi_{convection} + \Phi_{evaporation} + \Phi_{streambed} + \Phi_{groundwater}$$

Stream temperature is an expression of heat energy per unit volume, which in turn is an indication of the rate of heat exchange between a stream and its environment. The heat transfer processes that control stream temperature include solar radiation, longwave radiation, convection, evaporation and bed conduction (Wunderlich, 1972; Jobson and Keefer, 1979; Beschta and Weatherred, 1984; Sinokrot and Stefan, 1993; Boyd, 1996). With the exception of solar radiation, which only delivers heat energy, these processes are capable of both introducing and removing heat from a stream. **Figure A-53** displays heat energy processes that solely control heat energy transfer to/from a stream.

Figure A-53. Heat Energy Processes

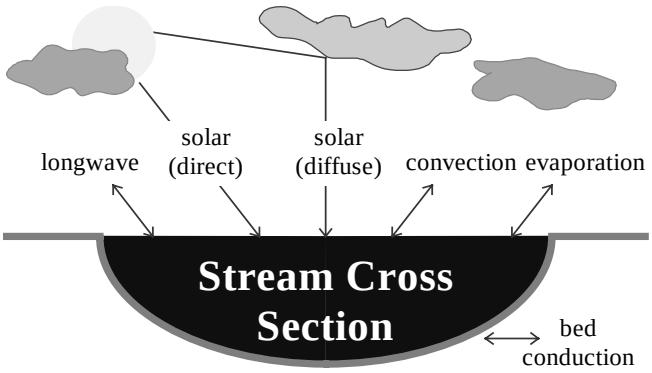

When a stream surface is exposed to midday solar radiation, large quantities of heat will be delivered to the stream system (Brown 1969, Beschta et al. 1987). Some of the incoming solar radiation will reflect off the stream surface, depending on the elevation of the sun. All solar radiation outside the visible spectrum (0.36μ to 0.76μ) is absorbed in the first meter below the stream surface and only visible light penetrates to greater depths (Wunderlich, 1972). Sellers (1965) reported that 50% of solar energy passing through the stream surface is absorbed in the first 10 cm of the water column. Removal of riparian vegetation, and the shade it provides, contributes to elevated stream temperatures (Rishel et al., 1982; Brown, 1983; Beschta et al., 1987). The principal source of heat energy delivered to the water column is solar energy striking the stream surface directly (Brown 1970). Exposure to direct solar radiation will often cause a dramatic increase in stream temperatures. The ability of riparian vegetation to shade the stream throughout the day depends on vegetation height, width, density and position relative to the stream, as well as stream aspect.

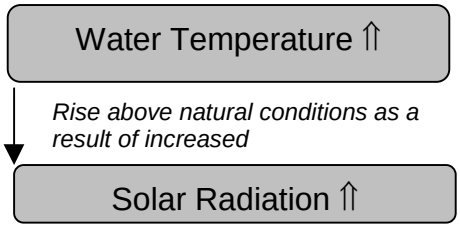

Both the atmosphere and vegetation along stream banks emit longwave radiation that can heat the stream surface. Water is nearly opaque to longwave radiation and complete absorption of all wavelengths greater than 1.2μ occurs in the first 5 cm below the surface (Wunderlich, 1972). Longwave radiation has a cooling influence when emitted from the stream surface. The net transfer of heat via longwave radiation usually balances so that the amount of heat entering is similar to the rate of heat leaving the stream (Beschta and Weatherred, 1984; Boyd, 1996).

Evaporation occurs in response to internal energy of the stream (molecular motion) that randomly expels water molecules into the overlying air mass. Evaporation is the most effective method of dissipating heat from water (Parker and Krenkel, 1969). As stream temperatures increase, so does the rate of evaporation. Air movement (wind) and low vapor pressures increase the rate of evaporation and accelerate stream cooling (Harbeck and Meyers, 1970).

Convection transfers heat between the stream and the air via molecular and turbulent conduction (Beschta and Weatherred, 1984). Heat is transferred in the direction of warmer to cooler. Air can have a warming influence on the stream when the stream is cooler. The opposite is also true. The amount of convective heat transfer between the stream and air is low (Parker and Krenkel, 1969; Brown, 1983). Nevertheless, this should not be interpretted to mean that air temperatures do not affect stream temperature.

Depending on streambed composition, shallow streams (less than 20 cm) may allow solar radiation to warm the streambed (Brown, 1969). Large cobble (> 25 cm diameter) dominated streambeds in shallow streams may store and conduct heat as long as the bed is warmer than the stream. Bed conduction may cause maximum stream temperatures to occur later in the day, possibly into the evening hours.

The instantaneous heat transfer rate experienced by the stream is the summation of the individual processes:

$$\Phi_{Total} = \Phi_{Solar} + \Phi_{Longwave} + \Phi_{Evaporation} + \Phi_{Convection} + \Phi_{Conduction} .$$

Solar Radiation (Φ_{Solar}) is a function of the solar angle, solar azimuth, atmosphere, topography, location and riparian vegetation. Simulation is based on methodologies developed by Ibqal (1983) and Beschta and Weatherred (1984). *Longwave Radiation* ($\Phi_{Longwave}$) is derived by the Stefan-Boltzmann Law and is a function of the emissivity of the body, the Stefan-Boltzmann constant and the temperature of the body (Wunderlich, 1972). *Evaporation* ($\Phi_{Evaporation}$) relies on a Dalton-type equation that utilizes an exchange coefficient, the latent heat of vaporization, wind speed, saturation vapor pressure and vapor pressure (Wunderlich, 1972). *Convection* ($\Phi_{Convection}$) is a function of the Bowen Ratio and terms include atmospheric pressure, and water and air temperatures. *Bed Conduction* ($\Phi_{Conduction}$) simulates the theoretical relationship ($\Phi_{Conduction} = K \cdot dT_b / dz$), where calculations are a function of thermal conductivity of the bed (K) and the temperature gradient of the bed (dT_b/dz) (Sinokrot and Stefan, 1993). Bed conduction is solved with empirical equations developed by Beschta and Weatherred (1984).

The ultimate source of heat energy is solar radiation both diffuse and direct. Secondary sources of heat energy include long-wave radiation, from the atmosphere and streamside vegetation, streambed conduction and in some cases, groundwater exchange at the water-stream bed interface. Several processes dissipate heat energy at the air-water interface, namely: evaporation, convection and back radiation. Heat energy is acquired by the stream system when the flux of heat energy entering the stream is greater than the flux of heat energy leaving. The net energy flux provides the rate at which energy is gained or lost per unit area and is represented as the instantaneous summation of all heat energy components.

Non-Uniform Heat Energy Transfer Equation

The rate change in stream temperature is driven by the heat energy flux (Φ_i). It is easily shown that a defined volume of water will attain a predictable rate change in temperature, provided an accurate prediction of the heat energy flux. The rate change in stream temperature (T) is calculated as shown in **Equation A-4**.

Equation A-3. Rate Change in Temperature Caused by Heat Energy Thermodynamics,

$$\frac{\partial T}{\partial t} = \left(\frac{Ax_i \cdot \Phi_i}{\rho \cdot c_p \cdot V_i} \right),$$

Which reduces to,

$$\frac{\partial T}{\partial t} = \left(\frac{\Phi_i}{\rho \cdot c_p \cdot D_i} \right).$$

Where,

Ax_i:	cross-sectional area (m^2)
C_p:	specific heat of water (cal $kg^{-1} \cdot {}^oC^{-1}$)
D_i:	average stream depth (m)
t:	time (s)
T:	Temperature (^oC)
V_i:	volume (m^3)
Φ_i:	total heat energy flux (cal $m^{-2} \cdot s^{-1}$)
ρ:	density of water (kg/m^3)

Advection (U_x) redistributes heat energy in the positive longitudinal direction. No heat energy is lost or gained by the system during advection, and instead, heat energy is transferred downstream as a function of flow velocity. In the case where flow is uniform, the rate change in temperature due to advection is expressed in the first order partial differential equation below.

Equation A-4. Rate Change in Temperature Caused by Advection,

$$\frac{\partial T}{\partial t} = -U_x \cdot \frac{\partial T}{\partial x}$$

Dispersion processes occur in both the upstream and downstream direction along the longitudinal axis. Heat energy contained in the system is conserved throughout dispersion, and similar to advection, heat energy is simply moved throughout the system. The rate change in temperature due to dispersion is expressed in the second order partial differential equation below.

Equation A-5. Rate Change in Temperature Caused by Dispersion,

$$\frac{\partial T}{\partial t} = D_L \cdot \frac{\partial^2 T}{\partial x^2}$$

The dispersion coefficient (D_L) may be calculated by stream dimensions, roughness and flow (Fischer et. al. 1979). In streams that exhibit high flow velocities and low longitudinal temperature gradients, it may be assumed that the system is advection dominated and the dispersion coefficient may be set to zero (Sinokrot and Stefan 1993). In the event that dispersion effects are considered significant, the appropriate value for the dispersion coefficient can be estimated with a practical approach developed and employed in the QUAL 2e model (Brown and Barnwell 1987). An advantage to this approach is that each parameter is easily measured, or in the case of Manning's coefficient (n) and the dispersion constant (K_d), estimated.

Equation A-6. Physical Dispersion Coefficient,

$$D_L = C \cdot K_d \cdot n \cdot U_x \cdot D^{\frac{5}{6}}$$

Where,

C:	Unit conversion C = 3.82 for English units C = 1.00 for Metric units
D:	Average stream depth (m)
D_L:	Dispersion coefficient (m^2/s)
K_d:	Dispersion constant
n:	Manning's coefficient
U_x:	Average flow velocity (m/s)

The simultaneous non-uniform one-dimensional transfer of heat energy is the summation of the rate change in temperature due to heat energy thermodynamics, advection and dispersion. Given that the stream is subject to steady flow conditions and is well mixed, transverse temperature gradients are negligible (Sinokrot and Stefan 1993). An assumption of non-uniform flow implies that cross-sectional area and flow velocity vary with respect to longitudinal position. The following second ordered parabolic partial differential equation describes the rate change in temperature for non-uniform flow.

Equation A-7. Non-Uniform One-dimensional Heat Energy Transfer,

$$\frac{\partial T}{\partial t} = -U_x \cdot \frac{\partial T}{\partial x} + D_L \cdot \frac{\partial^2 T}{\partial x^2} + \frac{\Phi}{c_p \cdot \rho \cdot D_i}$$

Steady Flow: $\frac{\partial U_x}{\partial t} = 0$

Non-Uniform Flow: $\frac{\partial U_x}{\partial x} \neq 0$

The solution to the *one-dimensional heat energy transfer equation* is essentially the summation of thermodynamic heat energy exchange between the stream system and the surrounding environment and physical processes that redistribute heat energy within the stream system. It is important to note that all heat energy introduced into the stream is conserved, with the net heat energy value reflected as stream temperature magnitude. Further, heat energy is transient within the stream system, due to longitudinal transfer of heat energy (i.e., advection and dispersion). The net heat energy flux (Φ) is calculated at every distance step and time step based on physical and empirical formulations developed for each significant energy component. The dispersion coefficient (D_L) is assumed to equal zero.

Boundary Conditions and Initial Values

The temperatures at the upstream boundary (i_o) for all time steps (t_o ,t_1,..., t_{M-1}, t_M) are supplied by the upstream temperature inputs. At the downstream boundary temperature at longitudinal position i_{n+1} is assumed to equals that of i_n with respect to time t. Initial values of the temperatures at each distance node (i_o ,i_1,..., i_{N-1}, i_N) occurring at the starting time (t_o) can be input by the model user or assumed to equal the boundary condition at time t_o.

Spatial and Temporal Scale

The lengths of the defined reaches are limited by hydrologic, riparian and channel morphology homogeneity. Reach length determinations are based on no major surface inflow from merging surface or subsurface water bodies, homogenous riparian characteristics, stream aspect, width, flow volume, velocity and/or depth. The temperature model is designed to analyze and predict stream temperature for one day and is primarily concerned with daily prediction of the diurnal energy flux and resulting temperatures on August 20, 1999. Prediction time steps are limited by stability considerations for the finite difference solution method.

Site Potential Development Matrix

1. Physiographic units developed by Clausntzer and Crowe (1997) list potential overstory streambank and terrace vegetation types. Average heights of overstory vegetation are derived for each physiographic unit (Clausntzer and Crowe 1997) and are presented. Where vegetation height is less than the average vegetation height for the appropriate physiographic unit, values are increased to "potentials" as detailed in **Figure A-27** and **Table A-19**. Vegetation density values are assumed to equal 80% for all potential vegetation conditions.

Recall **Figure A-27.** Physiographic Units of the Upper Grande Ronde Sub-Basin (Clausnitzer and Crowe, 1997)

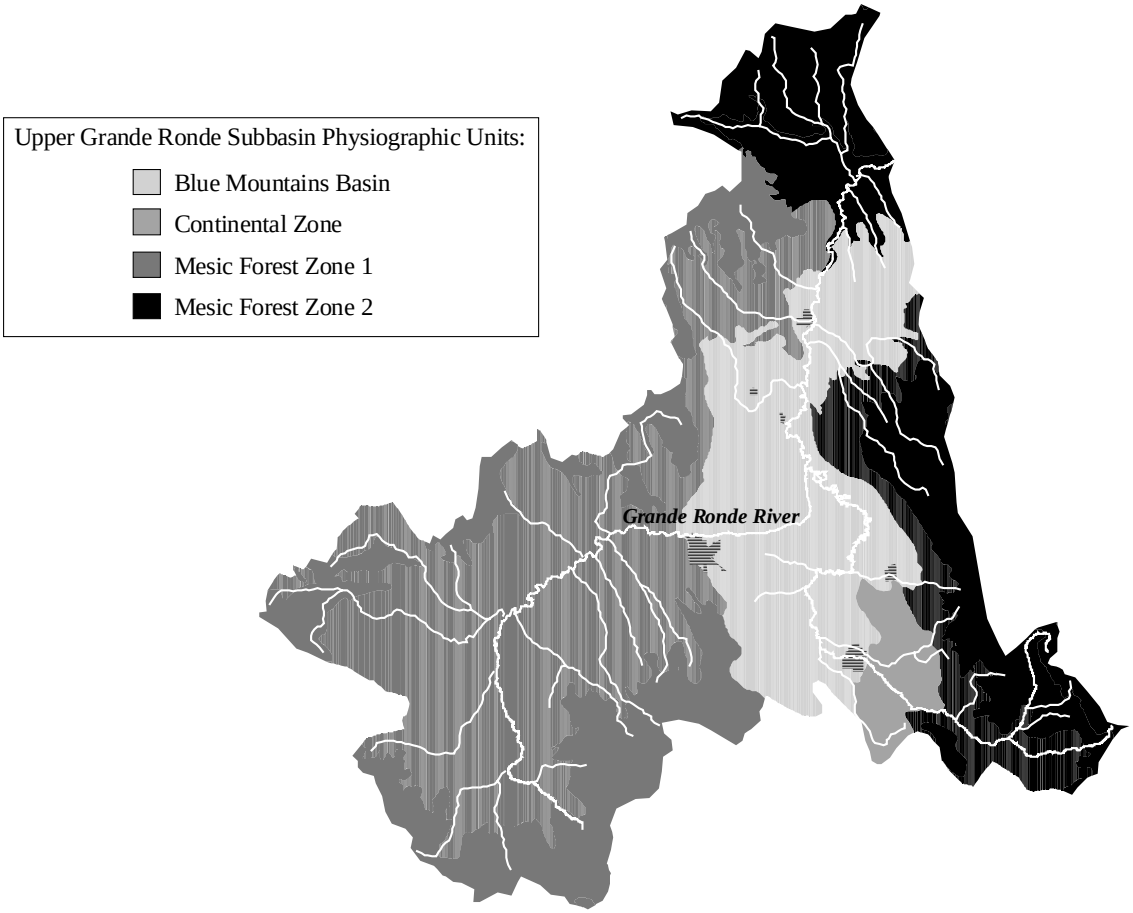

Recall **Table A-19.** Physiographic Unit Vegetation Characteristics				
Physiographic Unit	Elevation (feet)	Potential Terrace/Streambank Overstory Vegetation	Height (feet)	Assumed Density
Continental Zone and Blue Mountain Basin Zone	All	Quaking Aspen	70	
		Black cottonwood	100	
		Ponderosa Pine	125	
		Douglas fir	140	
		Mountain alder	40	
		Composite Dimension	**95**	**80%**
Mesic Forest Zone 1	<4,800	Quaking Aspen	70	
		Black cottonwood	100	
		Ponderosa Pine	125	
		Douglas fir	140	
		Grand fir	125	
		Composite Dimension	**112**	**80%**
	>4,800	Lodgepole pine	50	
		Subalpine fir	40	
		Engelmann spruce	80	
		Composite Dimension	**57**	**80%**
Mesic Forest Zone 2	<4,800	Black cottonwood	100	
		Ponderosa pine	125	
		Douglas fir	140	
		Grand fir	125	
		Engelmann spruce	80	
		Composite Dimension	**114**	**80%**
	>4,800	Lodgepole pine	50	
		Subalpine fir	40	
		Engelmann spruce	80	
		Composite Dimension	**57**	**80%**

The Oregon Department of Agriculture (ODA) has suggested potential heights for black cottonwoods along the Grande Ronde River within agricultural areas. Assumptions were based upon **Silvics of North American Trees**[5] and a soils map of the Grande Ronde valley. Potential black cottonwood height depends upon riparian soil types, thus ODA has given three site potential classes based upon existing soil types. Please recall that **Table A-20** summarizes the different potential black cottonwood heights at various locations in the Grande Ronde valley.

Recall **Table A-20**. Potential Black Cottonwood Heights in the Grande Ronde River Valley			
Location	Site Classification	Percentage of Bank	Potential Height (ft)
Island City to Head of State Ditch	1	35%	140
	2	50%	97
	3	15%	70
	Average Potential Black Cottonwood Height⇒		**108**
State Ditch	1	25%	140
	2	12.5%	97
	3	62.5%	70
	Average Potential Black Cottonwood Height⇒		**91**
Bottom of State Ditch to Imbler	1	20%	140
	2	50%	97
	3	30%	70
	Average Potential Black Cottonwood Height⇒		**98**
Imbler to Rhinehart	1	3%	140
	2	85%	97
	3	12%	70
	Average Potential Black Cottonwood Height⇒		**95**

2. Tributary temperatures are assumed to be below 64^{o}F.
3. Bankfull channel widths are reduced to values listed in **Table A-21** when exceeding these values (see **Figure A-55**).

Table A-21. Grande Ronde River Channel Width Reductions	
Grande Ronde Mainstem Reaches	Maximum Bankfull Channel Width
Tanner Gulch Sheep Cr. Confluences	65 feet
Sheep Cr. to Fly Cr. Confluences	82 feet
Fly Cr. to Indian Cr. Confluences	98 feet
Indian Cr. to Lookingglass Cr. Confluences	115 feet
Lookingglass Cr. Wallowa R. Confluences	131 feet

[5] Burns, R. M. and B. H. Honkala (1990). Silvics of North American Trees. Vol2, Hardwoods. Washington, D.C., U.S. Department of Agriculture.

4. Increase sinuosity in unconfined channels until either sinuosity equals 1.7 or wetted width to depth ratio is 20 or less. Unconfined channels were identified by McIntosh (1992) and confirmed with valley morphology mapping by surface slopes derived from DEMs (see **Figure A-56**).

Table A-22. Grande Ronde River Unconfined Channels

Grande Ronde Mainstem Reaches	Distance from Mouth (miles)
Vey Meadow	169.2 to 163.8
Upstream Meadow Cr.	154.0 to 150.9
Downstream Beaver Cr.	149.3 to 146.7
Upstream Jordan Cr.	144.8 to 142.4
Downstream Jordan Cr.	140.6 to 140.0
Upstream Five Points Cr.	138.3 to 136.5
Grande Ronde Valley	130.8 to 104.4
Lower Valley	102.6 to 95.1

5. Where width to depth ratios are greater than 30, decrease wetted widths by 2% increments until width to depth ratios equal 30.
6. Conserving instream flow and adding tributary flow where appropriate derives potential flow volumes (see **Figure A-57**).

Figure A-54. Streambank Vegetation Height - Current Conditions and Potential

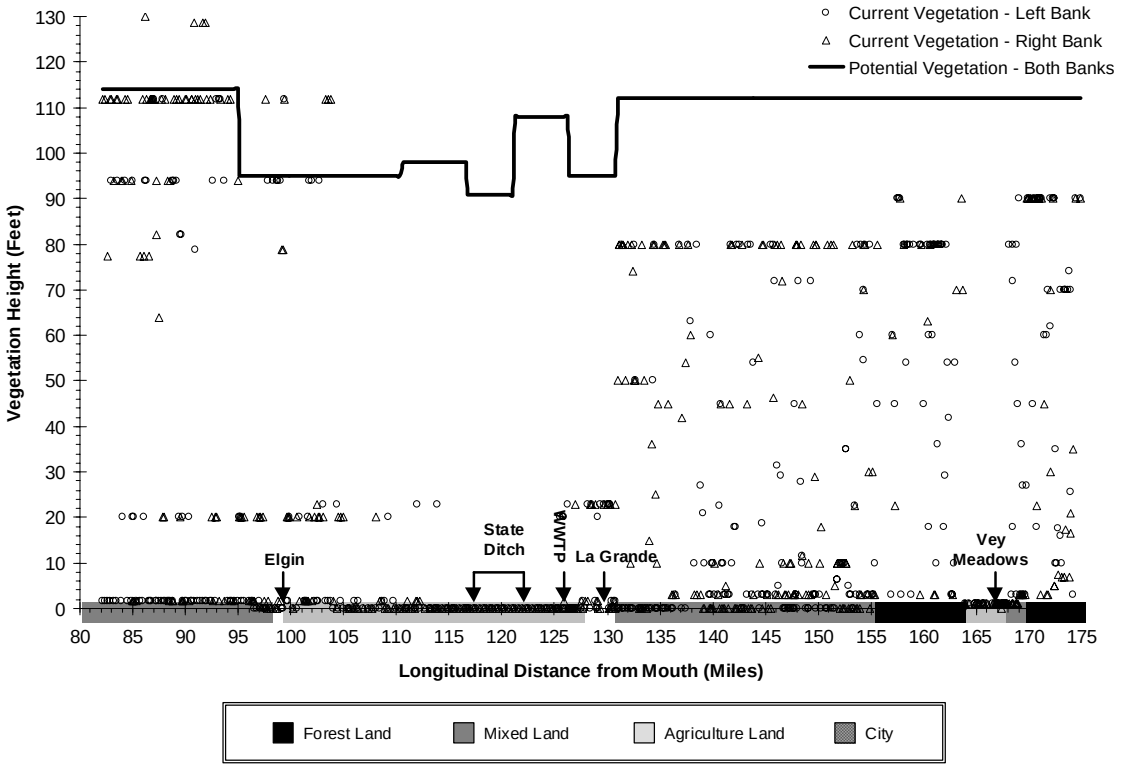

Figure A-55. Bankfull Channel Width - Current Conditions and Potential

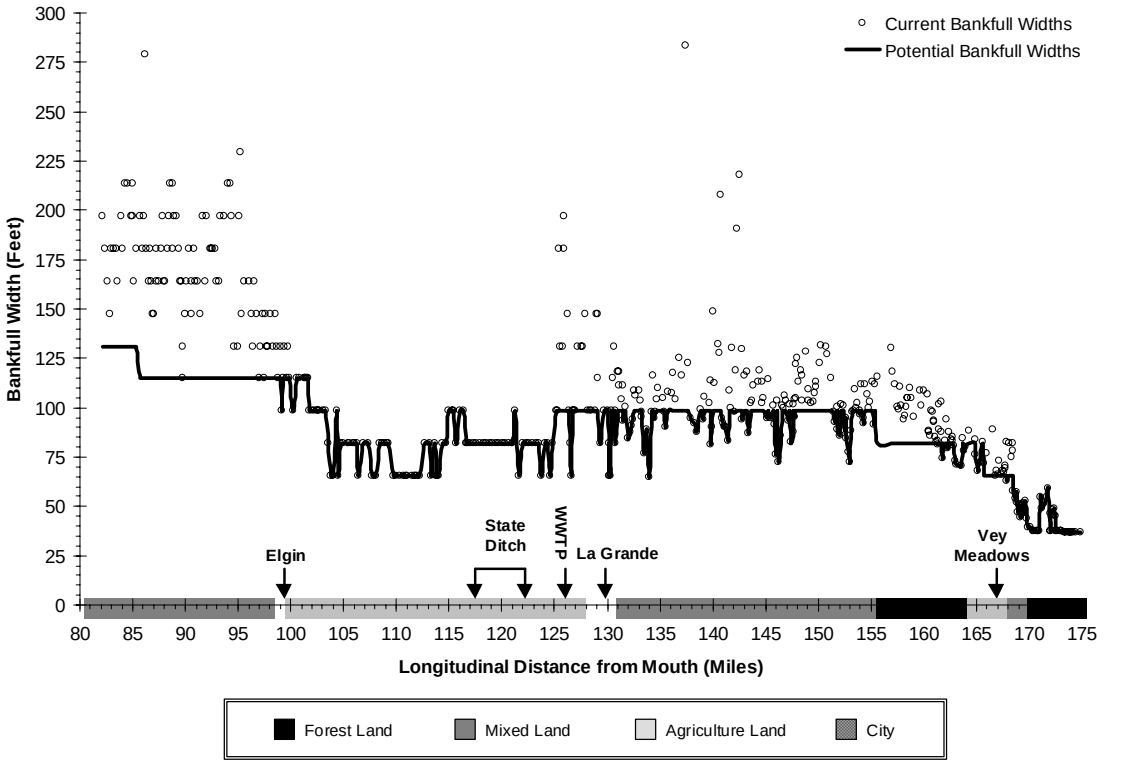

Figure A-56. Sinuosity - Current Conditions and Potential

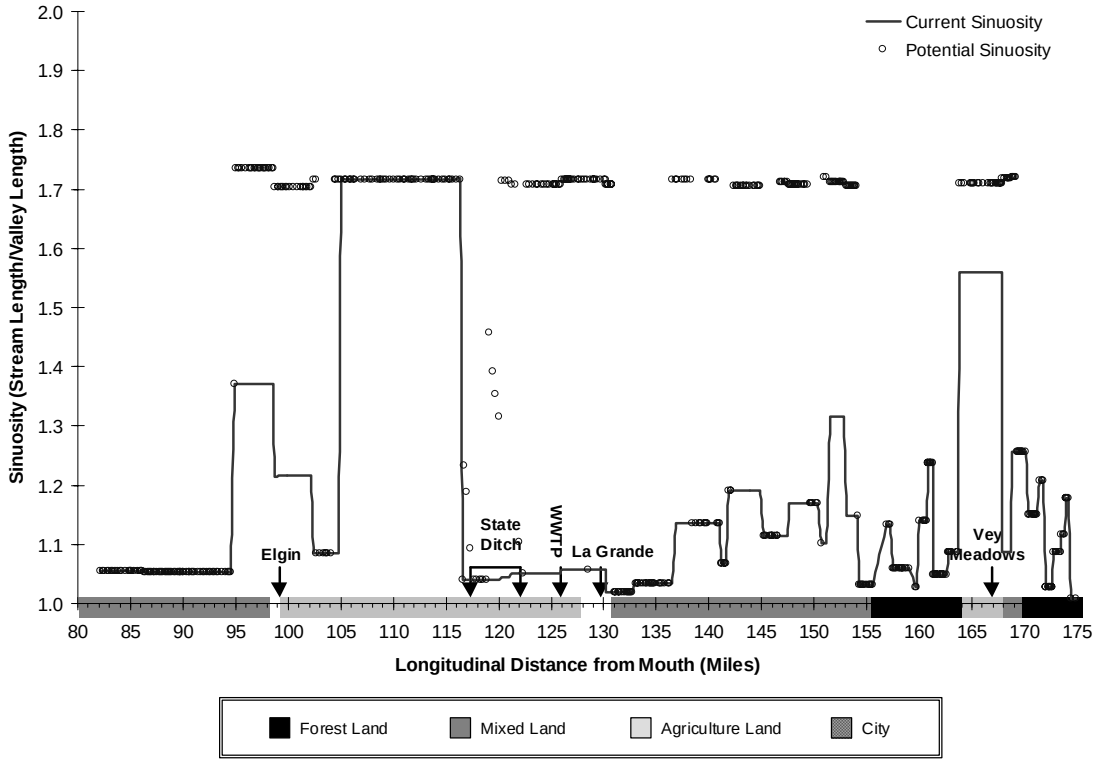

Figure A-57. August 20, 1999 Flow Volume - Current Conditions and Potential

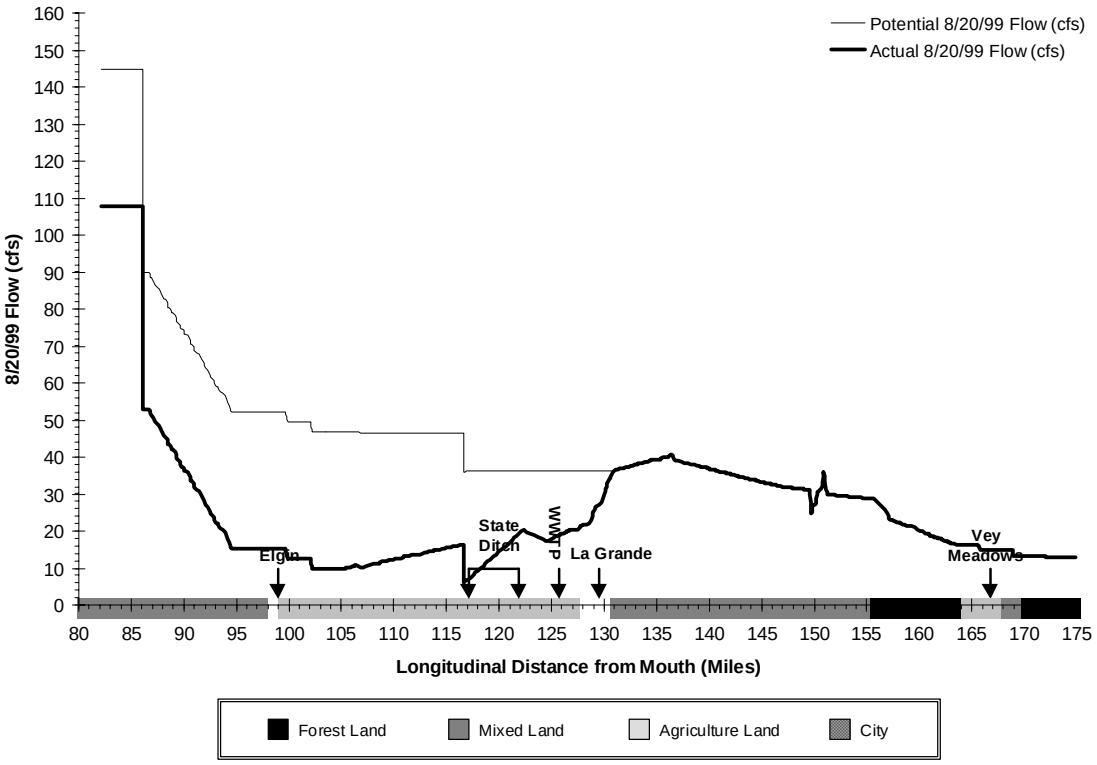

Results

Validation

Spatial Data Validation	*Continuous Data Validation*
n = 499	n = 155
R^2 = 0.93	R^2 = 0.91
Average Standard Error = 1.44°F	Average Standard Error = 1.60°F
Average Deviation = 1.21 °F	Average Deviation = 1.71 °F

Spatial Data Validation

Figure A-58. Grande Ronde River observed and predicted spatial temperature data on 8/20/99.

n = 499

R^2 = 0.93

Standard Error = 1.44°F

Average Deviation = 1.21°F

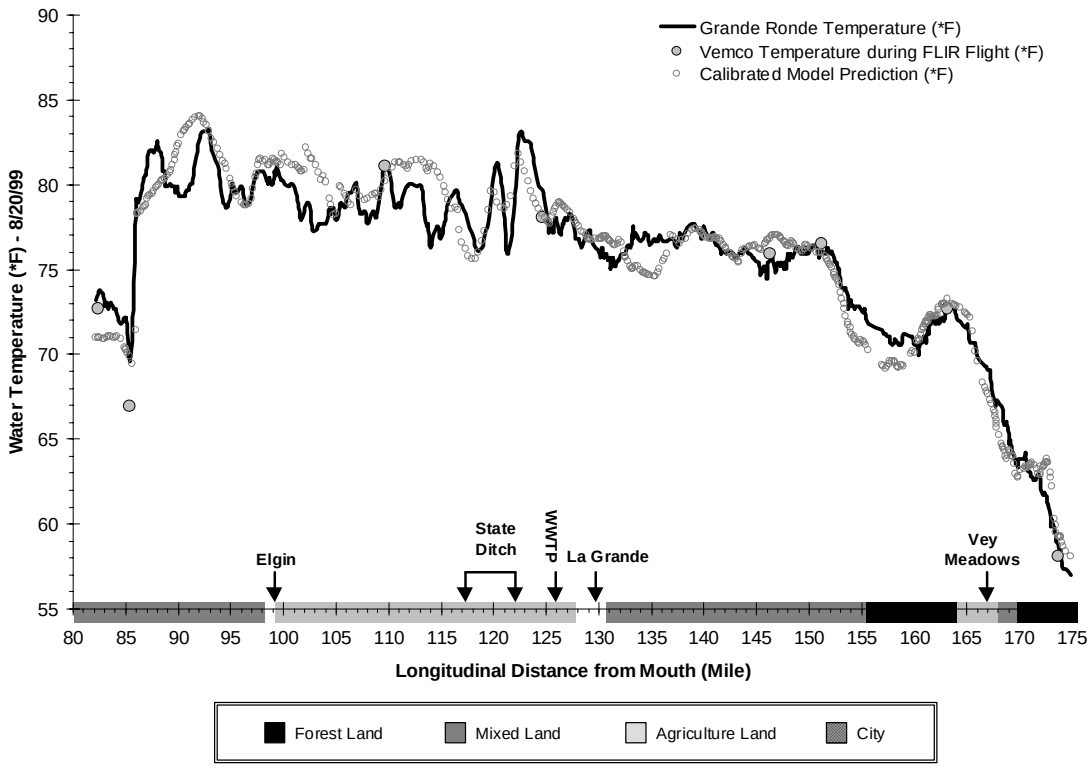

Continuous Data Validation

Figure A-59. Grande Ronde River Downstream Vey Meadow (Continuous Node 2)

$R^2 = 0.70$
Standard Error = 3.85°F
Average Deviation = 3.26°F

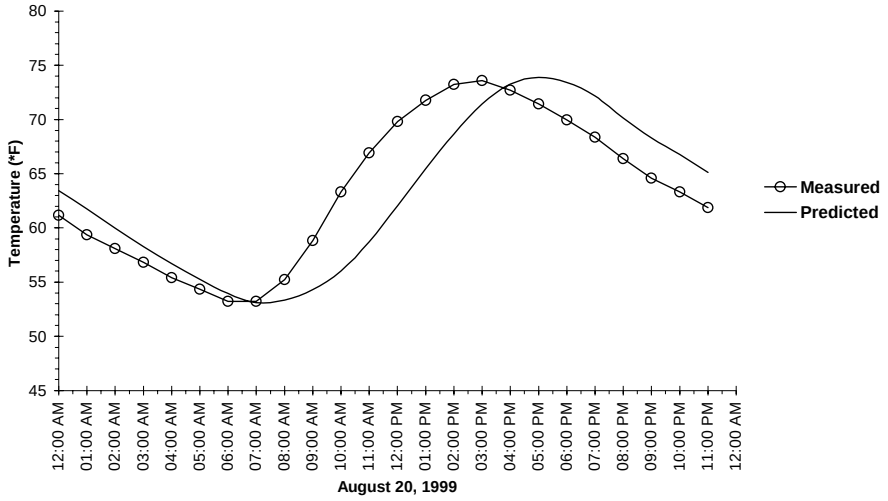

Figure A-60. Grande Ronde River Upstream Meadow Creek (Continuous Node 3)

$R^2 = 0.95$
Standard Error = 1.67°F
Average Deviation = 1.99°F

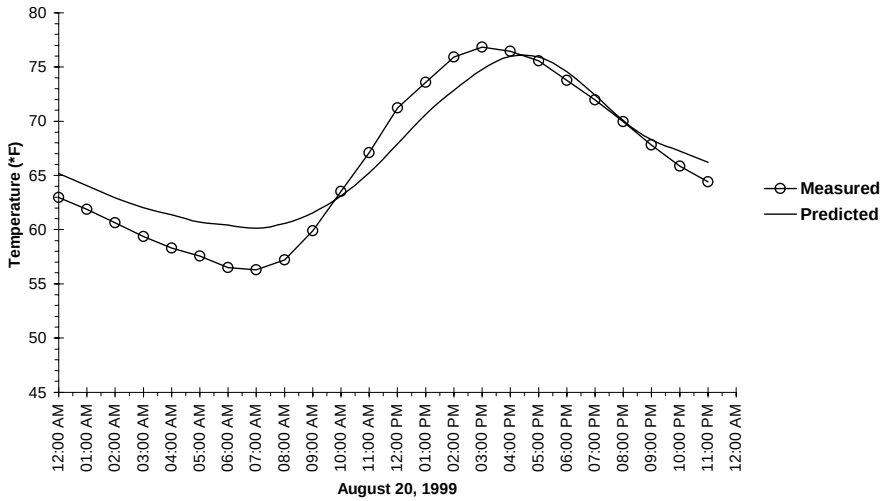

Figure A-61. Grande Ronde River Upstream Red Bridge (Continuous Node 4)

$R^2 = 0.97$
Standard Error = 0.47^oF
Average Deviation = 0.50^oF

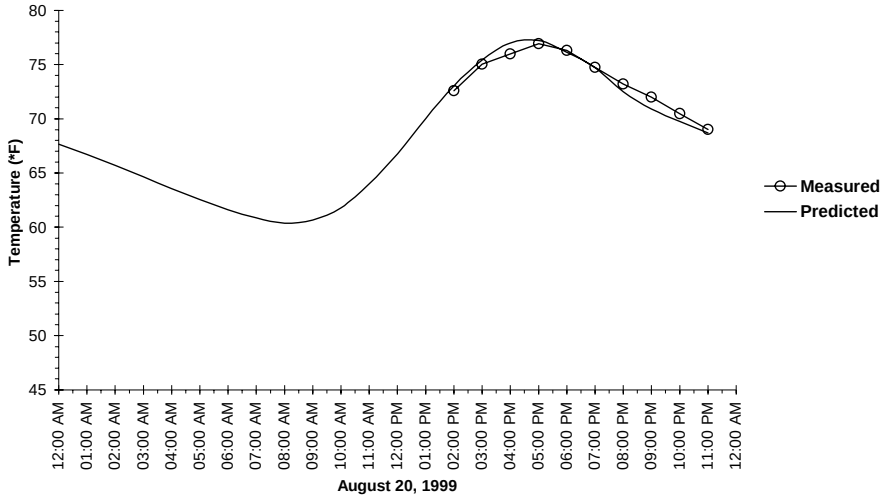

Figure A-62. Grande Ronde River Upstream Pierce Lane (Continuous Node 5)

$R^2 = 0.97$
Standard Error = 0.76^oF
Average Deviation = 1.24^oF

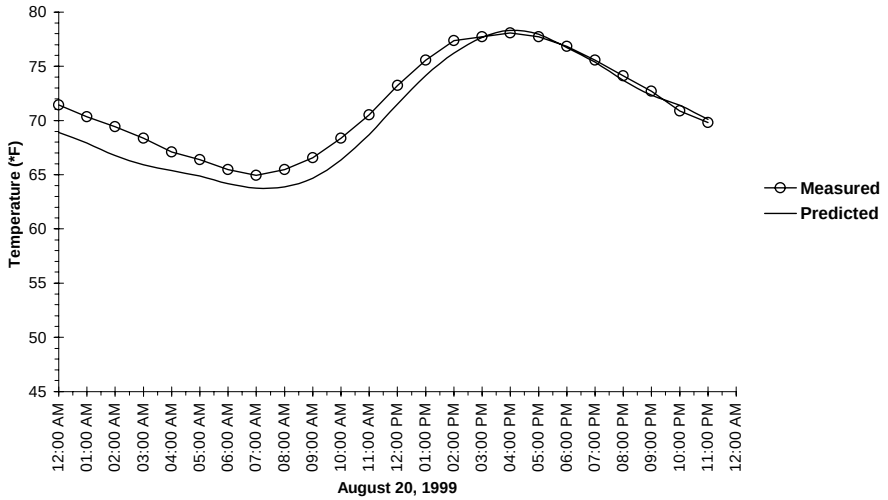

Figure A-63. Grande Ronde River at Striker Lane (Continuous Node 6)

$R^2 = 0.97$
Standard Error = 0.72^oF
Average Deviation = 0.58^oF

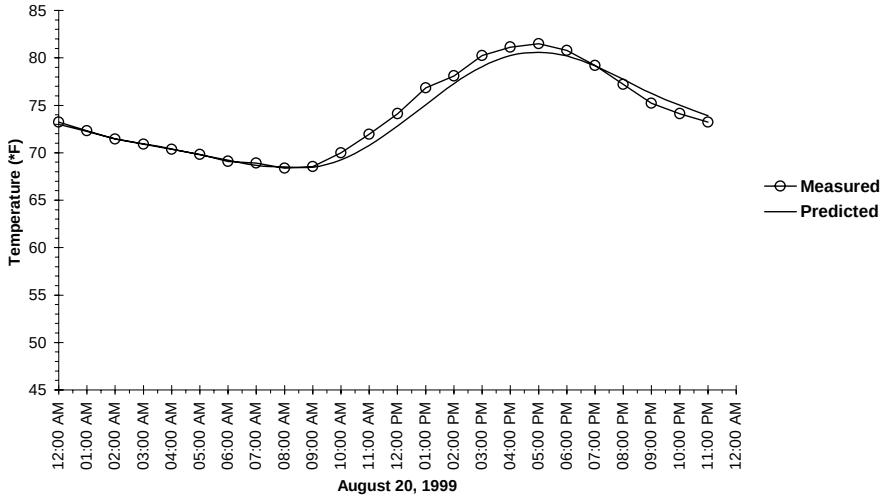

Figure A-64. Grande Ronde River Downstream Palmer Junction (Continuous Node 7)

$R^2 = 0.98$
Standard Error = 0.72^oF
Average Deviation = 0.95^oF

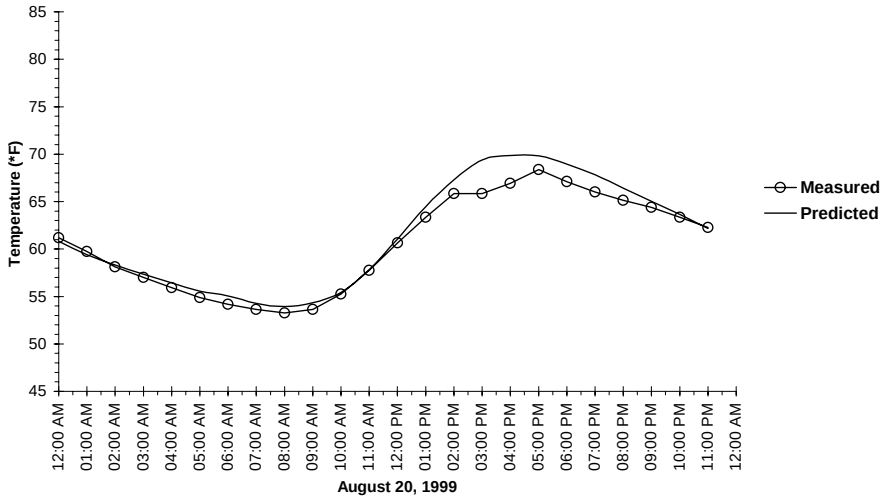

Figure A-65. Grande Ronde River at Rondowa (Continuous Node 8)

$R^2 = 0.84$
Standard Error = 2.99°F
Average Deviation = 3.46°F

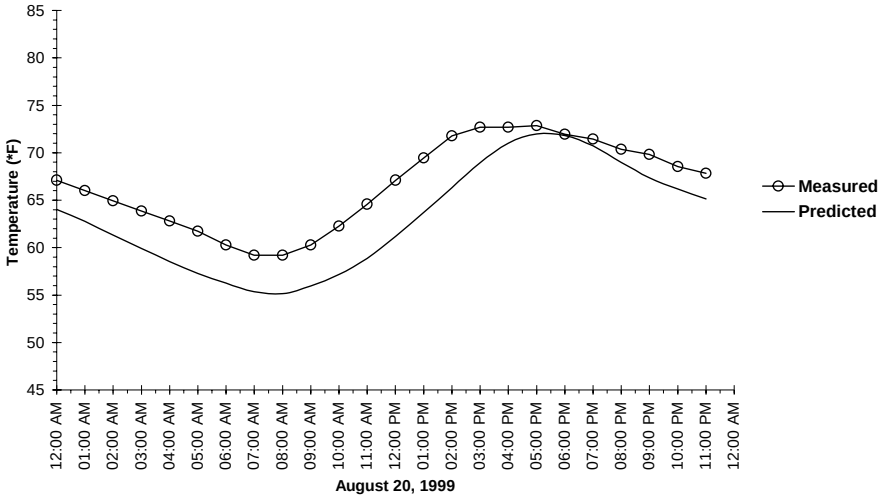

Temperature Scenario Simulations

Figure A-66. Potential Vegetation Scenario

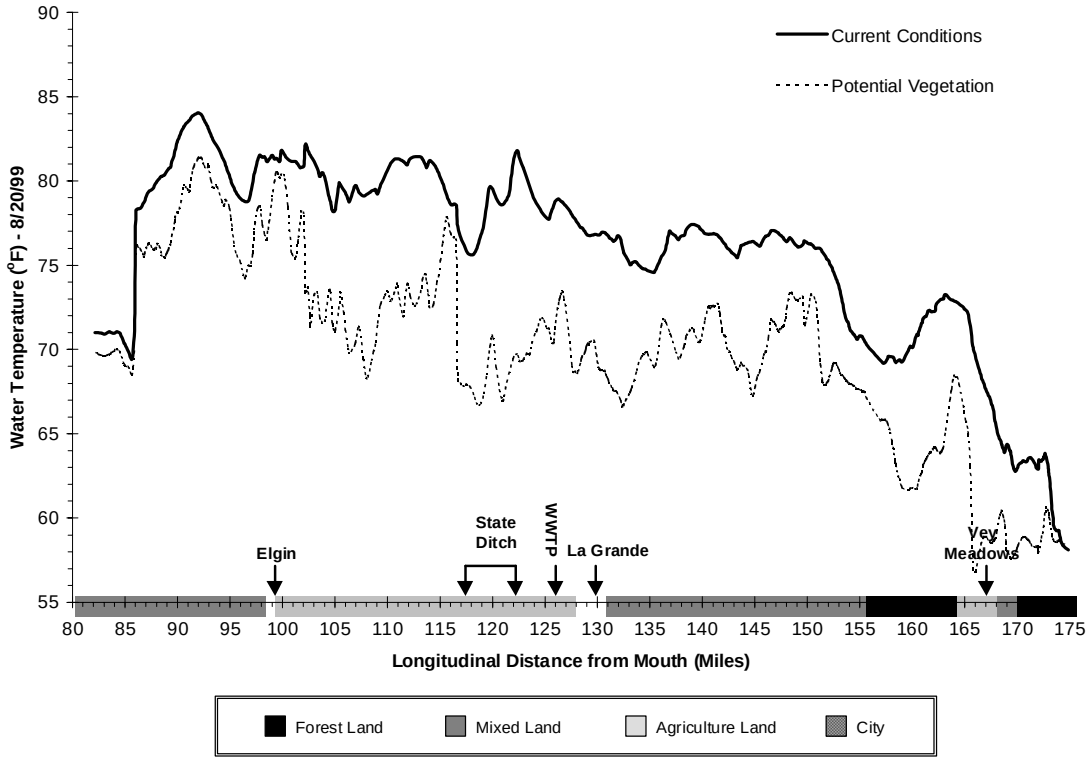

Figure A-67. Bankfull Channel Width Reduction Scenario

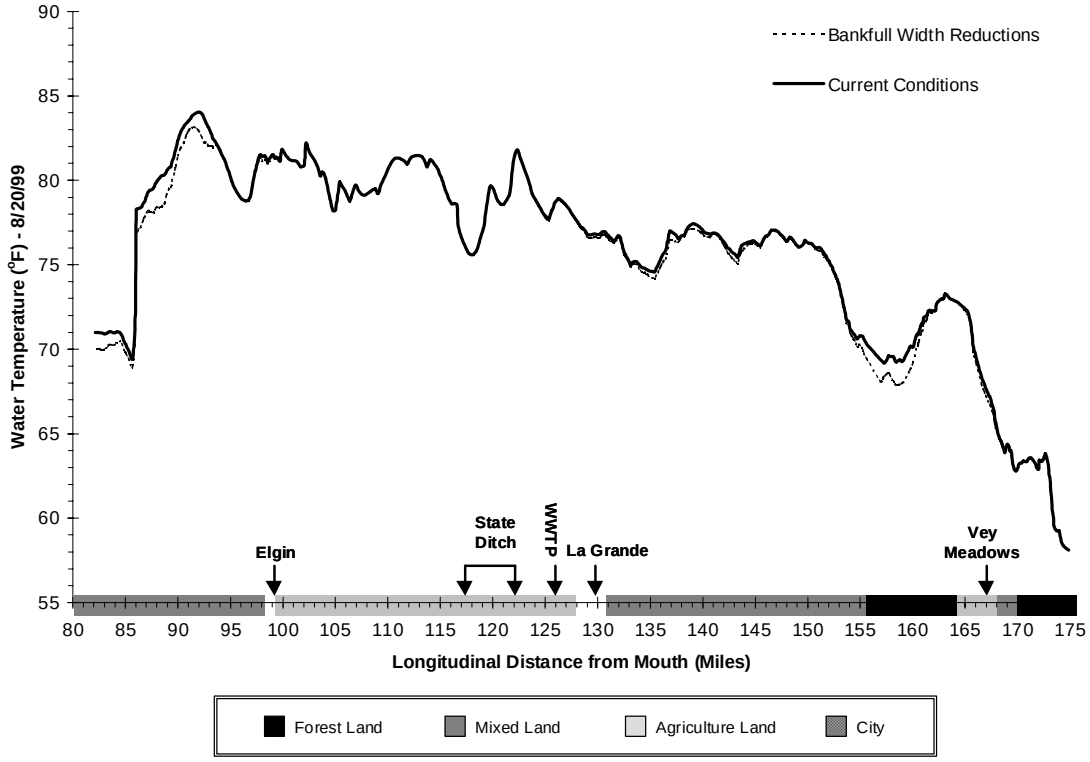

Figure A-68. Tributary Temperature Reduction (Less than 64°F) Scenario

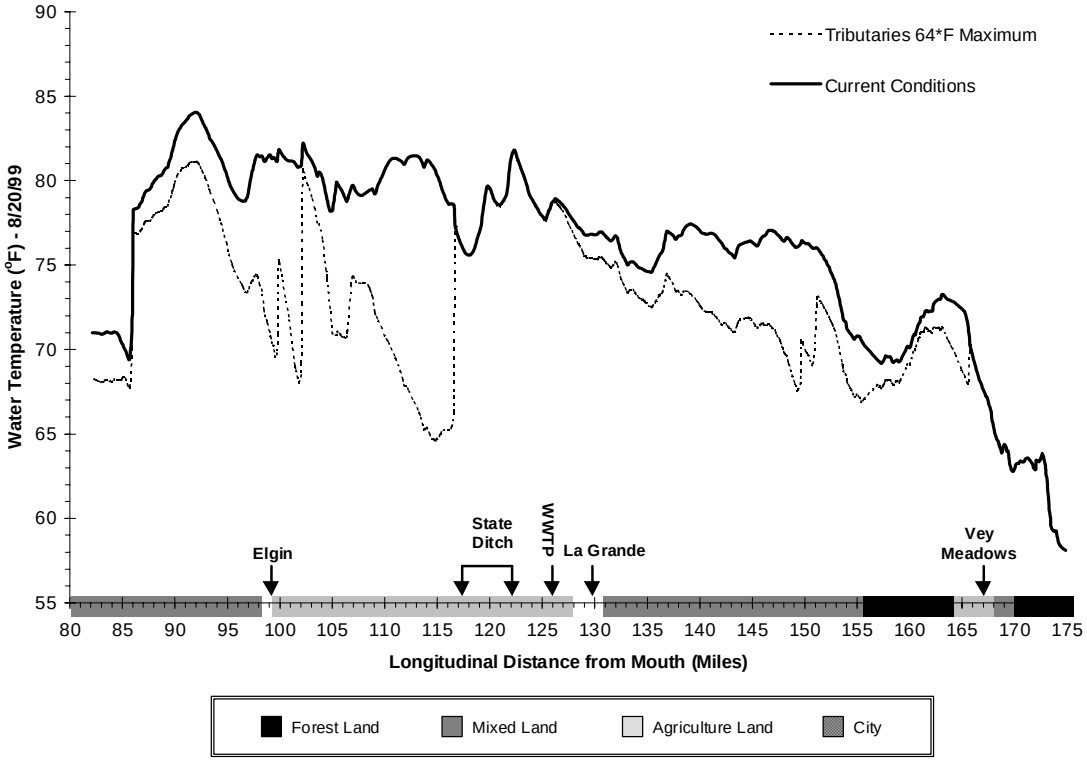

Figure A-69. Sinuosity Increases and Width:Depth Reduction Scenario

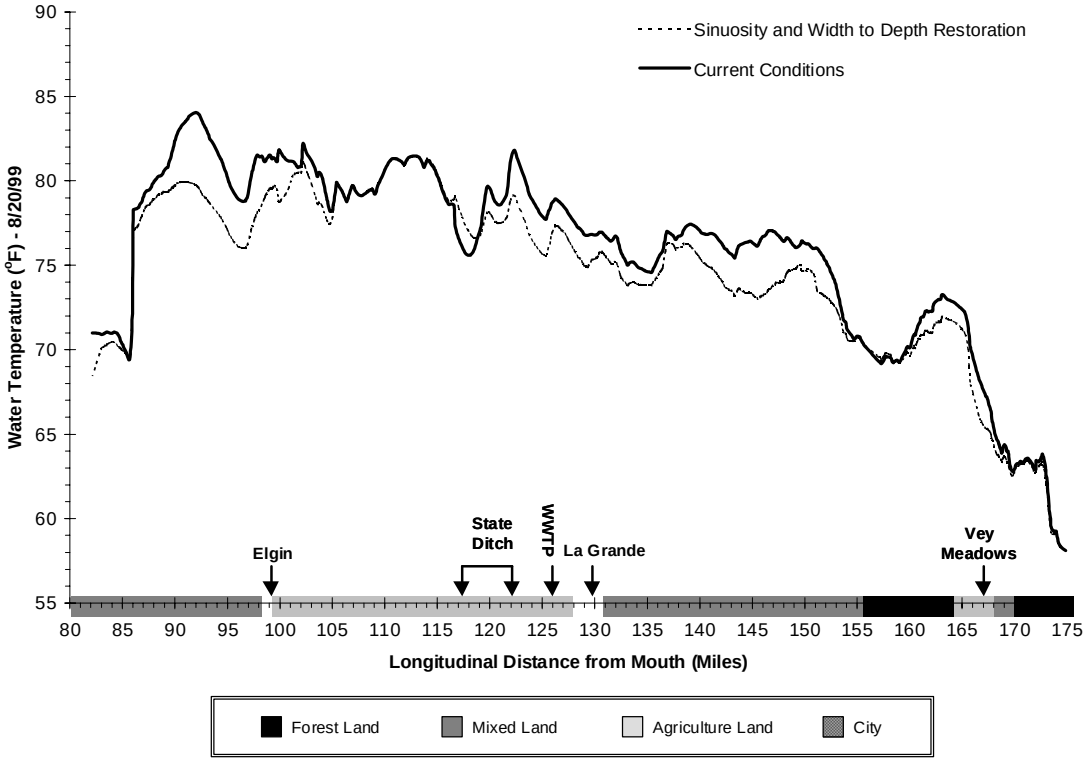

Figure A-70. Combination Scenario

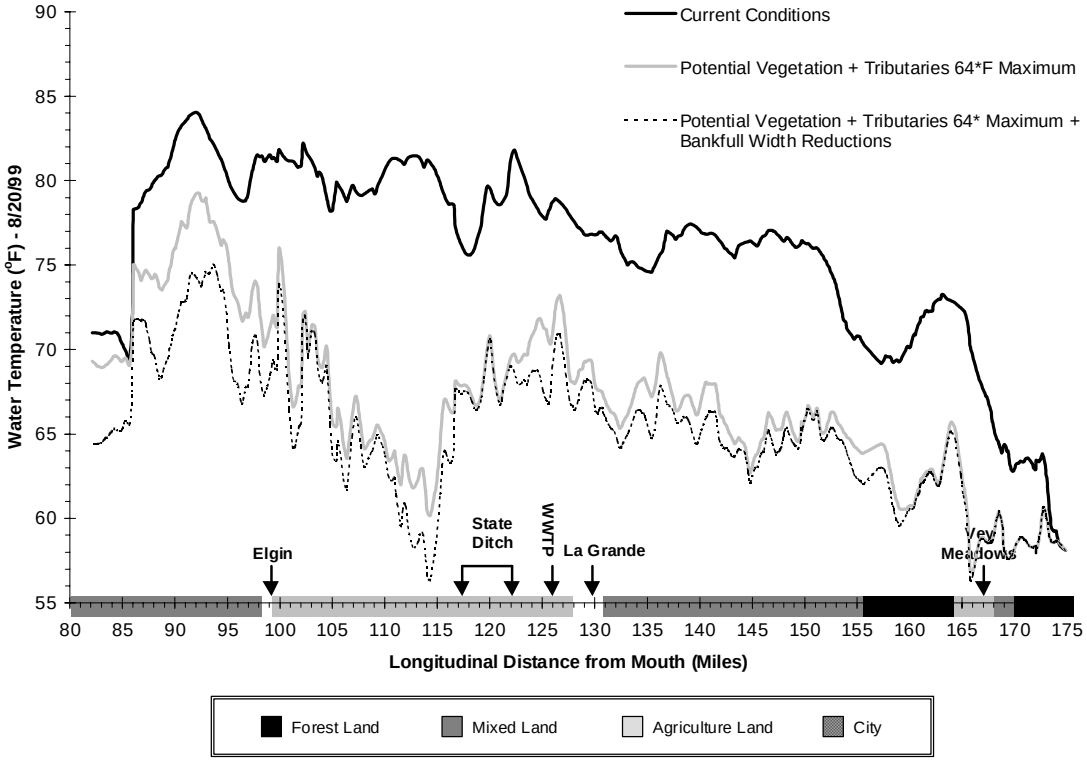

Figure A-71. Site Potential Scenario

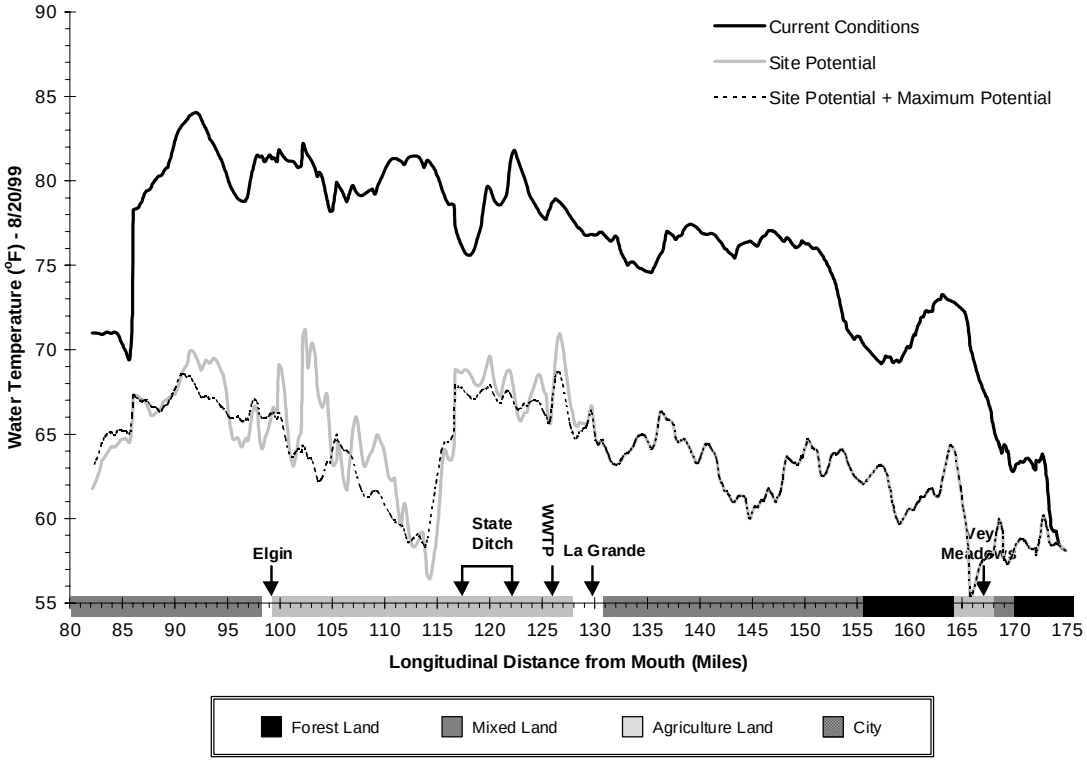

Figure A-72. Modeling Scenario Temperature Results
Percent of River Below Specified Temperature